**CLIC1 regulation of glioblastoma**

Kamaldeep Randhawa
Department of Cellular and Molecular Medicine
Brain and Mind Research Institute
Faculty of Medicine
University of Ottawa
June 2024
Ottawa, Ontario, Canada

Supervisor: Dr. Arezu Jahani-Asl
Department of Cellular and Molecular Medicine
Brain and Mind Research Institute
Faculty of Medicine
University Of Ottawa,
June 2024

A thesis submitted to the University of Ottawa in partial fulfilment of the Master of Science degree requirements

## Table of Contents

## Abstract

Glioblastoma (GB) is the most lethal neurological malignancy of the central nervous system, with a median survival of 18 months despite intense treatment involving maximal surgical resection, ionizing radiation (IR), and temozolomide (TMZ). The inevitability of GB recurrence is in part driven by a population of self-renewing cancer stem cells known as brain tumor stem cells (BTSCs) that can evade conventional treatment modalities. Targeting the signaling pathways that sustains BTSCs holds promise for combating GB recurrence. Notably, the elevated expression of the cytokine receptor Oncostatin M Receptor (OSMR) and the frequent co-occurrence of the mutant Epidermal Growth Factor Receptor (EGFR) gene, Epidermal Growth Factor Receptor variant III (EGFRvIII), within BTSCs, contribute to the establishment of highly tumorigenic and treatment-resistant cells. However, the mechanisms by which the OSMR/EGFRvIII complex sustains BTSCs and promotes tumourigenesis remain largely unknown.

In this study, we identified a novel binding partner of OSMR, Chloride Intracellular Channel 1 (CLIC1), in patient-derived BTSCs through a Mammalian Membrane Two-Hybrid High Throughput (MaMTH-HTS) screen and endogenous validation with proximity ligation assay analysis. Functional assays demonstrated that CLIC1 affects the viability, proliferation, and self-renewal of BTSCs *in vitro*, and tumour progression *in vivo*. Mechanistically, the functional capacity of BTSCs to form tumours upon intracranial injection is mediated by the EGFRvIII/STAT3 pathway, as genetic deletion of CLIC1 resulted in impaired STAT3 activation and reduced EGFRvIII levels. Finally, we demonstrated that OSMR is required for CLIC1 function at the plasma membrane.

Our data suggest that CLIC1 is potentially a viable therapeutic target for suppressing OSMR/EGFRvIII/STAT3 oncogenic signalling and depleting the resistant BTSCs in GB. This work provides new insights into the molecular underpinnings of GB but also lays the foundation for future research aimed at developing targeted therapies against CLIC1 and its associated pathways to improve treatment outcomes for patients of GB.

## Acknowledgements

I would first like to thank Dr. Jahani-Asl for providing me this opportunity to join her lab and take part in research efforts for neuro-oncological research and for her support both technically/theoretically and financially through her CIHR grants. Also, I would like to thank Dr. Jahani-Asl for taking the time to assist in the editorial process of this thesis in addition to providing opportunities to present our work at national and international conferences.

I would like to extend a big thank you to Dr. Dianbo Qu and Dr. Amir Hossein Mansourabadi for taking the time to impart their expertise as well as my lab mates and friends for their continual support through my academic journey. Their kindness, support, and resilience has enriched this process and made it exceptionally memorable and fulfilling.

I would like to thank all the members of my thesis advisory committee, Dr. Yannick Benoit, Dr. Shawn Beug and Dr. Saverio Gentile for their guidance and feedback.

Finally, I would like to thank Manveer, Japdeep and Gursharan for their tremendous support. I could not have undertaken this journey without you.

## Contributions

The experiments in this thesis were performed under the supervision and consultation from Dr. Jahani-Asl. I performed immunofluorescence under the guidance of the Cell Biology and Image Acquisition Core at the University of Ottawa. The Mammalian Membrane Two Hybrid – High Throughput Screen was performed by the Dr. Igor Stagljar Lab. The siRNA screen and *in vivo* studies were performed by Dr. Dianbo Qu. Electrophysiological studies were performed by Dr. Michele Mazzanti.

## List of Figures

## List of Tables

## List of Abbreviations

| | |
|---|---|
| APC | Antigen-presenting cells |
| AREG | Amphiregulin |
| BCNU | Bis-chloroethylnitrosourea |
| BCRP | Breast Cancer Resistance Protein |
| BTSCs | Brain Tumour Stem Cells |
| BSA | Bovine Serum Albumin |
| CAFs | Cancer associated fibroblasts |
| CCL2 | Chemokine (C-C motif) ligand 2 |
| CCL5 | Chemokine (C-C motif) ligand 2 |
| CFTR | Cystic fibrosis transmembrane conductance regulator |
| CLC | Cardiotrophin-like cytokine |
| CLIC | Chloride Intracellular Channel |
| CLIC1 | Chloride Intracellular Channel 1 |
| CNTF | Ciliary neurotrophic factor |
| CNV | Copy number variations |
| CSC | Cancer stem cell |
| CSF-1 | Colony Stimulating Factor 1 |
| CT-1 | Cardiotrophin 1 |
| CXCL10 | C-X-C motif chemokine 10 |
| DIDS | 4,4′-diisothiocyanostilbene-2,2′-disulfonic acid |
| DMSO | Dimethyl sulfoxide |
| ECM | Extracellular Matrix |
| EGF | Epidermal Growth Factor |
| EGFR | Epidermal growth factor receptor |
| EGFRvIII | Epidermal growth factor receptor variant III |
| EMT | Epithelial to mesenchymal transition |
| EPGN | Epigen |
| EPR | Epiregulin |
| FITC | Fluorescein isothiocyanate |
| FBS | Fetal bovine serum |
| $GABA_A$ | γ-Aminobutyric acid type A |

| | |
|---|---|
| GAL4TF | GAL4 transcription factor |
| GAMs | Glioma associated macrophages |
| GB | Glioblastoma |
| GDP | Guanosine diphosphate |
| GFP | Green fluorescence protein |
| GO | Gene Ontology |
| GST | Glutathione transferases |
| GTP | Guanosine triphosphate |
| HBEGF | Heparin-binding EGF-like growth factor |
| HCC | Hepatocellular carcinoma |
| HGG | High grade gliomas |
| IAA94 | Indanyloxyacetic Acid 94 |
| iNOS | Inducible nitric oxide synthase |
| IR | Ionizing radiation |
| JAK | Janus Kinase |
| LIF | Leukemia inhibitory factor |
| LIFR | Leukemia inhibitory factor receptor |
| MaMTH-HTS | Mammalian Membrane Two-Hybrid High Throughput |
| MB | Medulloblastoma |
| MDM2 | Murine double minute 2 |
| MDR | Multi drug resistance |
| MDR1 | Multi-drug Resistance Protein 1 |
| MES | Mesenchymal |
| MGMT | Methylguanine-DNA methyltransferase |
| MMP | Matrix metalloproteinase |
| MØ | Macrophages |
| MRP1 | MDR-Associated Protein 1 |
| NF1 | Neurofibromatosis type 1 |
| NHE9 | $Na^+/H^+$ exchanger 9 |
| NK | Natural killer |
| NOD-SCID | Nonobese diabetic/severe combined immunodeficiency |
| NSCs | Neural stem cells |
| NTD | Amino terminal domain |

| | |
|---|---|
| OPN | Osteopontin |
| OSM | Oncostatin M |
| OSMR | Oncostatin M Receptor |
| OXPHOS | Oxidative phosphorylation |
| PCCs | Pancreatic cancer cells |
| PDA | Pancreatic ductal adenocarcinoma |
| PDGFR | Platelet-derived growth factor receptors |
| PI3K | Phosphoinositide 3-kinase |
| PIP2 | Phosphorylates phosphatidylinositol 4,5 bisphosphate |
| PIP3 | Phosphatidylinositol 3,4,4-triphosphate |
| PM | Plasma membrane |
| PSCs | Pancreatic stellate cells |
| PTEN | Phosphatase and tensin homolog |
| ROS | Reactive oxygen species |
| RTKs | Receptor tyrosine kinases |
| RVD | Regulatory volume decrease |
| RVI | Regulatory volume increase |
| SCF | Stem cell frequency |
| SCID | Severe combined immunodeficient |
| SDF-1 | Stromal cell-derived factor 1 |
| STAT3 | Signal transducer and activator of transcription 3 |
| TCGA | The Cancer Genome Atlas Consortium |
| TGFA | Transforming growth factor-α |
| TKD | Tyrosine kinase domain |
| TME | Tumour microenvironment |
| TMZ | Temozolomide |
| TP53 | Tumour protein 53 |
| V-ATPase | Vacuole ATPase |

# 1. Introduction

## 1.1. Glioblastoma Heterogeneity

Glioblastoma (GB) is a highly lethal neurological malignancy with a median survival of 18 months, representing a significant clinical challenge[1,2]. The annual incidence rate of GB ranges from 0.59-5 per 100,000 persons according to international studies, marking it as the most common malignant brain tumour[3]. GB is characterized by genetic and phenotypic heterogeneity and highly invasive cells that accelerate tumour growth and pose major barriers to treatment[4–7]. The current standard of care includes maximal surgical resection of the tumour followed by ionizing radiation (IR) and temozolomide (TMZ). Despite these intense efforts, the outlook for GB patients remains grim as recurrence is inevitable[8]. One of the main obstacles for treatment efficiency is tumour heterogeneity which facilitates the selection of resistant subpopulations. Tumour heterogeneity' includes both inter-tumour heterogeneity, variance observed at a population level, and intra-tumour heterogeneity, which accounts for differences within individual tumours[9]. High resolution classification of heterogeneity and its drivers serves to improve diagnosis and prognosis[10].

### 1.1.1. Inter-patient heterogeneity

Patient specific mutations and epigenetic alterations ensures no two patients will behave the same clinically. A singular driver of GB does not exist, rather, many different oncogenic programs, genetic mutations and extrinsic factors contributes to brain tumour formation. Commonly affected tumour suppressor genes include tumour protein 53 (TP53) neurofibromatosis type 1 (NF1), and phosphatase and tensin homolog (PTEN). Affected oncogenes often include platelet-derived growth factor receptors (PDGFR), epidermal growth factor receptor (EGFR), and murine double minute 2 (MDM2) **(Figure 1)**[11–13].

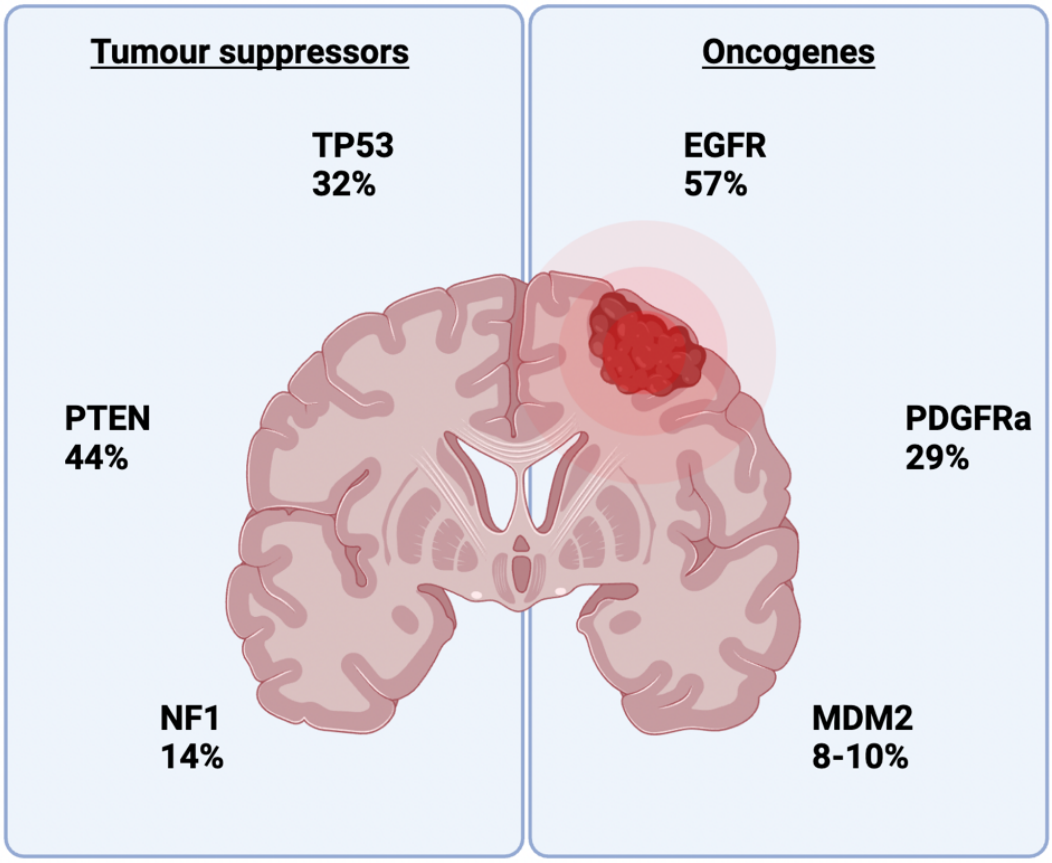


**Figure 1. Commonly altered genes and frequency of their modifications in glioblastoma.** Tumour suppressors include TP53, PTEN, and NF1 which are altered in 32%, 40%, and 14% of GB cases, respectively[14–16]. Oncogenes include EGFR, PDGFRa and MDM2 which are altered in 57%, 29% and 8-10% of cases, respectively[17–19]. Created using Biorender.com.

Among these genes, an active mutant of EGFR, termed EGFR variant III (EGFRvIII) is the most common. EGFRvIII is constitutively active leading to the activation of key oncogenic signalling pathways. Notably, the presence of EGFRvIII leads to the upregulation of a key cytokine receptor, Oncostatin M Receptor (OSMR), which is significantly correlated with poor patient prognosis[20].

In addition to gene mutations, most GB cells carry copy number variations (CNV) in chromosome 7 and 10 (+7/-10), a molecular event that involves either duplications or deletions of genomic segments. For instance, most GB cells have multiple copies of the EGFR gene and mutations/deletions in the PTEN tumour suppressor. Upregulation of EGFR

is associated with uncontrollable phosphorylation and low levels of PTEN are correlated with poor prognosis and therapy resistance[21]. The number of gains and losses varies among patients, thus contributing to inter-patient heteogeneity[22,23].

Finally, the tumour microenvironment (TME), which comprises brain-resident cells, immune and vascular cells, shows variability among patients. While myeloid cells, including macrophages, dendritic cells, monocytes, and granulocytes, remains relatively consistent across patients, there are notable variations in the total number of T-cells. Specifically, $CD4^+$ T-cells and regulatory T-cells remain largely absent whereas $CD8^+$ cytotoxic T-cells and natural killer (NK) cells are shown to vary greatly between patients[24,25]. Heterogeneity amongst patients challenges the development of universal agents and treatment modalities such that the optimal course of action becomes difficult to gauge. This shifts the emphasis towards individualized therapies, necessitating the understanding of complex cellular networks.

### 1.1.2. Intra-tumoral heterogeneity

Transcriptional analyses have revealed the existence of 4 GB subtypes: classical, mesenchymal (MES), proneural, and neural[26]. These subtypes are distinguished largely based on expression levels of key proteins, including EGFR, NF1, PDGFRA/IDH1[26–28] **(Figure 2).**

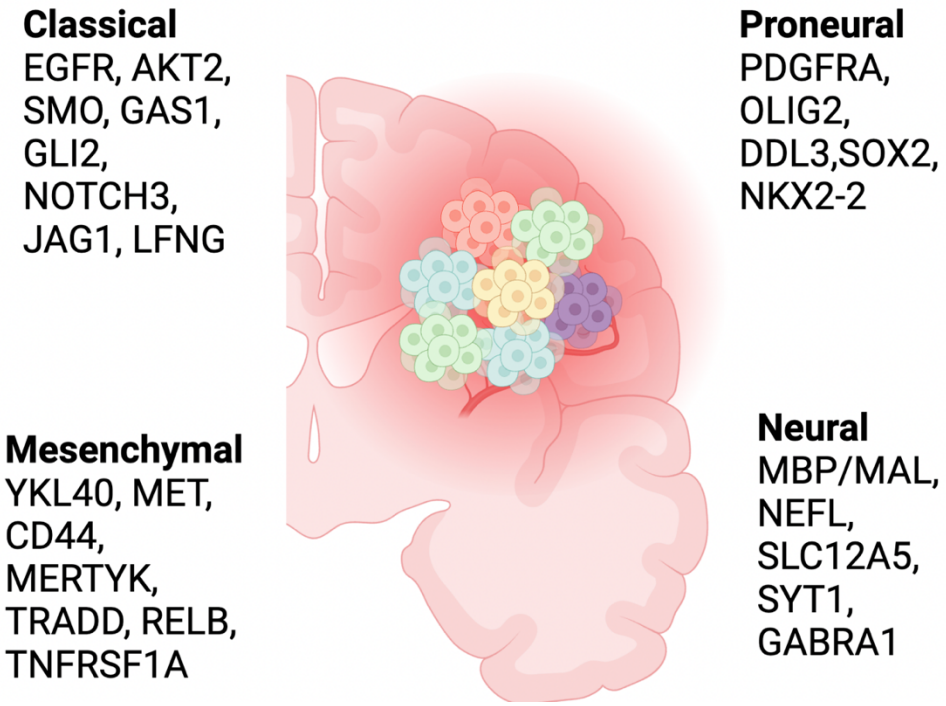


**Figure 2. Glioblastoma subtypes**. Each GB subtype is associated with a specific gene expression pattern. The classical subtype exhibits alterations in EGFR, AKT2, SMO, GAS1, GLI2, NOTCH3, JAG1, LFNG. The proneural signature includes modifications to PDGFRA, OLIG2, DDL3, SOX2, NKX2-2. The mesenchymal subtype is associated with the expression of YKL40, MET, CD44, MERTYK, TRADD, RELB, TNFRSF1A. Finally, the neural subtype expresses MBP/MAL, NEFL, SLC12A5, SYT1, GABRA1[27]. Created using Biorender.com.

Each subtype demonstrates varying drug sensitivity, with the MES subtype being the most aggressive and treatment resistance. Single cell RNA-sequencing experiments have demonstrated that within an individual GB tumour, cells exhibiting characteristics of various subtypes are present[24,29]. In addition, GBs evolve over time, with over 60% of tumours exhibiting a branched pattern of evolution whereby the molecular subtype of the tumour changes upon recurrence[30]. Treatment modalities (IR and TMZ) alter both the genotype and

the phenotype of GB. Longitudinal transcriptome analyses using 91 paired samples taken from patient's pre-treatment and upon recurrence, demonstrated that only 55% of GB samples retain their original molecular subtype[31]. In another study, Wang et al. demonstrated that 66% of primary GB switched their subtype at relapse. Strikingly, the MES subtype was the most stable primary GB subtype, while the classical and proneural subtypes were less frequently observed[32,33]. Recurrent GB tumours possess heightened malignant potential, which may be attributed to their increased stemness and preferential selection of therapy resistant subclones that emerge and expand[34]. Even prior to the selective pressure of chemotherapy and IR, GB tumours exhibit remarkable plasticity; proliferative, self-renewal, differentiative, and infiltrative abilities vary significantly between single cell-derived clones. As such, multiple biopsies are necessary to comprehensively classify a tumour as the intrinsic plasticity adds several layers of complexity[8,35].

### 1.1.3. Models of heterogeneity

Two models are proposed to account for tumour heterogeneity, clonal evolution and cancer stem cells. In the clonal evolution model, heterogeneity is ascribed to the result of stochastic mutations within individual tumour cells that persist through the course of natural selection[36,37]. Clones with the greatest fitness expand while those with selective disadvantages are competed against. Notably, clonal advantages vary along a spatial-temporal landscape as the requirements across tumour regions change. For instance, areas within a tumour may become less hospitable due to the depletion of oxygen, in such a case, "hypoxia-fit"" clones would thrive. In another case, highly vascularized and nutrient dense spaces may select for clones that possess high proliferative capacities. Therapeutic interventions further enhance the complex sub-clonal architecture, as treatment resistant cells emerge and expand[38–40].

In contrast, the cancer stem cell (CSC) model holds that a subset of cancer cells possess indefinite self-renewal capabilities and maintain tumour growth. In this context, tumours are organized along a hierarchy, with the CSCs cells being at the top, and differentiated cells being at the bottom[36,41]. Cellular heterogeneity is orchestrated through processes of differentiation, which are again, spatio-temporally regulated in a cell-intrinsic and extrinsic manner. Importantly, the hierarchy is bi-directional, with CSCs exhibiting high degrees of

plasticity. In GB, single-cell RNA seq data demonstrates that a stemness continuum exists across the bulk tumour and interconversions between a CSC state and non-CSC state are made possible through cross-talks with the TME[42,43]. Secretion of growth factors, cytokines, chemokines, and exosomes by immune, inflammatory, endothelial, adipocyte, and fibroblast cells influences the acquisition of CSC features[44].

### 1.1.4. Brain tumour stem cells

The discovery of a population of GB CSCs termed brain tumour stem cells (BTSCs) has transformed our understanding of GB pathogenesis and the many barriers posed by their existence. Slow cycling or dormant BTSCs can evade conventional treatments (IR and TMZ) and re-enter the cell cycle to undergo self-renewal and recapitulate all cellular subpopulations of the tumour, effectively maintaining heterogeneity[45–49]. BTSCs originating from different populations are highly diverse, with extensive genomic diversity and plasticity[47,49,50]. For instance, proliferative, self-renewal and tumourigenic capabilities vary between different BTSC populations, which also show variable expression of NSC markers such as NESTIN, SOX2, VIMENTIN, and CD133. Furthermore, BTSCs exhibit differential abilities to reversibly exit the cell cycle. This is achieved by repressing cell cycle machinery such as cyclins, and cyclin dependent kinases (CDKs), while increasing the activity of CDK inhibitors, p21 and p27, to prevent unidirectional passage through the cell cycle[51].Whereas some BTSCs are highly proliferative, resembling normal transit amplifying cells, many are quiescent. Quiescence represents one category of cell cycle arrest that corresponds to a transient or prolonged period of dormancy often referred to as the $G_0$ phase. Other categories of arrested states include terminal differentiation and senescence, which are distinguished from quiescence due to their lack of reversibility[51]. On the other hand, transit amplification is the process by which stem cells differentiate into an “amplified” precursor cell, undergoing a series of mitotic divisions to expand the progeny of differentiated cells, while maintaining the NSC pool[52]. BTSCs are therefore classified into two categories of precursor states, stem-like and progenitor-like, with the latter being significantly more tumourigenic[53]. Understanding the dynamic behaviour of BTSCs is essential in the development of targeted therapies to combat GB. Fortunately, their ability to recapitulate heterogenous tumours provides critical insights into their behaviour. To study BTSCs, their characteristics should be understood in comparison to normal NSCs[48,54,55]. BTSCs display similar phenotypic and functional

characteristics as NSCs and are often cultured under similar conditions[48,55]. The neurosphere culturing system enables BTSCs to: (1) generate clonally derived cells resembling neurospheres, (2) proliferate and self-renew, (3) retain similar tumour characteristics to parent cells, (4) differentiate to recapitulate the phenotypic and functional heterogeneity of the tumours from which they are derived[56,57]. This fourth ability makes BTSCs an invaluable tool for modelling GB heterogeneity.

### 1.2. Key oncogenic pathways of glioblastoma: RTKs

Receptor tyrosine kinases (RTKs) represent a class of transmembrane proteins that are commonly dysregulated in signal transduction pathways[58–60]. They translate extracellular stimuli into internal responses, regulating proliferation, self-renewal, growth, apoptosis, migration, and invasion of many cancers **(Figure 3)**[61–69]. Receptor specific ligands induce dimerization of receptor chains and subsequent trans-auto phosphorylation of the intracellular tyrosine kinase domain (TKD) to induce downstream signalling cascades. In GB, the Ras pathway is upregulated in nearly all tumours, however, activating mutations are rare[70]. Rather, upstream RTKs like EGFR can dysregulate this pathway. Ras is a guanosine-binding protein that cycles between inactive guanosine diphosphate (GDP) form and active guanosine triphosphate (GTP) form. Ras-GTP activates downstream effectors such as Raf and MAPK which initiate a phosphorylation cascade, leading to cell cycle progression, angiogenesis, survival, and migration[71–75]. RTKs also initiate the PI3K/PTEN/AKT pathway which regulates survival, cell cycle, and growth. Upon growth factor stimulation of an RTK, PI3K is recruited to the plasma membrane (PM) where it phosphorylates phosphatidylinositol 4,5 bisphosphate (PIP2), to phosphatidylinositol 3,4,4-triphosphate (PIP3), which in turn leads to the phosphorylation of the serine/threonine kinase AKT. Active AKT propagates phosphorylation marks onto different proteins in the PM, cytosol, or in the nucleus, supporting growth, and survival[76,77]. PTEN is a negative regulator of this process which converts PIP3 back to PIP2, thus terminating the signal. In GB, PTEN mutations are found in 41% of all cases[78]. The signal transducer and activator of transcription 3 (STAT3) transcription factor is also activated by RTKs, such as EGFR. Once activated, STAT3 proteins dimerize and move into the nucleus where they bind target genes such as Cyclin D1 or VEGF to promote cell cycle progression and angiogenesis, respectively[79]. STAT3 activation is correlated with poor prognosis and promotes an immunosuppressive TME[80].

The TP53 pathway also plays an important role in GB signalling. The TP53 gene, located on human chromosome 17p13, is a highly dysregulated tumour suppressor. TP53 encodes P53, a highly unstable transcription factor. It is negatively regulated by murine double minute 2 (MDM2), a ubiquitin ligase. MDM2 marks P53 for ubiquitin mediated degradation. In response to stress signals, such as DNA damage, MDM2 is phosphorylated and P53 is subsequently released, thus stabilizing its levels[81]. P53 is then able to induce cell cycle arrest or apoptosis[82]. In GB, P53 inactivation occurs in ~30% of all cases and corresponds to increased self-renewal, invasion, proliferation. In addition, P53 inactivation is associated with disrupted apoptosis and an enhanced chemo-resistant phenotype[83–87].

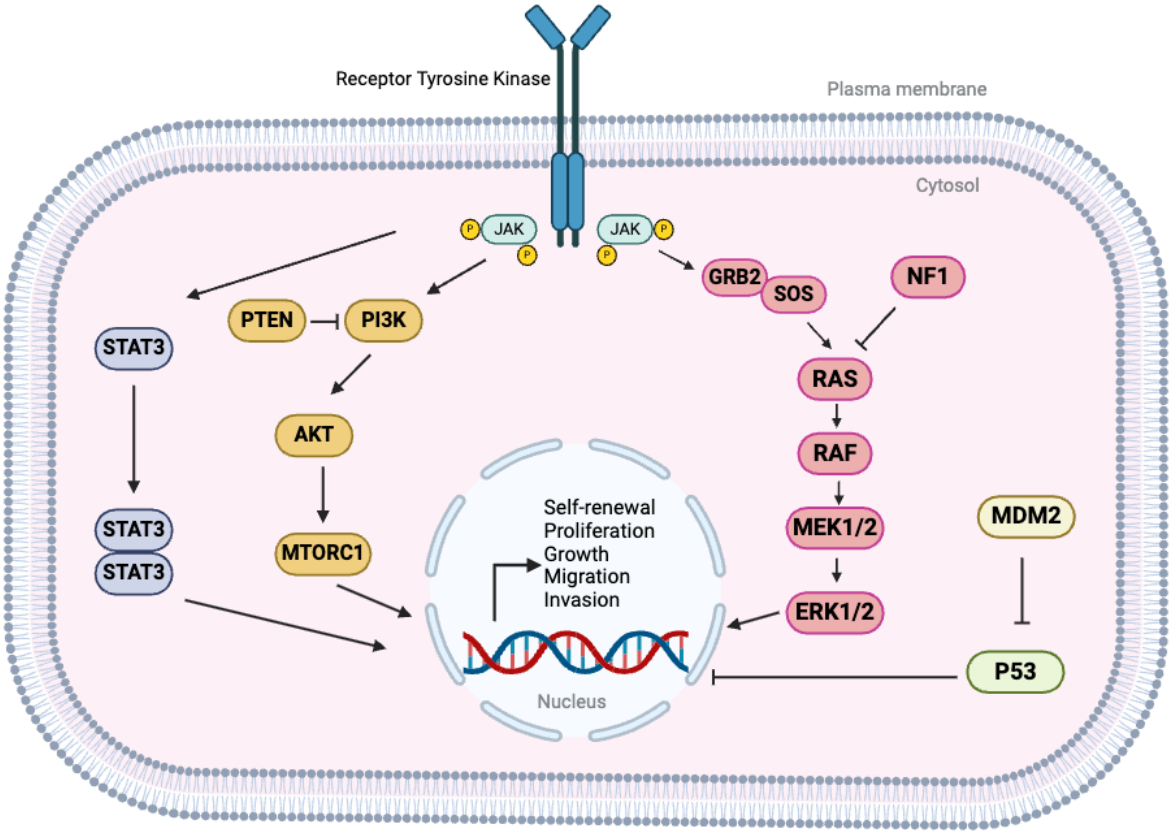


**Figure 3. Simplified RTK regulated signalling pathway in glioblastoma.** Activation of RTK induces downstream signalling to STAT3, PI3K/AKT, RAS/RAF/MEK/ERK to promote self-renewal, proliferation, growth, migration, and invasion. Created with BioRender.com.

### 1.2.1. EGFR signalling

Upregulation of EGFR is one of the most common abnormalities, observed in ~50% of all GB cases[88,89]. While EGFR is sometimes only expressed in a fraction of bulk tumour cells, in most cases, EGFR amplification is observed across the entirety of the tumour mass[90]. EGFR is a RTK which possesses an extracellular ligand binding domain, a single transmembrane region, tyrosine kinase activity and a C-terminal region. There are 7 ligands that bind EGFR: EGF (the canonical ligand), transforming growth factor-α (TGFA), heparin-binding EGF-like growth factor (HBEGF), amphiregulin (AREG), betacellulin (BTC), epiregulin (EPR), and epigen (EPGN)[91–96]. Binding of ligands induces receptor homo- and hetero- dimerization with others in the ERBB family, induction of tyrosine kinase activity and subsequent autophosphorylation at tyrosine residues such as Y992, Y1045, Y1068, Y1148, and Y1173 in the C-terminal tail[88,97]. Signalling through EGFR results in the activation of various downstream oncogenic pathways including RAS/MAPK/ERK, PI3K/PTEN/AKT, JAK/STAT, and PLC/PKC pathway, leading to proliferation, invasion, and angiogenesis[90].

In addition to gene amplification, ~50% of EGFR-amplified tumours express epidermal growth factor receptor variant III (EGFRvIII), a tumour specific variant in which exons 2-7 are deleted[89]. EGFRvIII lacks major components of its extracellular ligand binding domain and remains constitutively active/phosphorylated, independent of ligand stimulation. Constitutive tyrosine kinase activity at low levels leads persistent intracellular signalling, which is augmented by impaired internalization, and degradation[98–100]. Signalling mediated by EGFRvIII is believed to influence critical aspects of oncogenesis, including proliferation, resistance, invasion, and migration[101–105]. EGFRvIII is often found in molecular clusters at the PM and shares overlapping signaling pathways with EGFR while also exhibiting independent signaling capabilities[17]. Unlike EGFR, which is broadly expressed throughout the tumour, EGFRvIII is observed in distinct cell populations, specifically, the CSC niche. Interestingly, EGFRvIII and CD133, a marker for BTSCs, are frequently co-expressed and delineate the BTSC subpopulation. Co-expression of EGFRvIII and CD133 corresponds to BTSCs with the greatest self-renewal and tumourigenic properties **(Figure 4)**[100].

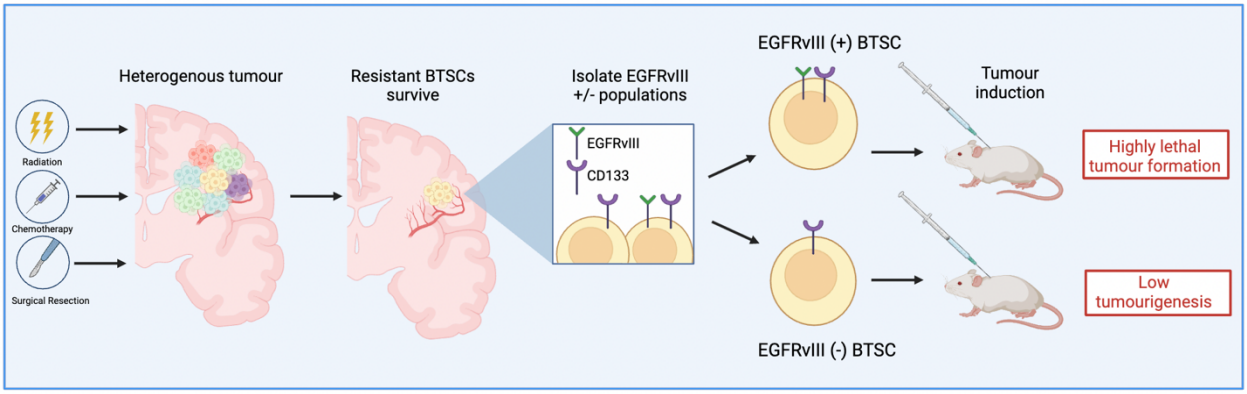


**Figure 4. EGFRvIII delineates highly tumourigenic BTSCs.** Treatment of GB with radiation, chemotherapy and surgical resection often fails to eliminate resistant BTSC populations. Isolation of EGFRvIII+/CD133+ BTSCs and subsequent injection into 6–8 week nonobese diabetic/severe combined immunodeficiency (NOD-SCID) mice leads to highly lethal tumour formation. In contrast, mice receiving EGFRvIII-/CD133+ BTSCs form tumours at a significantly lower rate with poor tumourigenic capabilities. Created with BioRender.com.

### 1.2.2. EGFR mediated cellular transformation

The subventricular zone of the forebrain lateral ventricles and the dentate gyrus in the hippocampus, house adult NSCs[106]. These neurogenic niches are integral for the genesis of new neurons into pre-existing neural circuity and overall brain plasticity. The main implication however, of an adult NSC pool is its susceptibility to malignant transformation[107,108]. For instance, Holland et al. demonstrated that delivering a constitutively active form of EGFR, into astrocytic progenitors of a genetic mouse model, can induce glial transformation with very similar features to human gliomas. Notably, EGFR-induced mutagenesis required two additional mutations: deletion of INK4a–ARF locus[109]. This genetic region encodes two tumour suppressors molecules (p16INK4a and p19ARF) that regulate cell cycle progression[110,111]. Interestingly, both the NSC (Nestin expressing) and astrocytic compartments (GFAP expressing) are equally permissive for gliomagenesis[112]. Therefore, in the presence of active EGFR signalling, cells of the glial lineage with dysregulated cell cycles, are suspectable to the development of glioma-like lesions[109].

### 1.2.3. EGFRvIII induces STAT3 activation to promote GB progression

Transcriptional variation among GB cells of different lineages intricately influences the behaviour of oncogenes and thus challenges the selection of appropriate therapeutic targets. For instance, de la Iglesia et al. demonstrated that STAT3 takes on either a pro-oncogenic or pro-tumour suppressive role in GB, depending on the status of EGFRvIII. In the presence of EGFRvIII, STAT3 functions in a tumourigenic capacity whereby it forms a complex with EGFRvIII in the nucleus of glial cells and drives the expression of gene networks involved in tumourigenesis[113,114]. Loss of STAT3 attenuates EGFRvIII driven transformation, proliferation and tumourigenesis. In contrast, suppression of STAT3 in PTEN deficient (EGFRvIII negative) GB cells increases proliferation, invasion, and their tumourigenic capacity[113]. One mechanism by which STAT3 exerts its tumour suppressive effects is through suppression of chemokine IL8, which is frequently upregulated in PTEN deficient GB. Activated STAT3 occupies the promoter of IL8 and represses its expression thereby blocking proliferation, invasion, and tumourigenesis[114]. In another study, Puram et al identified inducible nitric oxide synthase (iNOS) as a direct target gene of STAT3 during astrocyte transformation in the presence of EGFRvIII. Loss of iNOS significantly attenuates proliferation, invasion and tumourigenesis. However, in PTEN deficient (EGFRvIII negative) astrocytes, iNOS inhibition does not significantly influence proliferation and invasion. Thus, depending on the presence or absence of EGFRvIII, STAT3 takes on a pro-oncogenic or pro-tumour suppressive role. These studies underscore the importance of mapping the genetic landscape of GB tumours and to decipher multifaceted interactions between proteins to determine appropriate therapeutic targets.

### 1.2.4. EGFRvIII drives proneural-mesenchymal transition

At present, TMZ is the first line systemic chemotherapeutic agent used for patients with GB[115]. However, in almost all cases, disease recurrence in inevitable. Complex multifactorial processes such as methylation status of O6-methylguanine-DNA methyltransferase (MGMT), extracellular vesicles, epithelial to mesenchymal transition (EMT), and BTSCs influence resistance and recurrence[116–119]. Among these mechanisms, EMT provides an important mechanism of resistance. The process of EMT converts immotile epithelial-like cells, into motile mesenchymal like cells. During this process, cells can acquire CSC-like features and

form tumours more easily[120,121]. Preventing shifts towards mesenchymal-like states represents an attractive but challenging approach with the potential to significantly improve clinical management of cancer.

In GB, the proneural subtype is known to undergo a switch to MES upon recurrence. In MES form, cells acquire heightened capacity for proliferation, self-renewal, and therapeutic resistance[122–124]. In addition, the MES subtype is closely associated with BTSC features, a primary cell type that challenges therapeutic success[116]. EGFRvIII has recently been suggested to promote resistance to TMZ by promoting EMT. To investigate the relationship between EGFRvIII status and TMZ sensitivity, Shi et al. followed up with GB patients with EGFRvIII negative (-) or positive (+) status. They found that EGFRvIII (-) patients had prolonged survival with TMZ treatment, while no significant difference was observed in overall survival for EGFRvIII (+) patients regardless of TMZ treatment. This indicates that EGFRvIII status affects TMZ sensitivity, with EGFRvIII (-) patients receiving more benefit. Furthermore, in addition to the expected increase in proliferation, migration and tumourigenesis, exogenous expression of EGFRvIII in BTSCs significantly reduced proneural signatures (SOX2, NOTCH1, OLIG2, and CD13) and increased MES markers (CD44, BCL2A1, LYN, and WT1). These results suggest that EGFRvIII plays a critical role in orchestrating treatment resistance by inducing MES states in BTSCs.

Despite a well characterized role in GB pathogenesis, targeted therapies towards EGFR and EGFRvIII using tyrosine kinase inhibitors as a monotherapy or antibodies, have shown limited efficacy in patients[97]. For instance, in response to gefinitib and lapatinib, first generation EGFR inhibitors, EGFR acquires a T790M resistance mutation which renders these drugs ineffective[125,126]. A targeted EGFRvIII vaccine, Rindopepimut (CDX-110) was proven to be safe, immunogenic and tumour specific in a phase I clinical trial but failed in a double-blind randomized phase III trial with a control condition[127–130]. The infectiveness of EGFR and EGFRvIII-targeted therapies may be explained by our knowledge gaps in understanding their mechanism of tumourigenesis[131,132]. Therefore, it becomes imperative to identify EGFR and EGFRvIII dependent pathway(s) and drug targets to modulate EGFR and EGFRvIII in tandem with complimentary pathways to develop novel therapeutic approaches. This feat leads us to analyze the relationship between tumours and their microenvironment.

## 1.3. Cytokine Signalling

Cancer stromal cells in the TME promote cancer progression through several paracrine mechanisms[133–135]. One such mechanism is through a dysregulated stroma, which can enhance the production and release of cytokines. Cytokines are small (15-20kDa) secreted proteins that mediate cell communication in the TME[136].

### 1.3.1. Tumour Microenvironment

Cancer cells exist in a complex and reciprocal relationship with their microenvironment. This milieu is composed of soluble factors, vasculature, stromal cells, immune cells, and the extracellular matrix[137,138]. Other components of the TME include specific environmental conditions such as acidic pH, high concentration of reactive oxygen species (ROS) and/or hypoxia[137]. Exploitation of the local environment and hijacking of non-transformed cells, enables a cancer permissive niche[139,140]. Regular interactions between tumour cells and their adjacent allies stimulates clonal evolution, development of heterogeneity, multi-drug resistance, invasion, and migration[140–145]. Immunosuppression is a main driver of cancer progression. The mechanism to achieve such a state involves release of cytokines, expression of specific cell surface proteins, or the production of metabolites. Amongst these mechanisms, cytokines are master regulators of the TME, representing the main communication link between cancer cells, stroma, and immune cells[146].

The cellular make-up of the glioma TME includes astrocytes, microglia, T-cells, cancer associated fibroblasts, and macrophages **(Figure 5)**. Amongst each population, the glioma associated macrophages (GAMs) dominate up to 50% of the TME[147]. GAMs are divided into two categories: pro-tumour or anti-tumour. Pro-tumour GAMs can inhibit immune responses and enhance tumour progression. They lack specific expression of T cell coactivators (CD86, CD80, and CD40), and release anti-inflammatory cytokines such as IL-6, IL-10, IL-13 and TGF-β. In an immunosuppressed state, cancer cells evade detection and destruction. Many IL-6 cytokines are also shown to elicit cancer promoting features, making them an attractive target for inhibition. In contrast, anti-tumour GAM release pro-inflammatory cytokines such as TNF-α, IL-1β, IL-12, IL-23, and NO. These cytokines promote an immune response that consequently enhances the detection and destruction of tumour cells[146,148–153].

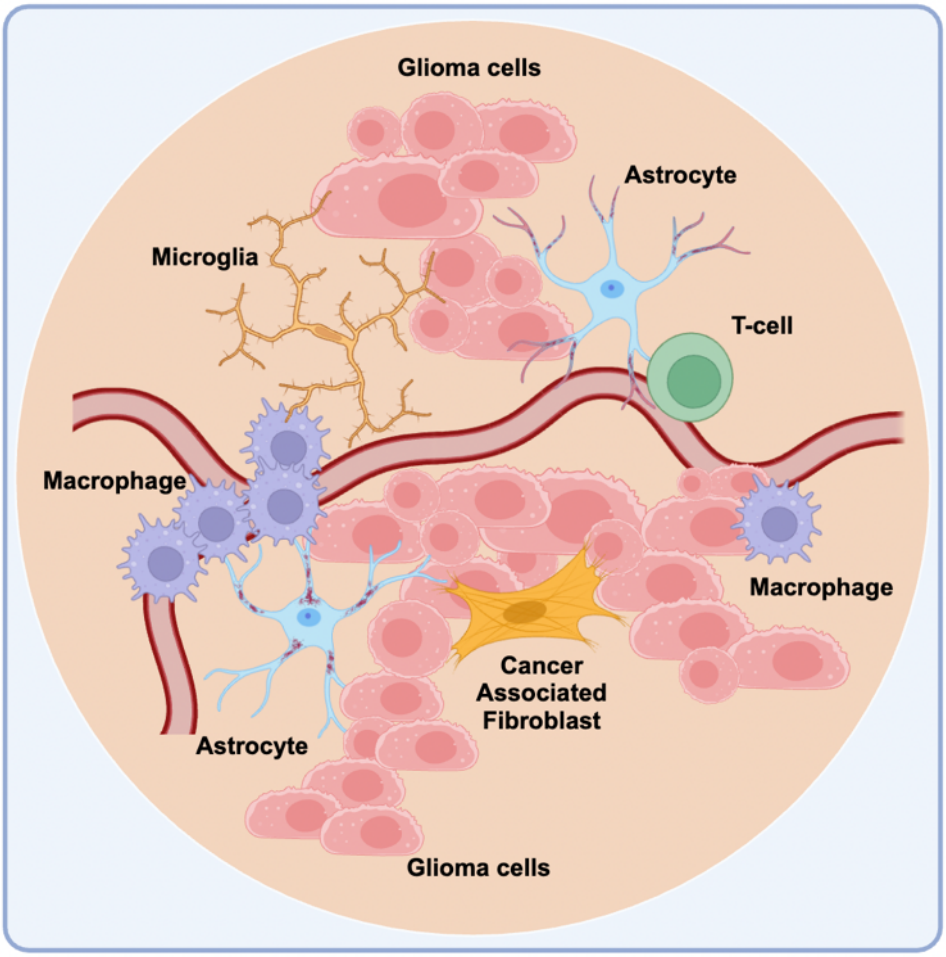


**Figure 5: Tumour microenvironment in glioblastoma.** The figure describes a simplified view of the microenvironment present in the diseased brain. Tumour cells emerge and expand in a permissive microenvironment. Different cell types include glioma cells that interact with astrocytes, microglia, T-cells, cancer associated fibroblasts, and macrophages which promotes tumour growth, angiogenesis, EMT, metastasis, and resistance. Created with BioRender.com.

### 1.3.2. IL-6 Family of cytokines

The Interleukin 6 family of cytokines consists of eight members: IL-6, IL-11, ciliary neurotrophic factor (CNTF), leukemia inhibitory factor (LIF), oncostatin M (OSM), cardiotrophin 1 (CT-1), cardiotrophin-like cytokine (CLC), and IL-27. Each member shares a common gp130 (130kDa) signalling subunit. After ligand binding, IL-6 receptors dimerize with gp130 and recruit janus kinases (JAK) triggering several intracellular pathways including STAT, PI3K, and MAPK[148,154,155], with STAT3 being a critical mediator of cytokine induced

tumourigenesis through its activation of genes involved with increased proliferation, survival, EMT, and transformation[148,149,156].

### 1.3.3. Oncostatin M/Oncostatin M Receptor signalling

An important cytokine involved with such immunopathogenesis is OSM, a member of the IL-6 family of cytokines. OSM is mainly secreted by activated immune cells such as macrophages, T-lymphocytes, dendritic cells and neutrophils. In addition, microglia, neurons, and fibroblasts also secrete OSM. OSMR is expressed on solid tumour tissue cells, endothelial cells, dendritic cells and stromal cells[20,157,158]. OSM binds to the heterodimeric OSM receptor (OSMR) composed of gp130/OSMRβ to propagate external signals **(Figure 6)**[158] .

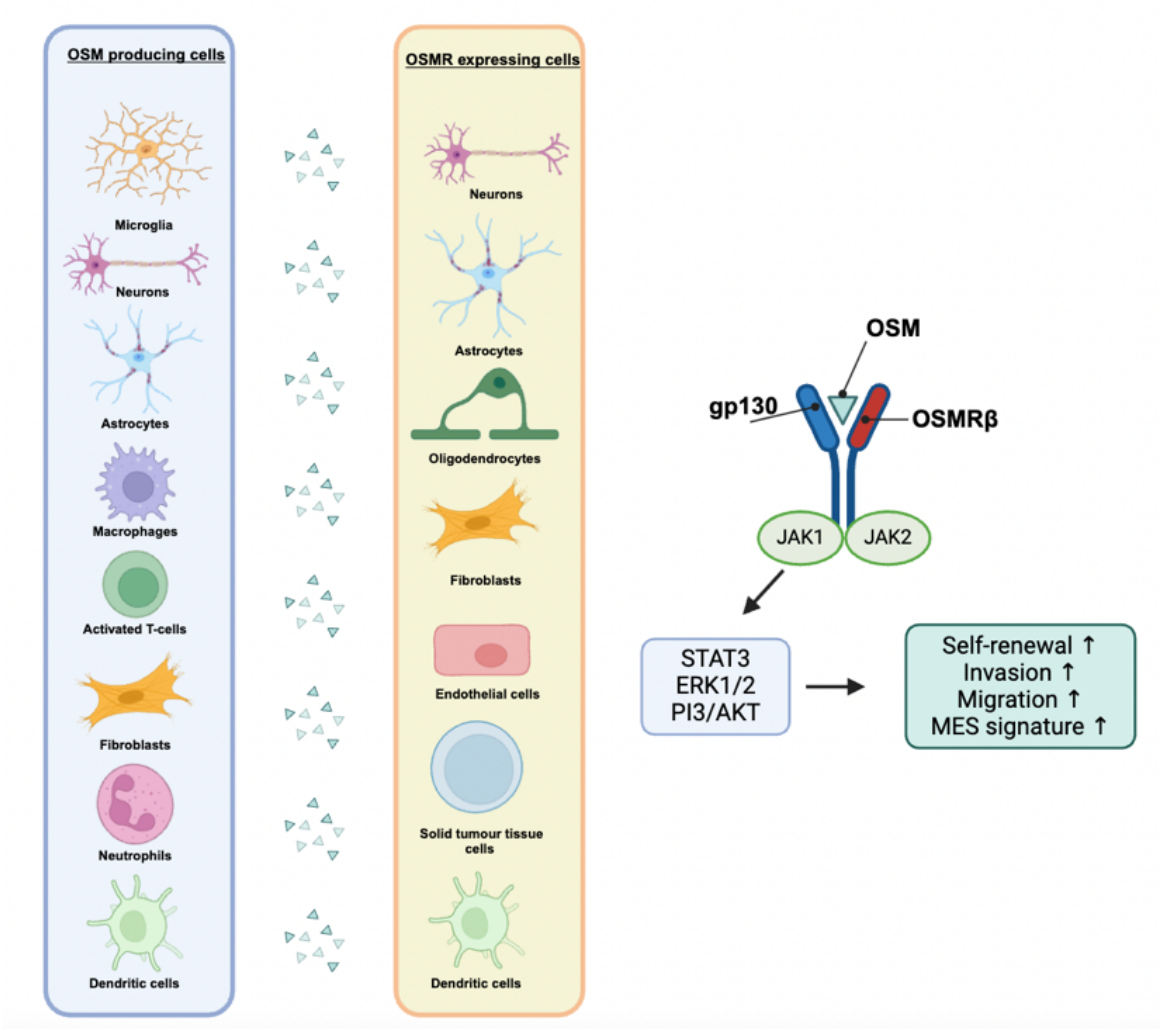

**Figure 6. OSM and OSMR expressing cells.** OSM is produced and released by microglia, neurons, astrocytes, macrophages, activated T-cells, fibroblasts, neutrophils and dendritic cells. OSM binds to OSMR present on fibroblasts, endothelial cells, BTSCs, and dendritic cells. OSM-OSMR leads to recruitment of JAK1/2 which activates downstream effectors STAT3, ERK1/2, and PI3K/AKT leading to increased capacity for self-renewal, increased invasion, migration and MES signature in GB cells. Created with BioRender.com.

Low affinity binding takes place between OSM and gp130 which is strengthened when a second receptor chain is recruited, either OSMRβ or LIFRα[159]. The intracellular domains of both OSMR and gp130 lack intrinsic kinase domains and thus rely upon the recruitment of receptor associated JAKs to transmit signals[160]. Upon ligand binding, OSM signals are propagated by JAK1 and JAK2 which transphosphorylate each other and the intracellular domains of the receptor complex. OSM/OSMR signalling leads to the activation of key oncogenic signalling pathways including MAP kinase cascade, the PI3K pathway and STAT3[160]. OSM dysregulation is reported in a variety of different cancers where it exhibits pleiotropic effects. Initially recognized as a tumour suppressor, OSM was observed to demonstrate inhibitory effects on several tumors like melanoma, lung carcinoma, neuroblastoma, and breast carcinoma[161,162]. However, additional studies revealed synergistic effects on tumorigenesis and chronic inflammation[163–166].

#### 1.3.3.1. OSM/OSMR in glioblastoma

The MES subtype of GB is the most aggressive and treatment resistant subtype. Both cell-intrinsic and extrinsic mechanisms are suggested to drive malignant transformation. In GB, OSM is implicated in MES transitions[167,168]. OSMR is highly expressed in the MES subtype of GB and has low expression in the proneural subtype. Treatment of GB cell lines (LN18 and LN229) with OSM increases the MES signature (YKL40/CHI3L1, fibronectin) and decreases the proneural signature (Olig2). This is associated with increased invasion, migration, and self-renewal. Notably, OSM-mediated signalling contributes to the aggressiveness of GB in a STAT3-dependent manner[169]. Depletion of STAT3 inhibits the OSM-mediated induction of MES genes[156,169]. The major source of OSM comes from GAMs, which enrich themselves close to the MES subtype. Notably, the Cancer Genome Atlas Consortium (TCGA) MES gene expression pattern is highly expressed in immune cells in addition to the GB MES cells. Interestingly, the number of MES-like GB cells is proportional to the abundance of immune cells. Depletion of macrophages using clodronate has been demonstrated to decrease MES-

like GB cells. These macrophages have high expression of OSM which is matched by a high expression of OSMR in the malignant cells, indicative of a ligand-receptor interaction. While the GAMs induce MES transition of GB cells, they are reciprocally affected by GB cells **(Figure 7)**[156]. For instance, GB cells release Colony Stimulating Factor 1 (CSF1) and C-X-C motif chemokine 10 (CXCL10), which maintains the function and survival of GAMs and promotes invasion of GB[170]. Other chemokines such as stromal cell-derived factor 1 (SDF-1) and osteopontin (OPN) promote recruitment of macrophages to the tumour site[171]. GB derived chemokine (C-C motif) ligand 2 (CCL2) and chemokine (C-C motif) ligand 5 (CCL5) recruit regulatory T-cells which inhibit the function of $CD4^+$ and $CD8^+$ effector T cells, natural killer (NK) cells, and antigen-presenting cells (APC)[172–174]. CCL2 also induces the production and secretion of macrophage derived IL-6, IL-10, which in turn, promotes GB invasion[175]. Thus, a reciprocal relationship exists between tumour cells and their TME's which promotes GB progression.

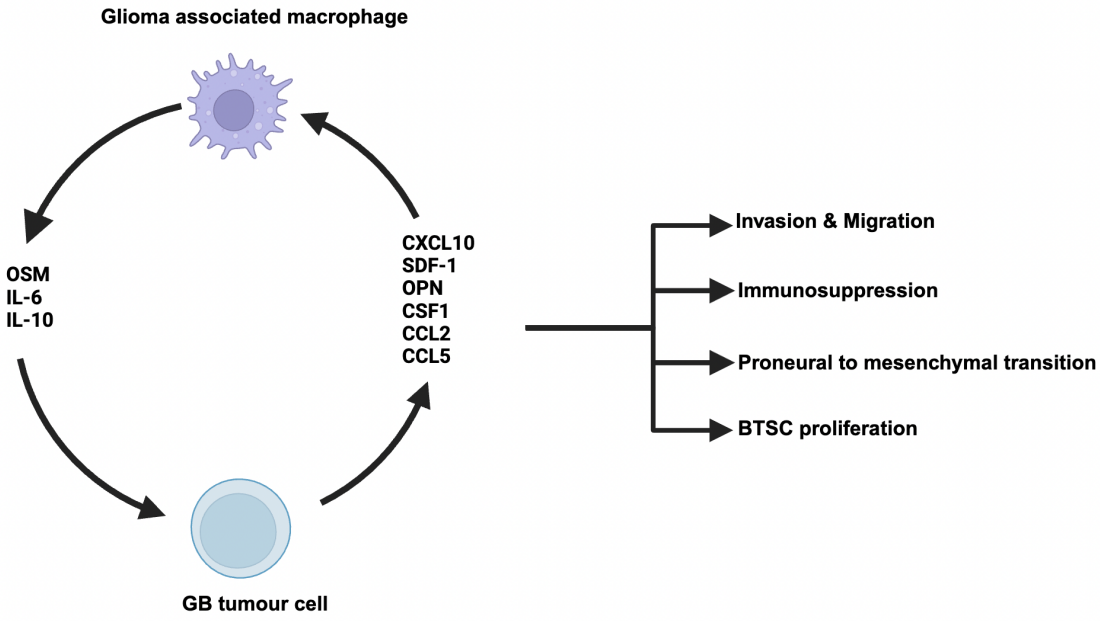


**Figure 7. Reciprocal relationship between GB cells and glioma associated macrophages.** Glioma associated macrophages are known to be a source of OSM, IL-6, and IL-10 which in turn, leads to the secretion of CXXL10, SDF-1, OPN, CSF-1, CCL2, and CCL5. Secretion of cytokines and chemokines promotes invasion and migration, immunosuppression, proneural to mesenchymal transitions and BTSC proliferation. Created using Biorender.com.

#### 1.3.3.1.1. OSMR orchestrates feedforward signalling with EGFRvIII and STAT3 in GB

The tumourigenic mechanisms of EGFRvIII are not fully understood. Recently, Jahani et al. conducted global RNA sequencing to demonstrate that OSMR is highly expressed in all EGFRvIII expressing human BTSCs and mouse astrocytes. Notably, they found that OSMR has a common network of target genes with EGFRvIII. This discovery led them to an important finding that OSMR functions an essential co-receptor of the oncogenic EGFRvIII and can also form a complex with phosphorylated (active) wild type EGFR which leads to the activation of STAT3. Concurrently, they showed that STAT3 binds to the OSMR promoter to upregulate its expression thus orchestrating a feed-forward mechanism in GB **(Figure 8)**[20]. Phosphorylation of EGFR and EGFRvIII is required for its binding to OSMR and subsequent activation of STAT3. Loss of OSMR attenuates EGFRvIII and STAT3 phosphorylation, thus supressing downstream signalling pathways and blocking brain tumor formation[20]. This study highlights the promiscuous and heterodimeric binding that takes place between EGFRvIII and receptors in GB cells. Furthermore, it highlights the potential of OSMR as a therapeutic target for GB.

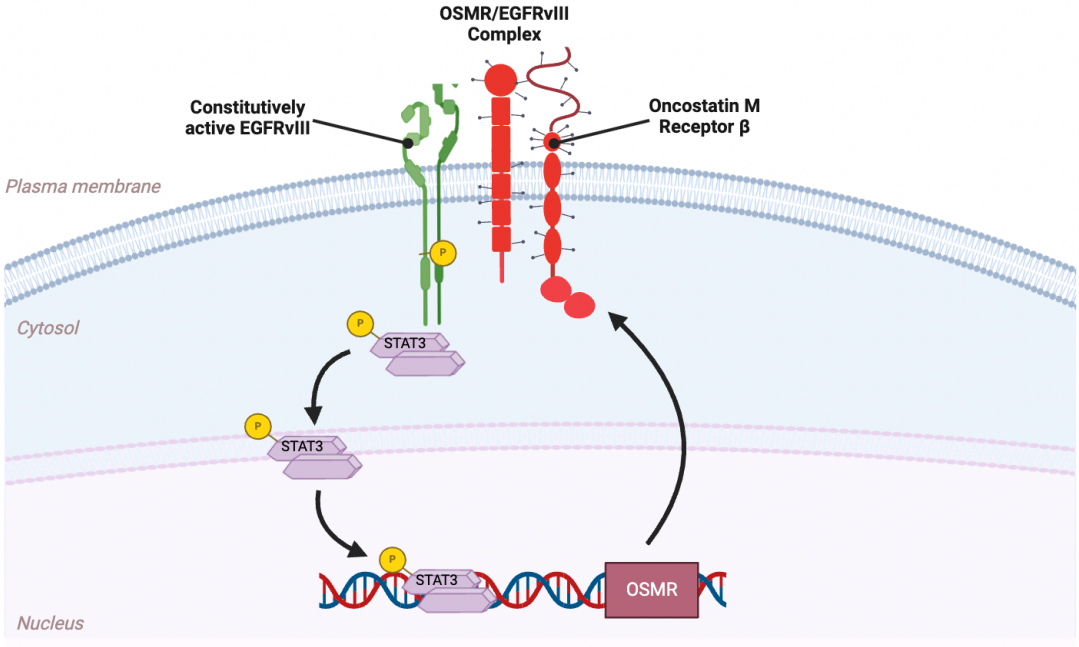


**Figure 8. OSMR orchestrates feedforward loop in BTSCs.** OSMR binds constitutively active/phosphorylated EGFRvIII, leading to STAT3 phosphorylation. Active STAT3 proteins dimerize and move into the nucleus and drive expression of OSMR, leading to positive feedback. Created using Biorender.com.

#### 1.3.3.2. OSM/OSMR in breast cancer ECM remodeling

Dynamic restructuring of the extracellular matrix (ECM) provides an opportunity for tumour cells to grow and escape their local environment[176]. In breast cancer, OSM/OSMR mediate the biochemical signals that drive ECM remodelling. Both OSM and OSMR are highly upregulated in the human breast cancer stroma[177]. The stroma harbour cancer associated fibroblasts (CAFs), which are a central component of primary and metastatic TMEs[178]. Araujo et al. demonstrated that suppression of OSMR in mammary tumours significantly delays tumour onset, growth, lung metastasis and tumour burden at 14 weeks. Interestingly, this is associated with decreased levels of CAF-derived fibronectin, an extracellular matrix protein. The stromal OSM/OSMR axis is also a critical regulator of tumour progression. By orthotopically transplanting breast tumour cells into an *Osmr*-KO mouse or wild-type mice, researchers assessed the contribution of stromal OSM signalling. Results demonstrated that OSMR depletion in the TME delayed onset and growth of mammary tumours. Follow up single-cell RNA sequencing (scRNA-seq) analysis revealed that tumour infiltrating myeloid cells are mainly responsible for producing OSM while OSMR is mainly expressed by fibroblasts and some cancer epithelial clusters. Furthermore, CAF activation via OSM enhances their contractile ability, enabling biomechanical reorganization of extracellular matrix proteins through active STAT3 signalling[177]. This upregulates genes associated with CAF activation (SERPINB4, THBS1, RARRES1, and TNC) and is associated with invasion and poor prognosis in breast cancer patients[177,179]. Additionally, OSM/OSMR signalling remodels the TME through chemokine secretion and myeloid cell recruitment, as evidenced by microarray and transcriptomic analyses showing upregulation of pathways related to leukocyte chemotaxis and inflammation[177,180,181]. OSM induces expression of key chemoattractants (CXCL10, CXCL12, CXCL7, and CCL20) *in vitro* and accordingly promotes immune cell colonization at the tumour site *in vivo*. Abrogation of OSMR signalling in *Osmr*-KO mice reduces populations of F4/80-positive macrophages and Ly6G-positive myeloid cells[177]. The tumour infiltrating immune cells adopt a protumoural and immunosuppressive phenotype as evidenced by CXCR4 and CCR5 positivity[177,180,181]. Overall, OSM in breast cancer organizes a protumoural crosstalk between cancer cells, the immune system and the ECM which has major implications in tumour progression.

#### 1.3.3.3. OSM/OSMR promote pro-tumourigenic TME in pancreatic cancer

In pancreatic ductal adenocarcinoma (PDA), heterocellular OSM/OSMR signalling reprograms CAFs and orchestrates interactions among immune cells, cancer cells and stromal components, fostering a pro-tumourigenic microenvironment conducive of tumour growth and metastasis[182]. Elevated OSM and OSMR expression in PDA correlates with poor prognosis, with OSMR localized to stromal and epithelial compartments, and OSM expressed by immune cells[182]. PDA is regulated by a complex microenvironment composed of inflammatory CAFs, $CD4^+$ regulatory T-cells, myeloid derived suppressor cells and macrophages (MØ) which infiltrate early during tumour development. These cell types utilize matrix metalloproteinase (MMP) and IL-6 signalling to promote tumour progression while concurrently suppressing anti-tumour immunity[183,184].

Lee et al. demonstrated that co-culturing pancreatic cancer cells (PCCs), MØs and pancreatic stellate cells (PSCs) upregulates expression of several pro-tumoural cytokines (IL6, LIF, CXCL1, GM-CSF and CCL2) previously shown to activate the cancer stroma and promote an immunosuppressive microenvironment[182,185–189]. They determined that Individual signals are released in a cell-specific manner whereby MØs express tumour necrosis factor (Tnf) and OSM, PSCs release Il6, Cxcl9 and Cxcl10, and PCCs express Csf2 and Cxcl5. Strikingly, OSM stimulation of CAFs drives a phenotypic shift from myofibroblastic to inflammatory, characterized by increased expression of Il6, Il4ra Cxcl1, Mt2. This process is accompanied by upregulation of OSMR with concaminent activation of several signal transduction pathways (PI3K-AKT-mTOR, MEK-MAPK and EMT). Finally, they performed orthotopic transplantation of PCCs into *Osm* deficient mice which resulted in decreased tumour size, no overt metastasis, and a shift towards a more immunogenic microenvironment[182]. Overall, these results demonstrate that OSM/OSMR establishes a pro-tumourigenic microenvironment that enables PDA progression.

#### 1.3.3.4. OSM in cancer cell plasticity

Cancer cell plasticity is a non-mutational process that enables malignant cells to dynamically acquire distinct functional and phenotypic characteristics in response

environmental cues[190,191]. The developmentally regulated process of EMT has been linked to cancer plasticity. EMT enables transitions of cancer cells from a more differentiated/epithelial state into a stem-like/MES state[192]. This process is mediated by the TME, whereby cytokines, chemokines and growth factors drive phenotypic and functional transitions[193].

Junk et al. explored the role of 28 cytokines in promoting EMT and CSC acquisition. Their results demonstrated that six of the nine cytokines that drove the expansion of MES/CSC (CD24−/CD44+) from epithelial/non-CSC (CD24+/CD44−) are from the IL-6 family of cytokines: IL-6, CNTF, CT-1, CLC, LIF and OSM. Of these members, OSM was the most potent inducer of EMT and CSC acquisition, concomitant with the greatest level of STAT3-Y-705 phosphorylation. Sustained exposure to OSM resulted in the progressive emergence of spindle-shaped and vimentin expressing, MES cells from epithelial/non-CSC that expressed E-cadherin at the cell periphery[163]. The loss of E-cadherin, a cell adhesin molecule, leads to metastatic dissemination and triggers EMT-related processes[194]. Junk et al. further demonstrated that OSM induction of EMT/CSC properties is STAT3 dependent and requires TGF-β/SMAD signaling. Flow cytometry analyses demonstrated that while OSM treatment expanded the CD24−/CD44+ MES/CSC pool from 1.7 to 33.8%, co-administration with a TGF-β receptor type I (TGFβRI) inhibitor SB431542 supressed expansion. Finally, global gene expression analyses demonstrated that OSM or TGF-β treatment induce highly similar changes in an EMT signature which facilitates invasion, migration, and drug tolerance[163]. This analysis reveals the importance of OSM mediated pathways in sustaining CSC features.

## 1.4. Ionic Homeostasis

### 1.4.1. Ions and Ion Channels

The PM serves as a semi-permeable barrier, selectively enabling ions such as sodium ($Na^+$), potassium ($K^+$), and chloride ($Cl^-$) to pass through and thereby establishing an electrochemical gradient. Ion channels are classified into three major superfamilies based on the stimuli that trigger their activity: voltage-gated, ligand-gated and mechano-sensitive ion channels[195]. Voltage-gated ion channels transmit electrical signals. They are activated/inactivated in response to changes in the resting membrane potential[196]. Ligand-

gated ion channels are opened is response to ligand binding to an orthostatic site, resulting in a conductive conformational change[197]. Mechanosensitive ion channels are biological force sensing systems that transmit mechanical stimuli[198].

All ion channels are specialized transmembrane proteins that facilitate the rapid and selective movement of ions across the membrane. These channels offer energetically favorable routes for ion flux, driven by the electrochemical gradients established by ion concentration differences across the membrane. This gradient serves as a source of energy for various cellular functions, including neuronal signaling, proliferation, motor control, apoptosis, and memory consolidation. The precise control of ionic fluxes is therefore essential for all life[195]. Beyond these traditional roles, aberrant expression and dysregulation of ion channels are implicated in various diseases, including cancer, where they contribute to tumor proliferation, self-renewal, invasion, migration, angiogenesis, and resistance to conventional therapies such as chemotherapy[199–201]. Due to their susceptibility to regulation by small molecules, PM ion channels are promising therapeutic targets and current efforts are aimed at elucidating their role in cancer.

### 1.4.2. The ion permeome and cancer

The ion permeome, a dynamic mosaic of channels, transporters and ion controlling proteins, is increasingly recognized as a pivotal player in tumorigenesis. In over 9000 cancer samples, genes responsible for the ion permeome show increased expression[202]. For example, voltage gated $Na^+$ channels are implicated in the invasion and metastases of breast cancer cells. In GB, the $Na^+/H^+$ exchanger (NHE9) is found to limit luminal acidification of lysosomes and EGFR turnover, thus sustaining EGFR-related signalling pathways and driving tumour growth and migration[203]. The mechanosensitive ion channel, Piezo1, orchestrates a feedforward mechanism to drive proliferation and stiffening of gliomas[204]. Invadopodia formation in metastatic prostate cancer cells require NALCN-mediated $Na^+$ influx to maintain $Ca^{2+}$ oscillations[205]. The mitochondrial potassium channel, $K_v1.3$, shows elevated expression in pancreatic, melanoma, and leukemia where its inhibition induces cell death in chemo resistant cells[206–208]. Of the ion channels, $Cl^-$ channels are considered one of the most active during tumourigenesis. Altered Cl- flux in tumours is mediated by the expression of several types of Cl- transporters including voltage-sensitive ClC subfamily, γ-Aminobutyric acid type A

($GABA_A$) receptors, $Ca^{2+}$ dependent Cl- channels, Maxi-Cl- channels, the cystic fibrosis transmembrane conductance regulator (CFTR), and volume-regulated channels[209–214]. These channels mediate electrostatic compensation, cell volume regulation, pH balance, cell fate changes, and motility of cancer cells[215]. The emerging understanding of the ion permeome's role in tumorigenesis seeks to transform our therapeutic interventions for a variety of cancers.

### 1.4.3. Chloride Intracellular Channel Family

The Chloride Intracellular Channel (CLIC) family are an emerging class of $Cl^-$ ion channels involved in cancer development[216–231]. There are six known members CLIC1, CLIC2, CLIC3, CLIC4, CLIC5 and CLIC6 that are highly conserved among metazoa[232–237]. Each member shares a ~240 amino acid sequence belonging to the glutathione transferases (GST) fold super- family. This fold is believed to serve a cellular detoxification purpose and CLICs are known to display dual roles as enzymes and ion channels[238,239]. These metamorphic proteins exist in an equilibrium between soluble globular form and integral membrane form, making them distinct from typical anionic channels. CLIC proteins predominantly exist in their soluble form and lack a membrane targeting leader sequence[240,241]. Biochemical and immnunocyto/histochemical assays demonstrate that CLICs are distributed throughout the nucleoplasm, cytoplasm, inner mitochondrial membrane, secretory vesicles, exosomes, lysosome, luminal membrane, and golgi apparatus[232,236,240–245]. Association with the PM is observed under pathological conditions[245]. CLIC proteins are involved with maintenance of mitochondrial functional integrity, generation of cellular ROS, involvement in mitochondrial stress response, activation of inflammasomes, acidification and proteolysis of phagosomes, and preservation of cytoskeletal filament integrity[236,246–248]. Several members of the CLIC family are associated with pathological conditions, including cardiac dysfunction, hearing loss, Alzheimer's disease, and all stages of cancer development, including initiation, progression, resistance, and recurrence[249–258].

## 1.5. Chloride Intracellular Channel 1

Among the CLIC family, the Chloride Intracellular Channel 1 (CLIC1) plays a prominent role in GB pathogenesis[230,231,244,249,250]. CLIC1 is a voltage-dependent ion channel belonging to the highly conserved class of CLIC proteins[259–261]. Soluble CLIC1 is a monomer that contains

a glutaredoxin-like active site, like the omega class of glutathione-S-transferases (GST) and forms a covalent bond with glutathione through Cys-24 present in its amino terminal domain (NTD)[260,262]**.** In tissues, CLIC1 is mainly found in soluble cytoplasmic form but can undergo major structural rearrangements to insert into lipid membranes in response to various stimuli. The transition of cytosolic CLIC1 to PM CLIC1 is regulated by oxidative stress, pH and presence of divalent cations **(Figure 8)**[262–264].

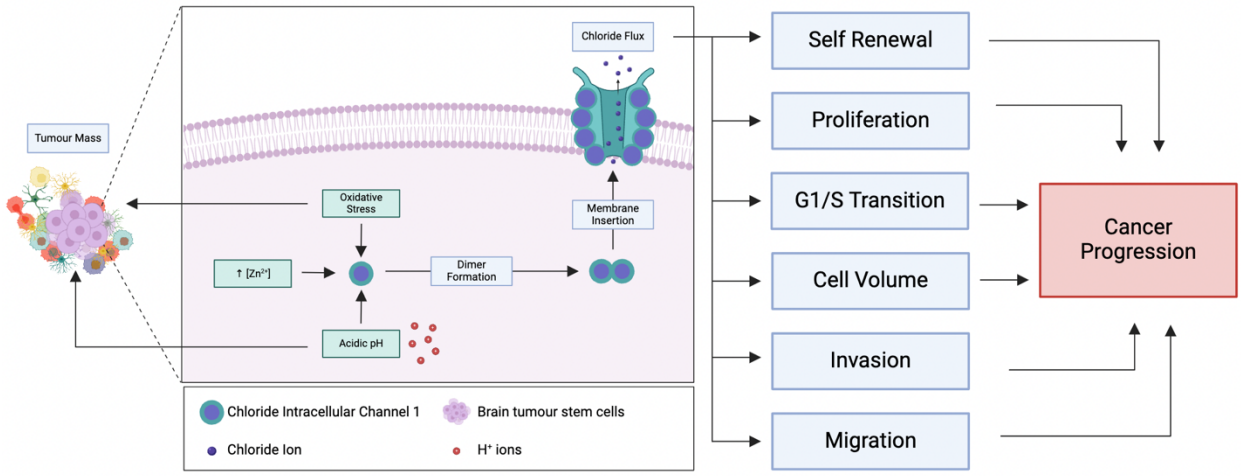


**Figure 9. Role of CLIC1 in cancer hallmark acquisition.** Chloride Intracellular Channel 1 is highly expressed in BTSCs. Structural regulation of CLIC1 by oxidative stress, divalent cations, and low pH promotes membrane insertion. Oxidative and acidic stress promote BTSC features. As a chloride ion channel, CLIC1 facilitates acquisition of different hallmarks of cancer: self-renewal, proliferation, cell volume, invasion and migration. Created with BioRender.com. Adapted from Randhawa et al. 2023[265].

### 1.5.1. CLIC1 structural regulation

The redox-sensitive motif of CLIC1 is proposed to be Cysteine-24, located on the luminal side of the membrane[266,267]. In the presence of excess ROS, CLIC1 is oxidized and forms an intramolecular disulphide bond between Cysteine-24 and Cysteine-59. This induces a reversible structural transition, transforming the monomer to a non-covalent dimer. The dimeric state exposes a large hydrophobic surface which serves as the dimer interface and subsequently enables the formation of $Cl^-$ ion channels. Redox sensitivity is eliminated when Cysteine-24 is mutated to serine. Notably, CLIC1's anion selectivity is Br ≈ Cl > I[259,261,262]. To create an ionic conducting pathway, CLIC1 is hypothesized to oligomerize. The putative transmembrane region of CLIC1 encompasses residues 24 to 46 and contains only two

charged residues, Arginine-29 and Lysine-37, which are likely to line the ionic path. Point mutations in these amino acids modifies biophysical characteristic of CLIC1 (conductance and open/close state kinetics)[268]. In contrast to oxidation, a reducing environment, such as in the presence of antioxidant molecules, reverses this process and prevents the formation of ion channels by CLIC1[262]. Taken together, CLIC1's structure and function are under redox regulation.

Furthermore, CLIC1 shows pH-dependent regulation, with studies indicating lower $Cl^-$ efflux activity at neutral pH and increased activity in acidic and alkaline environments. Tulk et al. carried out a valinomycin-dependent $Cl^-$ efflux assay over a range of pH values. They found that the Cl− efflux activity of CLIC1 was lowest at pH 7, with greater activity observed at higher (pH 9) and lower pH values (pH 5)[269]. In another study, Warton and colleagues discovered that at lower pH values, CLIC1 was more likely to be inserted into artificial membranes and function as an ion channel[270]. A recent study by Varela et al. found that CLIC1's ionic activity was minimal above pH 6.5[263]. By considering the isoelectric point (pI) of CLIC1 (4.5), these findings may be explained[270]. The pI is the pH value at which a protein achieves electrical neutrality. As the pH decreases towards 4.5, CLIC1 becomes electrically neutral. This transition to a net zero charge decreases repulsive forces between CLIC1 subunits which may facilitate oligomerization and ion channel formation[269]. In a similar vein, Peretti and colleagues found that CLIC1 channel activity regulates the G1/S transition which corresponds to a decrease in intracellular pH[249,271]. Taken together, CLIC1 shows strong pH dependence, with acidic and perhaps basic conditions promoting membrane insertion.

Finally, studies have highlighted the role of divalent cations, such as $Ca^{2+}$ and $Zn^{2+}$, in regulating CLIC1's ion channel function. Both $Ca^{2+}$ and $Zn^{2+}$ have been shown to affect membrane insertion properties in various proteins, and the presence of a bound $Ca^{2+}$ in C. elegans and drosophila homologues of CLIC1 have been noted[272–275]. Varela and colleagues demonstrated that the presence of $Zn^{2+}$ but not $Ca^{2+}$, increased the activity of CLIC1 at low pH, confirming previous studies demonstrating the importance of low pH on CLIC1 membrane insertion[269,276]. They also showed that CLIC1 has a direct binding affinity for $Zn^{2+}$. Notably, they found that only $Zn^{2+}$, and not $Ca^{2+}$, could effectively trigger membrane insertion[263]. Regulatory insights into CLIC1's membrane insertion is critical for its selection as a therapeutic target.

### 1.5.2. CLIC1 and Cancer

CLIC1 is normally expressed in the brain, kidney, liver, heart, and skeletal muscle[230,243,277,278], though its expression is elevated in human cancers including hepatocellular carcinoma (HCC), gallbladder carcinoma, gastric carcinoma, colorectal cancer, and brain cancer[225,228,278–280]. Changes in subcellular localization of CLIC1 from the cytosol to PM during cell cycle progression in response to extrinsic and intrinsic stimuli is shown to dictate its oncogenic function[230,244,281]. Through leveraging these intrinsic characteristics, it may be possible to selectively target CLIC1 for cancer therapy while sparing normal cells. Elucidation of the role of CLIC1 in cancer hallmark acquisition seeks to enhance our understanding of its role in tumourigenesis.

#### 1.5.2.1. CLIC1 regulation of BTSC self-renewal

Stem cells are specialized cells that have the capacity to replenish themselves or differentiate into different cell types. They also possess the ability to divide indefinitely, employing two distinct modes of symmetric or asymmetric divisions. Symmetric division results in the generation of two uncommitted daughter cells, effectively expanding the pool of stem cells. In contrast, asymmetric division yields one committed daughter cell alongside one uncommitted cell[282]. In cancer, this ability lends itself to the development of heterogenous tumours that are treatment resistant[5].

In ionic form, CLIC1 has been demonstrated to play a significant role in the self-renewal and proliferation of BTSCs[230]. Acidic microenvironments promote both BTSC phenotype and CLIC1 membrane insertion[263,270,283]. High expression of CLIC1 is also observed in BTSCs compared to wild-type NSCs[230]. Its involvement in self-renewal pathways and the promotion of stem-like features makes CLIC1 a key player in sustaining the viability and growth of BTSCs. To investigate the impact of CLIC1 inhibition in this context, Gritti and colleagues conducted a comprehensive study utilizing three distinct BTSC populations. These populations were subject to different culture conditions: stem cell permissive conditions to maintain their stem-like characteristics or fetal bovine serum (FBS) containing media to induce differentiation over a period of 14 day[250]. Notably, BTSCs exhibited high expression of CLIC1, whereas differentiated cells lost CLIC1 expression. The researchers also observed that treatment with Indanyloxyacetic Acid 94 (IAA94), the CLIC1 channel inhibitor, resulted in

a significant decrease in viability among BTSCs, providing further evidence of the vital role played by CLIC1 in the maintenance of BTSC viability. Importantly, the inhibitory effects of IAA94 were not observed in differentiated populations, underscoring the specific importance of CLIC1 in the maintenance of BTSCs. Furthermore, this study also revealed that the viability of human umbilical cord-derived MES stem cells (ucMSCs), which predominantly express CLIC1 in the cytosol and exhibit negligible CLIC1-mediated currents, were unaffected by treatment with IAA94. Malignant transformation of cells is associated with this change in localization and channel activity[284]. These findings suggest that inhibiting the CLIC1 mediated $Cl^-$ current may hold great potential for selectively impacting malignant BTSC populations while preserving the viability of normal stem cell populations.

#### 1.5.2.2. CLIC1 regulation of cell volume

Ions are critical regulators of cell volume. The volume of a cell corresponds to the amount of water it holds. This volume can change depending on the amount and transport of intracellular and extracellular osmolytes including $Na^+$, $K^+$, $Cl^-$, and taurine[285]. This transport generates an osmotic gradient that enables the diffusion of water across the PM. Small perturbations in cell size can adversely affect function by disrupting cell density[286]. Cells utilize two main mechanisms to rescue their volume in response to perturbations to their resting state. Regulatory volume increase (RVI) is a process that increases cell size in response to shrinkage. It is mainly achieved by $Na^+/H^+$ and $Cl^-/HCO_3^-$ exchangers. Conversely, when cells experience volume expansion, a compensatory mechanism known as regulatory volume decrease (RVD) activates, leading to the efflux of $K^+$ and $Cl^-$[287]. These homeostatic mechanisms ensure structural integrity and constancy of intracellular milieu[288].

Proliferation is a key cellular function that critically relies on volume regulation. As cells undergo cell division, dynamic changes in cell volume are required for the generation of two equally sized daughter cells. During the prophase to metaphase transition, cells undergo a significant volume decrease, reaching a minimum size at metaphase. This reduced volume is preferred by the cell and is referred to as pre-mitotic condensation. Salt and water efflux enables pre-mitotic condensation. During the final stages of cytokinesis, but prior to the complete division of their cytoplasm, the volume of two daughter cells will match the volume of the mother cell at prophase[289–291].

CLIC1 plays a crucial role in regulating both cell volume and the cell cycle. Francisco and colleagues found that genetic deletion of *Clic1* in a Math1-Cre; SmoM2 mouse model, resulted in decreased capacity for proliferation and increased apoptosis in medulloblastoma (MB) cells. Additionally, the researchers observed that suppressing *Clic1* caused cell swelling in addition to mitotic defects[224]. Knockdown of *Clic1* in mitotic cells also exhibited significantly decreased total currents, suggesting that CLIC1 ion channels are highly active during cell division. Furthermore, the study highlighted the cooperative role of CLIC1 with EAG2, a potassium ion channel known to be essential for cell volume reduction and the initiation of mitosis[292]. CLIC1 was found to be present at the PM during interphase and mitosis, whereas EAG2 was present only during mitosis. Colocalization of CLIC1 and EAG2 was observed during mitosis which supports the notion of KCl efflux required for cell shrinkage prior to division[290]. Furthermore, combined knockdown of CLIC1 and EAG2 synergistically reduced MB growth. Synergistic cell volume reduction was achieved by ectopic expression of CLIC1 and EAG2 in cerebellar granule neuron precursor cells obtained from MB tumours. Mechanistically, CLIC1 knockdown was shown to activate the P38/ MAPK osmolarity sensing pathway which inhibited mitotic entry. Moreover, P38 kinase activity suppression by P38 kinase inhibitors partially rescued the cell volume increase phenotype observed in CLIC1 knockdown cells[224]. Taken together, the findings suggest that CLIC1 cooperates with EAG2 to regulate mitotic entry, cell volume dynamics, proliferation, and tumour growth, indicating its potential as a therapeutic target.

#### 1.5.2.3. CLIC1 regulation of proliferation

In GB, CLIC1 in GB is hypothesized to be a cell cycle accelerator due to its regulation by ROS[249,250]. BTSCs harbour chronically altered metabolic conditions compared to wild type NSCs[293]. Higher basal levels of ROS in these cells can supports their survival by promoting G1/S phase transition[294,295]. CLIC1 has been shown to regulate the G1/S phase transition of BTSCs which corresponds to a peak in ROS[249,294,296]. Treatment of BTSCs with IAA94, the CLIC1 mediated current inhibitor, delays transition from the G1 phase, increases total time to complete the cell cycle, and significantly downregulates proliferation. IAA94 treatment also delays the expression of cyclin D1, an important regulator of G1/S transition[249,297]. The expression and phosphorylation of retinoblastoma (Rb), a tumour suppressor involved

with blocking S phase entry and cell growth, is also downregulated[250,298]. Rb binds and inhibits E2F transcription factors, which promote S phase entry. When Rb is phosphorylated, it releases E2F which can then stimulate G1/S transition[298]. Therefore, the attenuation of Rb phosphorylation indicates the arrest of the cell cycle at the G1 phase. Immunofluorescence and patch clamp experiments also show higher CLIC1 levels at the PM during G1/S phase[249]. Downregulation of CLIC1 and inhibition of the $Cl^-$ current via IAA94, attenuates the self-renewal capacity of BTSCs and stunts tumour growth *in vivo*[299]. The dysregulated metabolic conditions and heightened ROS levels in BTSCs underscore the pivotal role of CLIC1 in cell cycle regulation and tumour progression, suggesting its potential as a therapeutic target for GB treatment.

#### 1.5.2.4. CLIC1 regulation of invasion and migration

Coordinated cell migration plays a critical role in various biological processes including immunosurveillance, would healing and embryonic development[300]. In the context of embryonic development, the process of EMT bestows cells with migratory and invasive features, in addition to stem cell like properties and anti-apoptotic mechanisms[301]. The EMT process transforms immotile, tightly packed epithelial cells into migratory, loosely organized MES ones with the ability to travel large distances. EMT activating transcription factors such as E-cadherin, repress epithelial cell markers and promote MES signalling pathways such as Notch and Wnt[301,302]. Cancer cells co-opt these signal transduction pathways to acquire the hallmark of invasion and migration. High grade gliomas (HGG) invariably demonstrate a propensity to impinge upon neighbouring regions of the brain. In their invasive nature, gliomas must acquire a wedge-like shape, a direct consequence of cell shrinkage. This shrinkage necessitates that water be moved out of the cells which is accomplished by the secretion of $K^+$ and $Cl^-$. In this regard, gliomas must accumulate $Cl^-$ against its concentration gradient; the resting membrane potential of a glioma cell is $\sim -40$ mV whereas it's $\sim -80$ mV for a normal astrocyte. As the equilibrium potential for $Cl^-$ channels is more positive, opening of these channels causes efflux of $Cl^-$ ions, enabling cell shrinkage and invasion[303,304]. CLIC1 expression is strongly associated with the highly aggressive MES subtype of GB, which is associated with high infiltration rates, hypoxia, necrosis, inflammation, and multitherapy-resistant features as compared to other transcriptional subtypes. As such, MES GB patients tend to have poor survival. As the

astrocytic tumour grade increases, the expression of CLIC1 also rises. Interestingly, higher expression of CLIC1 is associated with poor patient survival. These findings highlight the critical role of CLIC1 in promoting the migration and invasion processes within GB, particularly in the aggressive MES subtype. Additionally, CLIC1 shows promise as a potential prognostic marker for predicting patient outcomes in GB[27,299,305–308].

### 1.6. Identification of components of the OSMR interactome including CLIC1 via Mammalian Membrane Two-Hybrid High Throughput (MaMTH-HTS) screening

Global approaches to identify OSMR-binding partners have revealed a shared gene network between OSMR and EGFRvIII, constituting the same receptor complex. However, OSMR demonstrates distinct downstream targets, independent from EGFRvIII. OSMR plays a crucial role in driving cells towards MES-like glioma states. Notably, a mitochondrial OSMR operates independently of EGFRvIII to sustain mitochondrial respiration. Deletion of OSMR disrupts oxidative phosphorylation, leading to increased ROS production and sensitizing BTSCs to IR, suggesting its involvement in multiple pathways driving GB pathogenesis. These findings prompted an inquiry into the mechanisms by which OSMR interacts with other key oncogenic players to sustain its signalling in both the absence and presence of EGFRvIII. To explore this, our laboratory conducted a Mammalian Membrane Two Hybrid High Throughput Screen (MaMTH-HTS) to elucidate potential interactions involving OSMR under varying conditions of EGFRvIII presence or absence. The screen was performed in HEK293T cells engineered to express or lack EGFRvIII. OSMR was used as a bait and a prey library of ~8000 open reading frames the Human ORFeome V8.1 collection was used, which enables high-throughput screens in multiple cell lines[309]. After rigorous screening, 177 OSMR-unique partners (including 52 PM proteins) and 137 OSMR/EGFRvIII hits (including 33 PM proteins) were identified. Our data revealed 29 candidate binding partners of OSMR that were commonly found in both groups, 7 of which were recognized as PM proteins. **(Figure 9).** The PM proteins consisted of both integral membrane proteins and proteins associated with the membrane. Using Gene Ontology (GO) terms, functional analyses of proteins clusters within each group highlighted metabolic processes and signalling as predominant categories across all groups **(Figure 9).** Additionally, the analyses revealed an enrichment of GO terms related to immune system processes in the OSMR-unique interactome, while regulation of biogenesis processes emerged as a top term in the OSMR-EGFRvIII category. Mapping the

interactome of OSMR serves as a valuable tool for delineating the molecular networks involved in different pathogenic conditions and aims to identify how OSMR regulates GB across different GB subtypes.

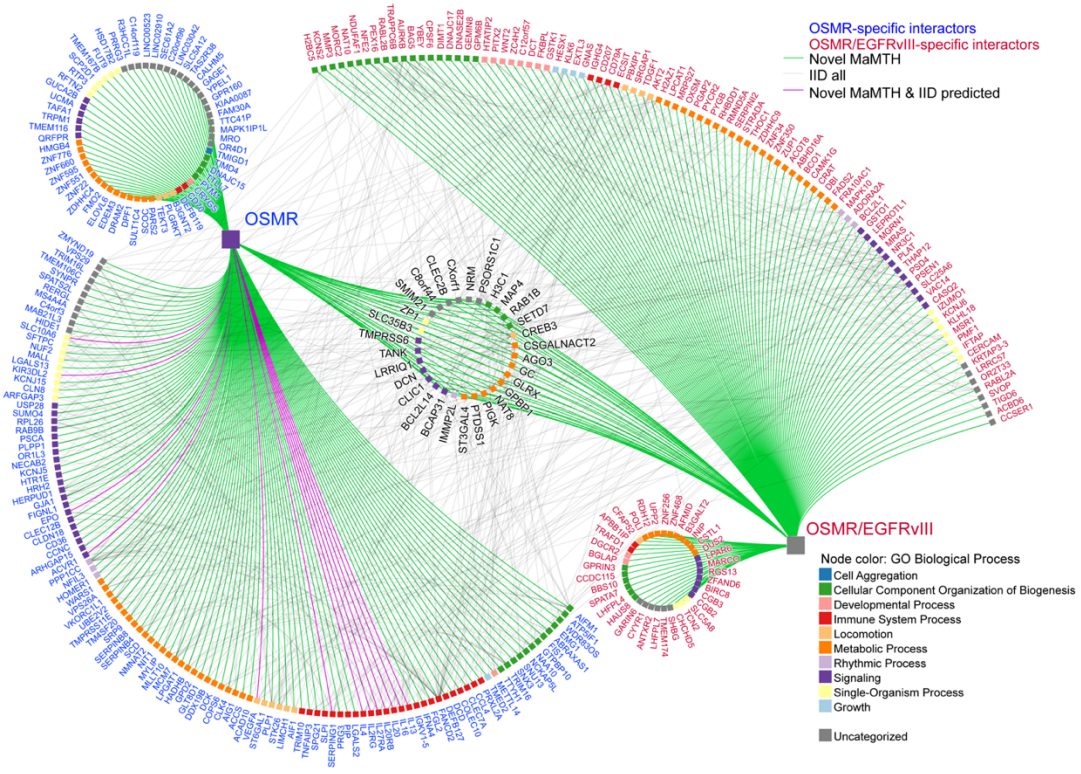


**Figure 10. MaMTH-HTS interactome for OSMR-unique and OSMR/EGFRvIII expressing cells.** OSMR specific interactions are shown in blue, OSMR/EGFRvIII interactions are shown in red. Common binding partners are shown in the center. Jahani et al. Unpublished.

### 1.7. Hypothesis and Aims

Hypothesis: CLIC1 functions as an essential regulator of OSMR/EGFRvIII in BTSCs to drive tumorigenesis.

Aim 1: To assess effects of CLIC1 on BTSC self-renewal and tumourigenesis.

Aim 2: To determine CLIC1's influence on downstream signals from OSMR/EGFRvIII.

## 2. Materials and Methods

### 2.1. Patient Derived BTSC culture

Primary human brain tumour stem cell lines (BTSC12, BTSC30, BTSC73, and BTSC147) were established following surgical excision of patient tumours. Tumour samples were placed into neurosphere culture conditions, as described[310]. Cells were maintained and grown in ultra-low-attachment flasks (Corning) in complete BTSC media: NeuroCult NS-A medium (StemCell Technologies, Inc., #05750), supplemented with penicillin-streptomycin (1:100, Sigma Aldrich, P4333), heparin (2 µg/ml, StemCell Technologies, Inc., #07980), human EGF (20 ng/ml, Miltenyi Biotec, #130-093-825) and human FGFb (10 ng/ml, Miltenyi Biotec, #130-093-838). Primary tumour spheres were expanded and cryopreserved in 10% dimethyl sulfoxide (DMSO) (Sigma-Aldrich) until use in experiments. BTSCs were passaged every 4-7 days or before necrotic core became visible (~200-250µm in size). This was accomplished by using a 10ml serological pipette to collect cells, centrifuging at 80 x g for 10 minutes, aspirating the supernatant and adding of 200µl of ACCUMAX (Innovative Cell Technologies, #AM105) for 10 minutes at 37°C in a water bath. This was followed by addition of 800ul of complete BTSC media. The pellet was gently mixed approximately 10-15 times using a P1000 followed by P200 pipettes sequentially to ensure complete dissociation of spheres. Cells were counted using 0.4% Trypan Blue Stain (Gibco, #15250-061) and plated at a density corresponding to the size of the flask and the desired duration of incubation **(Table 2)**.

**Table 1: Preparation of complete BTSC media**

| **Reagent** | **Final Concentration** | **Volume** |
|---|---|---|
| Streptomycin<br>(50 mg/mL)- penicillin<br>50,000 U/mL | 0.5mg/mL:500U/mL | 500 µL |
| Heparin (2 mg/mL; 1000 IU/mL) | 2ug/mL:1IU/mL | 50 µL |
| Human EGF (40 mg/mL) | 20ug/mL | 25 µL |
| Human FGF (20 mg/mL) | 10ug/mL | 25 µL |
| NeuroCult NS-A medium | N/A | 49.4 mL |
| Total | N/A | 50 mL |

**Table 2: Optimal BTSC plating densities**

| Platting Vessel | Number of cells for 2-3 day incubation | Number of cells for 6-7 day incubation | Volume BTSC Media |
|---|---|---|---|
| T-75 flask | $3 \times 10^6$ | $5 \times 10^5$ | 7 mL |
| T-25 flask | $1 \times 10^6$ | $2.5 \times 10^5$ | 3 mL |

### 2.2. Electroporation

To generate a transient knockdown (KD) of *Clic1* in patient derived BTSCs, a smart-pool of short interfering siRNAs was used. Briefly, 1 million cells were processed into a single cell suspension and subsequently mixed with ON TARGET-plus SMART pool human CLIC1 siRNA (Dharmacon, #L-009530-00-0005) at a concentration of 100nM, or ON TARGET-plus non-targeting pool (Dharmacon, #D-001810-10-05), at a concentration of 100nM. siRNA was delivered using the BTX™ Gemini X2 Electroporation System set at 250 volts, resistance 1050Ω, capacitance 250uF, and an electrode gap of 2mm. Electroporated cells were plated in a T-25 culture flask containing BTSC media and incubated at 37°C and 5% $CO_2$. Cells were plated for ELDA 24 hours after electroporation, while cells utilized for gene expression and immunoblotting were collected after 72 hours.

### 2.3. Gene Expression Analysis

Total RNAs were isolated from cells using the TRIzol method. Pelleted cells were incubated with 1 mL TRIzol digestive reagent (Invitrogen, #15596026) for 5 minutes at room temperature. Following this, 0.2ml chloroform (Sigma Aldrich, #288306) was added, vigorously shaken for 20 seconds, and incubated for 2-3 minutes at room temperature. After centrifugation at 12,000 x g for 15 minutes at 4°C, 0.5 ml of the upper aqueous phase was mixed with 0.5ml isopropanol in a clean tube. This mixture was incubated at room temperature for 15 minutes and then centrifuged at 12,000xg for 10 minutes at 4°C. The supernatant was discarded, and the RNA pellet was washed with 75% and 100% ethanol, each followed by centrifugation at 7500 x g for 5 minutes at 4°C. After air-drying for 10 minutes in a sterile biological hood, the RNA pellet was dissolved in 20-50 µL RNase-free water and incubated at 55-60°C for 10-15 minutes. Reverse transcription was performed using the 5X All-In-One RT MasterMix cDNA synthesis system (abm, #G492). The resulting cDNA was used for subsequent quantitative real-time PCR. For RT-qPCR analysis, the fluorescent dye

Green (Bio-Rad, #1725271) was employed. Primers **(Table 3)** were combined with 1µl of 5µm forward primer, 1µl of 5µm reverse primer, and 5µl SYBR Green to create the PCR mix. This mix, along with 3µl of 30 ng cDNA, was used to generate a final plated mix of 10µl total volume. The PCR was run on the QuantStudioTM 7 Flex Real-Time PCR System (Applied Biosystems). mRNA expression levels were normalized to the housekeeping gene beta-glucuronidase (GUSB).

**Table 3: qPCR primers used to assess gene expression**

| Gene | **Forward Primer Sequence** | **Reverse Primer Sequence** |
|---|---|---|
| GUSB | GCGTTCCTTTTGCGAGGAGA | GGTGGTATCAGTCTTGCTCAA |
| CLIC1 | ACCGCAGGTCGAATTCTTC | ACGGTGGTAACATTGAAGGTG |

### 2.4. Immunoblotting

BTSCs (~$5x10^5$ cells) were lysed in 1x RIPA Buffer (Thermo Fisher Scientific, #89900) with protease and phosphatase inhibitors (Thermo Fisher Scientific, #A32959). After cell lysis, protein concentration was determined by Bradford Assay (Bio-Rad), followed by electrophoresis on an 8-12% SDS-PAGE gel. Subsequently, proteins were transferred onto a Nitrocellulose Membrane 0.45µm (Bio-Rad, #1620115) at 100V for 1 hour and then at 120V for 20 minutes. Blocking for non-specific binding was performed using 5% bovine serum albumin (BSA) in 1X TBST for 1-2 hours. Membranes were incubated with primary antibody at 4°C overnight followed by HRP-conjugated secondary antibody incubation in 5% BSA for 1 hour at room temperature. Visualization of proteins of interest was achieved using ClarityTM Western ECL Substrate (BioRad, 170-5060) with a ChemiDoc Imaging System (Bio-Rad). The following antibodies were employed: OSMR (1:100, Santa Cruz Biotechnology, sc-271695, mouse), CLIC1 (1:200, Santa Cruz Biotechnology, sc-81873, mouse), Phospho-STAT3-Y705 (1:1,000; Abcam, ab76315, rabbit), STAT3 (1:1,000, Cell Signaling, #9132, rabbit), EGFR (1:500, Cell Signaling, #2232), $Na^+/K^+$ ATPase (1:1000, Abcam, Ab58475, rabbit), GAPDH (1:1000, Cell Signalling, #2118, rabbit), beta actin (1:1000, Cell Signalling, mouse). An in house EGFRvIII[311] antibody was employed.

### 2.5. Extreme Limiting Dilution Assay

The extreme limiting dilution assay (ELDA) was performed by dissociating spheres into a single-cell suspension followed by serial dilution using complete BTSC media containing serum-free NeuroCult NS-A medium (StemCell Technologies, Inc., #05750). The media was supplemented with 100 U/mL penicillin, 100 µg/mL streptomycin (Sigma Aldrich, P4333), heparin (2 µg/mL, StemCell Technologies, Inc., #07980), human EGF (20 ng/mL, Miltenyi Biotec, #130-093-825), and human FGF (10 ng/mL, Miltenyi Biotec, #130-093-838). Subsequently, 100µl of the diluted single-cell suspensions were plated in a 96-well plate, with 12 wells plated for dilutions of 25, 12, 6, 3, and 1 cell(s) per well. The plates were then incubated at 37°C and 5% $CO_2$ for 7 days, after which sphere formation was assessed. Data retrieved from the analysis was input into an online software available at https://bioinf.wehi.edu.au/software/elda/. The software provided information on the number of cells required to generate a positive well (with a sphere) for each condition and stem cell frequency (SCF), the proportion of stem cells within a given BTSC population.

### 2.6. Immunostaining

For immunostaining, BTSCs were plated on Lab-Tek II, CC2-treated chamber slide system (Thermo Fisher Scientific, #154941) in media containing complete BTSC media. Prior to plating cells, ACCUMAX was removed through an additional centrifugation step (120g x 10 mins) to enhance adherence. Cells were washed with warm 1x PBS and fixed with warm 4% paraformaldehyde (PFA) for 10 min at 37°C. 20% PFA was thawed at the time of use and the remainder was discarded. Next, cells were permeabilized with 0.5% Triton X-100 (Sigma Aldrich, #T8787) for 20 min and blocked for 1 h with 5% normal horse serum (NDS) in 1X-PBS. The cells were then incubated overnight at 4°C with primary antibodies to anti-OSMR (1:100, Santa Cruz Biotechnology, sc-271695, mouse), anti-CLIC1 (1:200, Santa Cruz Biotechnology, sc-81873, mouse), and an in house EGFRvIII antibody[311]. Cells were washed 3x with 1x PBS, 5 minutes each and then incubated with secondary Alexa fluor 488 goat (1:500, Thermofisher, A32740, mouse) and Alexa Fluor 594 goat (1:500, Thermofisher, A11032, mouse) for 1 h at room temperature. 2 mg/ml DAPI (Thermo Fisher Scientific, #D1306) was used to detect the nuclei and ProLong Gold Antifade Mountant (Thermo Fisher Scientific, #P36934) was used for mounting. Images were captured using a 40x oil or 100x oil objective on the Axio Observer 7.

### 2.7. Proximity Ligation Assay

The Proximity Ligation Assay was conducted in accordance with the Duolink In Situ Red Starter Kit's protocol (Sigma, #DUO92101). In brief, a single-cell suspension of BTSCs was plated on Nunc Lab-Tek II CC2 Chamber Slide System (Thermo Fisher Scientific, #154941) After dissociation, ACCUMAX was removed with an additional centrifugation step (120g x 5 minutes). The single cell suspension was plated at a density of 8 x $10^5$ cells per 200µl for 30-60 minutes. Prior to plating cells, chamber slides were warmed to 37°C. Subsequently, cells were washed with warm 1x PBS, fixed with warm 4% paraformaldehyde for 10 minutes at 37°, and then washed 3x with 1x PBS. Permeabilization was achieved using 0.5% Triton X-100 for 20 minutes, followed by blocking with the Duolink Blocking Solution provided in the starter kit. The samples were then incubated overnight at 4°C in a humid chamber with primary antibodies against the proteins of interest: OSMR (1:400, Abnova, H00009180-D01P, rabbit) and CLIC1 (1:400, Santa Cruz Biotechnology, sc-81873, mouse) were used. After overnight incubation, samples were washed with Wash Buffer A (available in the Starter Kit) and incubated with PLUS and MINUS oligonucleotide probes conjugated to secondary antibodies for 1 hour at 37 °C in a humid chamber. Following the incubation, samples were washed with Wash Buffer A and incubated with Ligation Buffer with Ligase (available in the Starter Kit) for 30 minutes at 37°C in a humid chamber. Rolling Circle Amplification (RCA) was achieved following washing samples with Wash Buffer A and incubating with polymerase and amplification solution (available in the Starter Kit) containing nucleotides for 100 minutes at 37 °C in a humid chamber, protected from light. Following RCA, samples were washed with Wash Buffer B and mounted with Duolink In Situ Mounting Medium with DAPI (DUO82040, Sigma). PLA signals were visualized and captured using a laser scanning microscope (Olympus LS, IXplore Pro Automated Microscope system) equipped with the adjoining imaging software (Zeiss) at 60x objective magnification. Stardist software on Fiji was utilized to quantify PLA signals.

### 2.8. Trypan Blue Population Growth Assay

The Cell Population Growth Assay involved processing BTSC spheres into a single-cell suspension using ACCUMAX dissociation solution (Stem Cell Technologies). Single cells were then plated at a density of 500 x $10^3$ cells per well (6-well plate) in 1.4 ml of complete BTSC media. Cells were collected at 1 day (24 hours), 3 days (72 hours), and 7 days (168 hours) post-plating, with live cell assessment using 0.4% trypan blue exclusion dye (Gibco

#15250-061). Cell counting was performed using an automated cell counter (Countess II FL Automated Cell Counter).

### 2.9. Cell Fractionation

The plasma membrane and cytoplasm were separated using the Thermofisher Subcellular Protein Fractionation Kit (Thermofisher, #78840), following the manufacturer's protocol. Briefly, 5 × $10^7$ BTSCs were rinsed once with 1ml of 1 × PBS containing 0.3% BSA and then with 1 ml of 0.9% sodium chloride solution. For cytoplasm extraction, cells were treated with 500µl of cytoplasmic extraction buffer (CEB) and shaken for approximately five minutes at 4°C. After centrifugation at 500 XG for 5 minutes, the supernatant was carefully collected. For plasma membrane extraction, the pellet was incubated with 500µl of membrane extraction buffer and shaken for approximately five minutes at 4°C. Subsequently, the cells were centrifuged at 3000 XG for 5 minutes, and the supernatant was collected. Protein concentration of cytosolic, and plasma membrane lysates was determined using the Bradford assay (Bio-Rad, #5000006) and 10ug of protein was loaded in a 10% SDS PAGE gel.

### 2.10. Mammalian Membrane Two Hybrid – High Throughput Screen

The MaMTH-HTS screen was performed in HEK293T cells engineered to express or lack EGFRvIII. OSMR was used as a bait and a prey library of ~8000 open reading frames the Human ORFeome V8.1 collection was used, which enables high-throughput screens in multiple cell lines [309]. At the C-terminus of the OSMR bait plasmid, a Math-HTS Bait tag (C/ub) was linked to a GAL4 transcription factor (GAL4TF). A fluorescent marker was also expressed with a P2A linker (C/ub-GAL4TF-P2A-tagBFP). The N-terminus of the prey proteins were fused to a Math-HTS Prey tag (N/ub) and P2A-mCherry at their C-terminus. The HEK293T cells contained a genomically integrated green fluorescence protein (GFP) under the control of a Gal4 promoter. The bait plasmid, either alone or in conjunction with an EGFRvIII expressing plasmid, is transfected into HEK293T cells containing the MaMTH-HTS 'Prey' library. Upon a protein-protein interaction between the bait and prey, a pseudo-ubiquitin complex forms, targeted by a deubiquitinating enzyme, which cleaves GAL4TF, allowing it to translocate to the nucleus and induce GFP expression via the GAL4 promoter.

### 2.11. siRNA counter screen

BTSC lines were plated with 70µl of media at 1000 cells/well in 96-well plate. Transfections were carried out using Lipofectamine RNAiMax (Thermofisher) after plating. 10pmol of siRNAs (Thermofisher) **(Table 4)** and 0.1µl of Lipofectamine RNAiMax (Thermofisher) for each well were diluted in 10µl of Opti-MEM (Thermofisher), respectively. Transfection mix of diluted siRNA and Lipofectamine RNAiMax were added to each well bringing the total volume of the well to 90µl of media. 48 hours after transfection, 10µl of PrestoBlue was added to each well. The plates were then incubated for 1 hour and read on a plate reader (BioTek) with the following settings: gain at 100, 10 flashes/well, read from bottom, excitation at 560nm and emission at 590 nm. Growth was normalized by dividing the value of each well to the average of the control wells. 3 or 4 replicate experiments were performed for each cell line.

**Table 4: List of target genes and associated siRNA sequences**

| Target Gene Name | Sense siRNA Sequence | Antisense siRNA Sequence |
|---|---|---|
| B-cell receptor-associated protein 31 | UGGUGACUCUCAUUUCGCAtt | UGCGAAAUGAGAGUCACCAgg |
| B-cell receptor-associated protein 31 | GCAAGUUGGAUGUCGGGAAtt | UUCCCGACAUCCAACUUGCct |
| B-cell receptor-associated protein 31 | GCACUAAGCAAAAACUAGAtt | UCUAGUUUUUGCUUAGUGCtg |
| BCL2-like 14 (apoptosis facilitator) | CCGAGUAGCUGAAAUUGUUtt | AACAAUUUCAGCUACUCGGtt |
| BCL2-like 14 (apoptosis facilitator) | CCAUAGAAUUCAAAAUCCUtt | AGGAUUUUGAAUUCUAUGGtg |
| BCL2-like 14 (apoptosis facilitator) | AAGAGAUUUUUGUAACUGAtt | UCAGUUACAAAAAUCUCUUtg |
| small integral membrane protein 21 | GCAUAUUUCGAAACUUUCUtt | AGAAAGUUUCGAAAUAUGCtg |
| small integral membrane protein 21 | GCUGGGAACAUUUAAACAAtt | UUGUUUAAAUGUUCCCAGCtg |
| small integral membrane protein 21 | CACCAUAUUCGUUUCUUCAtt | UGAAGAAACGAAUAUGGUGtt |
| chromosome 8 open reading frame 44 | CAGAUGUACCGAGUUUGAAtt | UUCAAACUCGGUACAUCUGgt |
| chromosome 8 open reading frame 44 | CCGAGUUUGAAAUCCCAGAtt | UCUGGGAUUUCAAACUCGGta |
| chromosome 8 open reading frame 44 | GUAUUAGAAUUAUUUCUGAtt | UCAGAAAUAAUUCUAAUACct |
| C-type lectin domain family 2, member B | GAAUUUUCUUAGGCGGUAUtt | AUACCGCCUAAGAAAAUUCat |

| | | |
|---|---|---|
| C-type lectin domain family 2, member B | AUACAACUGUUCCACUCAAtt | UUGAGUGGAACAGUUGUAUtt |
| C-type lectin domain family 2, member B | CAGCAACAGCUAGAUGUUAtt | UAACAUCUAGCUGUUGCUGca |
| chloride intracellular channel 1 | GGUUUUAGACAAUUACUUAtt | UAAGUAAUUGUCUAAAACCtt |
| chloride intracellular channel 1 | CAGCUGGGCUGGACAUAUUtt | AAUAUGUCCAGCCCAGCUGtg |
| chloride intracellular channel 1 | GUUUUAGACAAUUACUUAAtt | UUAAGUAAUUGUCUAAAACct |
| cAMP responsive element binding protein 3 | CUGUCUCUAUGGAUCUAGAtt | UCUAGAUCCAUAGAGACAGtt |
| cAMP responsive element binding protein 3 | GGCUAGUACUGACAGAUGAtt | UCAUCUGUCAGUACUAGCCta |
| cAMP responsive element binding protein 3 | GAGUGAGAGCUGUAGAAAAtt | UUUUCUACAGCUCUCACUCtc |
| chondroitin sulfate N-acetylgalactosaminyltransferase 2 | GGUCAUUAAUAAUCCUGAUtt | AUCAGGAUUAUUAAUGACCtc |
| chondroitin sulfate N-acetylgalactosaminyltransferase 2 | CUAGUGAUCUUUUAGAGUUtt | AACUCUAAAAGAUCACUAGgt |
| chondroitin sulfate N-acetylgalactosaminyltransferase 2 | GGACCUCUCAUGAAAGUGAtt | UCACUUUCAUGAGAGGUCCaa |
| SLIT and NTRK-like family, member 2 | CCAGUAGCCUAUUACCGAAtt | UUCGGUAAUAGGCUACUGGgt |
| SLIT and NTRK-like family, member 2 | GGAACCGUCUUGUCAAUGAtt | UCAUUGACAAGACGGUUCCat |
| SLIT and NTRK-like family, member 2 | GACUGUAUCCAAACGAAUUtt | AAUUCGUUUGGAUACAGUCtt |
| decorin | GCUGGACCGUUUCAACAGAtt | UCUGUUGAAACGGUCCAGCcc |
| decorin | AGAGGCUUAUUUGACUUUAtt | UAAAGUCAAAUAAGCCUCUct |
| decorin | GCUAGAUACUGGAAACCUAtt | UAGGUUUCCAGUAUCUAGCtt |
| eukaryotic translation initiation factor 2C, 3 | GAAGAGACAUCACACUCGAtt | UCGAGUGUGAUGUCUCUUCtg |
| eukaryotic translation initiation factor 2C, 3 | CAGUCGUCCUUCACACUAUtt | AUAGUGUGAAGGACGACUGgt |
| eukaryotic translation initiation factor 2C, 3 | CCAUAUGAGUUCGAUUUUUtt | AAAAAUCGAACUCAUAUGGgt |
| group-specific component (vitamin D binding protein) | GCUUAAACAUUUAUCACUUtt | AAGUGAUAAAUGUUUAAGCtg |
| group-specific component (vitamin D binding protein) | CUACCUGUUUUAAUGCUAAtt | UUAGCAUUAAAACAGGUAGtt |
| group-specific component (vitamin D binding protein) | GAUCCAAAGGAAUAUGCUAtt | UAGCAUAUUCCUUUGGAUCtt |
| glutaredoxin (thioltransferase) | CAACCACACUAACGAGAUUtt | AAUCUCGUUAGUGUGGUUGgt |
| glutaredoxin (thioltransferase) | GCAGUGAUCUAGUCUCUUUtt | AAAGAGACUAGAUCACUGCat |
| glutaredoxin (thioltransferase) | GAGUCUUUAUUGGUAAAGAtt | UCUUUACCAAUAAAGACUCga |

| | | |
|---|---|---|
| GC-rich promoter binding protein 1 | GCAUGGACAGAGAAUCGUUtt | AACGAUUCUCUGUCCAUGCaa |
| GC-rich promoter binding protein 1 | GGAAGUUCCCGUUCUCGUAtt | UACGAGAACGGGAACUUCCac |
| GC-rich promoter binding protein 1 | GAAAGGGAUAUAAACCGAAtt | UUCGGUUUAUAUCCCUUUCtt |
| histone cluster 1, H3a | CUGAACUGCUUAUUCGUAAtt | UUACGAAUAAGCAGUUCAGtg |
| histone cluster 1, H3a | GUAGGGCUAUUUGAGGACAtt | UGUCCUCAAAUAGCCCUACca |
| histone cluster 1, H3a | GCAAACAGUUGGCCACUAAtt | UUAGUGGCCAACUGUUUGCgt |
| IMP2 inner mitochondrial membrane peptidase-like (S. cerevisiae) | GUGGUGACAUUGUAUCAUUtt | AAUGAUACAAUGUCACCACgg |
| IMP2 inner mitochondrial membrane peptidase-like (S. cerevisiae) | GGGUUGAAGGUGAUCAUCAtt | UGAUGAUCACCUUCAACCCag |
| IMP2 inner mitochondrial membrane peptidase-like (S. cerevisiae) | AGAGAGUGAUUGCUCUUGAtt | UCAAGAGCAAUCACUCUCUta |
| leucine-rich repeats and IQ motif containing 1 | GGUCUUUGUGAUACACCUAtt | UAGGUGUAUCACAAAGACCtt |
| leucine-rich repeats and IQ motif containing 1 | CAGCUUGACUAAAAUCGUAtt | UACGAUUUUAGUCAAGCUGtt |
| leucine-rich repeats and IQ motif containing 1 | CUACCAUUGUAUACCUAGAtt | UCUAGGUAUACAAUGGUAGgt |
| N-acetyltransferase 8 (GCN5-related, putative) | CAGUCUUUUUGAUUCCCAUtt | AUGGGAAUCAAAAAGACUGaa |
| N-acetyltransferase 8 (GCN5-related, putative) | GCUUAUUGUCCAUUCACAUtt | AUGUGAAUGGACAAUAAGCtt |
| N-acetyltransferase 8 (GCN5-related, putative) | CAACCUUUCACUGCAAUGAtt | UCAUUGCAGUGAAAGGUUGgg |
| nurim (nuclear envelope membrane protein) | CCUUCUCGUCUUUGACUAUtt | AUAGUCAAAGACGAGAAGGat |
| nurim (nuclear envelope membrane protein) | CGGGCCCAGCUACAAAGAAtt | UUCUUUGUAGCUGGGCCCGga |
| nurim (nuclear envelope membrane protein) | GCCUCAAACAGGUAUACUAtt | UAGUAUACCUGUUUGAGGCcc |
| phosphatidylinositol glycan anchor biosynthesis, class K | GGACAUCGCACUGAUCUUUtt | AAAGAUCAGUGCGAUGUCCag |
| phosphatidylinositol glycan anchor biosynthesis, class K | GGCUCUAGCUAGUAGUCAAtt | UUGACUACUAGCUAGAGCCat |
| phosphatidylinositol glycan anchor biosynthesis, class K | CCAACAUAGAACUCGCGGAtt | UCCGCGAGUUCUAUGUUGGta |
| psoriasis susceptibility 1 candidate 1 | AGAAGUAACAUGUCCAAAAtt | UUUUGGACAUGUUACUUCUga |
| psoriasis susceptibility 1 candidate 1 | UCCAAGCAAUGAUAUCCAAtt | UUGGAUAUCAUUGCUUGGAgg |

| | | |
|---|---|---|
| psoriasis susceptibility 1 candidate 1 | GCAAUGAUAUCCAAGGAAUtt | AUUCCUUGGAUAUCAUUGCtt |
| phosphatidylserine synthase 1 | GGAUGAUGUGAACUACAAAtt | UUUGUAGUUCACAUCAUCCtt |
| phosphatidylserine synthase 1 | GAGUGUACCUUUUCAUGAUtt | AUCAUGAAAAGGUACACUCca |
| phosphatidylserine synthase 1 | CCAUCGUCAGCCUCAUGUAtt | UACAUGAGGCUGACGAUGGtg |
| RAB1B, member RAS oncogene family | GCUGAAAUCAAAAAGCGGAtt | UCCGCUUUUUGAUUUCAGCag |
| RAB1B, member RAS oncogene family | GCACCAGCCUUAACCCUCAtt | UGAGGGUUAAGGCUGGUGCcc |
| RAB1B, member RAS oncogene family | AGAGCGACCUCACCACCAAtt | UUGGUGGUGAGGUCGCUCUtg |
| SET domain containing (lysine methyltransferase) 7 | GGACCGCACUUUAUGGGAAtt | UUCCCAUAAAGUGCGGUCCtc |
| SET domain containing (lysine methyltransferase) 7 | GCACGUAUGUAGACGGAGAtt | UCUCCGUCUACAUACGUGCcc |
| SET domain containing (lysine methyltransferase) 7 | CCUGGACGAUGACGGAUUAtt | UAAUCCGUCAUCGUCCAGGtg |
| solute carrier family 35, member B3 | CCUACAUGAUAAUAGCUUUtt | AAAGCUAUUAUCAUGUAGGtt |
| solute carrier family 35, member B3 | CUGUAUGAUUUGAUAAACAtt | UGUUUAUCAAAUCAUACAGtg |
| solute carrier family 35, member B3 | GGACCUAUGGUUAUGCGUUtt | AACGCAUAACCAUAGGUCCga |
| ST3 beta-galactoside alpha-2,3-sialyltransferase 4 | GCAGACCAUUCACUACUAUtt | AUAGUAGUGAAUGGUCUGCtt |
| ST3 beta-galactoside alpha-2,3-sialyltransferase 4 | UCUGGGAUGUCAAUCCUAAtt | UUAGGAUUGACAUCCCAGAtg |
| ST3 beta-galactoside alpha-2,3-sialyltransferase 4 | GGAAGACAGUUUUUAUUUUtt | AAAAUAAAAACUGUCUUCCcg |
| TRAF family member-associated NFKB activator | CACUCAAGAUAACAAUUAUtt | AUAAUUGUUAUCUUGAGUGga |
| TRAF family member-associated NFKB activator | GAACUAUGAGCAGAGAAUAtt | UAUUCUCUGCUCAUAGUUCtc |
| TRAF family member-associated NFKB activator | GAGAUUCUGCAGUAAAAGAtt | UCUUUUACUGCAGAAUCUCta |
| transmembrane protease, serine 6 | GGAACUUACUACAACUCCAtt | UGGAGUUGUAGUAAGUUCCca |
| transmembrane protease, serine 6 | GCCUGUGAAGUGAACCUGAtt | UCAGGUUCACUUCACAGGCct |
| transmembrane protease, serine 6 | GCUGACCGCUGGGUGAUAAtt | UUAUCACCCAGCGGUCAGCga |
| zona pellucida glycoprotein 1 (sperm receptor) | CAGUCUUCUCGGCCGAUUAtt | UAAUCGGCCGAGAAGACUGca |
| zona pellucida glycoprotein 1 (sperm receptor) | ACACUGGGAUGUGAACAAAtt | UUUGUUCACAUCCCAGUGUtc |
| zona pellucida glycoprotein 1 (sperm receptor) | CACCCACUGUGGAACCACAtt | UGUGGUUCCACAGUGGGUGag |

### 2.12. Animals

All animal experiments were conducted under the guidelines of the Animal Care Committee (ACC) at the University of Ottawa in Ottawa, Ontario, Canada. Severe combined immunodeficient 6−8-week-old male mice were employed for the *in vivo* studies. Mice were maintained in regular pathogen-free housing conditions with standard access to food and drink.

### 2.13. Stereotaxic injections and bioluminescent imaging

Stereotaxic surgeries were conducted by injecting ~$3x10^5$ luciferase expressing CLIC1-CRISPR-BTSCs and control BTSCs into the right striata (0.8 mm lateral to the bregma, 1 mm dorsal, and 2.5 mm from the pial surface). Prior to injection, BTSCs were dissociated into single-cell suspensions in serum-free, antibiotic-free medium and tested for luciferase activity using IVIS imaging system. Kaplan-Meier survival plots were generated by collecting mice at the point of reaching the end stage (major body weight loss, dehydration, haunched back, piloerection, and lethargy). Median survivals were calculated using a log-rank test with GraphPad Prism, following previously described methods[312]. Briefly, the Kaplan-Meier approach estimated the probability of survival at each time point. Before any time elapses, all mice were considered “at risk”, however, no deaths occurred. Therefore, the probability of survival was input as a value of 1. Subsequently, information about the next elapsed time (day 7) included information about the how many participants experienced the event of interest (death). From this information, a survival probability was calculated using the formula: $S_{t+1} = S_t*((N_{t+1}-D_{t+1})/N_{t+1})$, where $S_t$ represents survival probability, $N_t$ represents number at risk, $D_t$ represents number of events. The survival probability for each subsequent time point is calculated in a similar fashion and a stair-step survival curve is plotted. For tumour volume assessment, the mice received intraperitoneal injections of 200 µL of 15 mg/mL d-luciferin (Thermo Fisher Scientific, #88292), underwent anesthesia via isoflurane inhalation, and were then subjected to weekly bioluminescence imaging using a CCD camera (IVIS, Xenogen). Subsequent collection and analysis of all bioluminescent data were performed utilizing IVIS software. Briefly, after initialization of the IVIS Spectrum system and acquiring an image, the images were analyzed using “ROI tools” in the tool palette. The ROI is selected which covers the area of interest. The IVIS imager captures pixels with specific photon intensity values, with brighter areas corresponding to higher photon detection, indicative of tumour induction.

## 2.14. Electrophysiology

Patch-clamp electrophysiology analyses were performed in a perforated-patch whole-cell configuration as previously described[250]. Briefly, the voltage protocol consisted of 800ms pulses from −60 mV to +60 mV (20 mV voltage steps). The CLIC1-mediated currents were isolated from the cells' other ionic currents by perfusing the specific inhibitor IAA94 (100 µmol/L). Patch-clamp solutions[313] included the following: bath (mmol/L): 125 NaCl, 5.5 KCl, 24 HEPES, 1 $MgCl_2$, 0.5 CaCl2, 5 D-glucose, 10 NaOH, pH 7.4; pipette (mmol/L): 135 KCl, 10 HEPES, 10 NaCl, 1 $MgCl_2$, pH 7.2.

# 3. Results

## 3.1. CLIC1 forms a complex with OSMR in BTSCs in the presence and absence of EGFRvIII

To understand how OSMR promotes tumorigenesis in GB that either harbour EGFRvIII or lack this mutation, our laboratory had conducted MaMTH in HEK293T cells in order to map global binding partners of OSMR **(Figure 10)**. Analyses of MaMTH data led to identification of 29 candidates as high confidence OSMR binding partners in cells harbouring or lacking EGFRvIII. This cluster of proteins exhibited diverse cell functions such as metabolic processes, signalling, biogenesis, development, and immune system processes **(Figure 10)**. OSMR has been previously demonstrated to play a critical role in the proliferation, self-renewal, and tumorigenesis of BTSCs[20,314]. Thus, prior to detailed investigation of OSMR candidate binding partners in patient derived BTSCs, we conducted a counter screen in which we employed siRNA-targeting each of these 29 hits followed by assessing cell viability using PrestoBlue analysis **(Figure 11a)**. Four patient derived BTSC lines were used in this assay (BTSC12, BTSC30, BTSC73 and BTSC147). Among the candidate binding partners, 12 demonstrated a substantial reduction in cell viability exceeding 50% **(Figure 11b)**. Notably, these proteins encompassed CLEC2B, CLIC1, CREB3, CSGALNACT2, DCN, EIF2C3, GC, GPBP1, HISTH3A, IMMP2L, NAT8, and ST3GAL4. Among these proteins, CLEC2B, CLIC1, and GPBP1 are plasma membrane proteins. In particular, CLIC1 emerged as the sole protein implicated in BTSCs, exhibiting heightened expression and playing pivotal roles in both proliferation and self-renewal. Like OSMR[169], CLIC1 is highly active in BTSCs compared to wild type NSCs and its expression correlates with the MES subtype of GB[230]. In addition, high expression of CLIC1 is correlated with poor prognosis in patients with GB and other cancers[226,230]. Inhibitors of CLIC1, such as biguanide based molecules or Indanyloxyacetic Acid 94 (IAA94) can exert antiproliferative and antiinvasive effects in BTSCs in addition to decreasing their capacity for self-renewal[250,315]. We therefore set out to investigate how CLIC1 regulates BTSCs and whether it interacts with OSMR physically and functionally to promote GB.

**Figure 11. siRNA counter screen of 29 candidate binding proteins of OSMR/EGFRvIII**
(a) Heat map detailing the impact of siRNA knockdown on 29 candidate binding proteins associated with OSMR/EGFRvIII in four BTSC lines (BTSC12, BTSC30, BTSC73, and BTSC147). The colour gradient, represented by column Z-scores, illustrates relative cell viability measured through PrestoBlue analysis. Blue indicates negative values, while yellow indicates positive values.
(b) PrestoBlue cell viability normalized to the control group (non-targeting siRNA), highlighting proteins that result in over 50% reduction in viability when knocked down, denoted in red. Data are presented as means ± SEM, n=3 biological replicants.

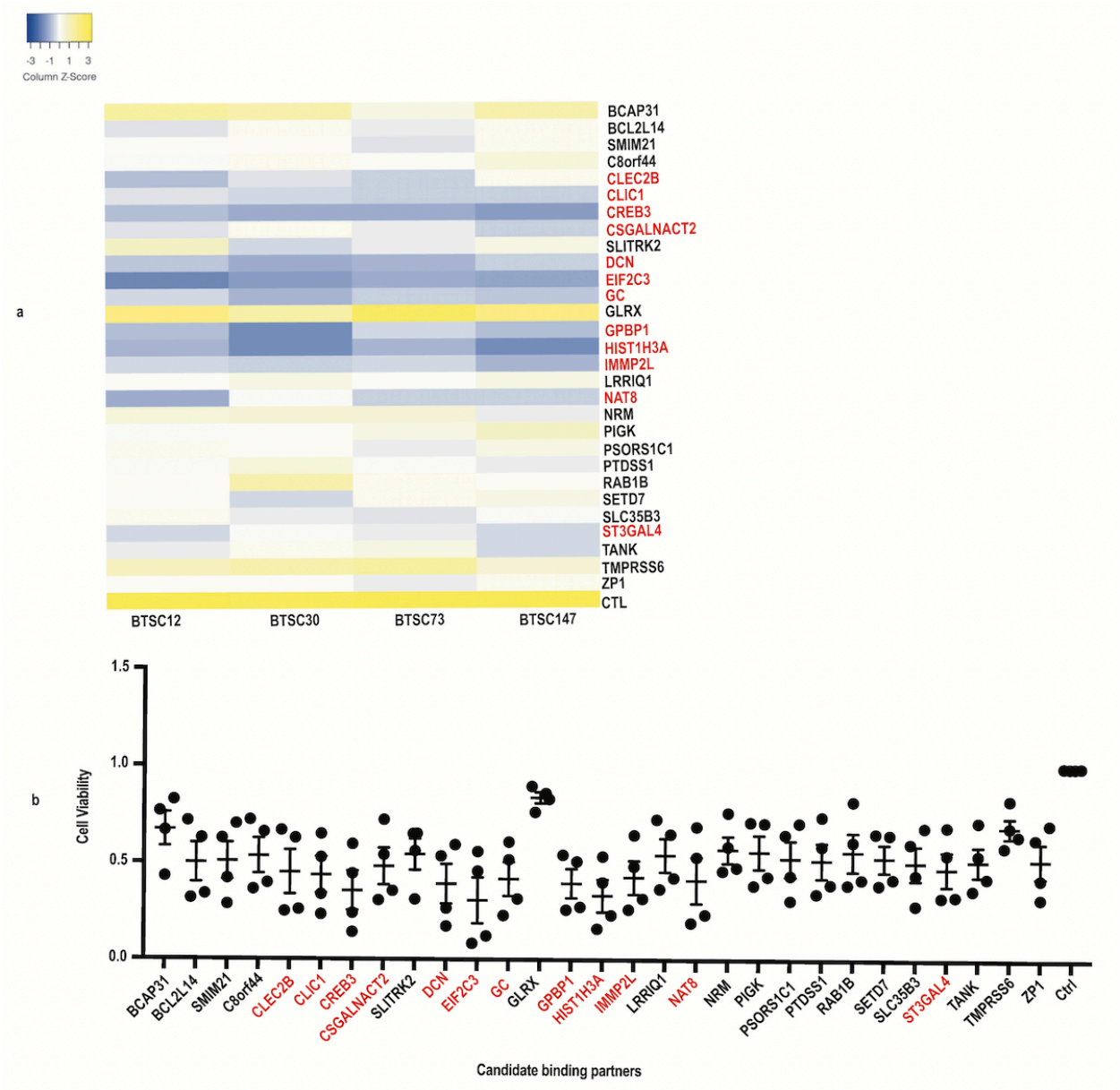
-3 -1 1 3
Column Z-Score
a
BCAP31
BCL2L14
SMIM21
C8orf44
CLEC2B
CLIC1
CREB3
CSGALNACT2
SLITRK2
DCN
EIF2C3
GC
GLRX
GPBP1
HIST1H3A
IMMP2L
LRRIQ1
NAT8
NRM
PIGK
PSORS1C1
PTDSS1
RAB1B
SETD7
SLC35B3
ST3GAL4
TANK
TMPRSS6
ZP1
CTL
BTSC12
BTSC30
BTSC73
BTSC147
b
Cell Viability
1.5
1.0
0.5
0.0
BCAP31
BCL2L14
SMIM21
C8orf44
CLEC2B
CLIC1
CREB3
CSGALNACT2
SLITRK2
DCN
EIF2C3
GC
GLRX
GPBP1
HIST1H3A
IMMP2L
LRRIQ1
NAT8
NRM
PIGK
PSORS1C1
PTDSS1
RAB1B
SETD7
SLC35B3
ST3GAL4
TANK
TMPRSS6
ZP1
Ctrl
Candidate binding partners

### 3.2. CLIC1 influences BTSC self-renewal

To begin with, we validated the results of siRNA counterscreen using a smartpool of 4 siRNA targeting CLIC1 and control non-targeting RNA (siCTL) in different BTSCs. Real-time qPCR was used to assess efficient knockdown of CLIC1 and GUSB was used as a housekeeping gene **(Figure 12a,d,g,j)**. Immunoblotting and densitometric analyses were performed to confirm knockdown of CLIC1 protein expression. Actin was used as loading control **(Figure 12b,e,h,k)**. BTSCs were plated for ELDA 1 day following electroporation. After confirming efficient knockdown of CLIC1, ELDA analysis was performed. In each of the four BTSC lines, siRNA mediated knockdown of CLIC1 significantly decreased self-renewal capacity and stem cell frequency **(Figure 12c,f,i,l)**. The results confirm that CLIC1 plays an important role in stemness of BTSCs regardless of their genetic background **(Table 5)**.

**Table 5. Mutational status of human BTSC lines**

| Line | Sex | Age | *EGFR* | *TP53* | *PTEN* | *IDH1* | *NF1* | CDK2A |
|---|---|---|---|---|---|---|---|---|
| BTSC12 | M | 59Y | wt | mut | mut | wt | NA | NA |
| BTSC30 | M | 67Y | wt | wt | mut | wt | NA | NA |
| BTSC73 | M | 52Y | vIII | mut | mut | wt | NA | homo del |
| BTSC147 | M | 55Y | vIII | mut | mut | wt | wt | homo del |

Mutant or wild-type status of genes frequently mutated in GB of 4 BTSC lines used in this study. vIII indicates EGFR variant III, an activating deletion characteristic of GBM, homo del indicates a homozygous deletion, NA – not available.

**Figure 12. Self-renewal capacity of BTSCs is attenuated upon CLIC1 knockdown**

(a,d,g,j) BTSC12, BTSC30, BTSC73, and BTSC147 cells were electroporated with siCLIC1 or siCTL. CLIC1 mRNA expression was evaluated by RT-qPCR. GUSB was used as a housekeeping gene. Data are presented as mean ± SD, n=3 biological replicates. (b,e,h,k) BTSCs were subject to immunoblotting using antibodies indicated on the blots. Densitometric quantification of CLIC1 protein expression level is normalized to actin, n=3 biological replicates.
(c,f,i,l) BTSCs were subject to ELDA analysis 24 hours following electroporation with siCLIC1 or siCTL. Percent stem cell frequency (SCF %) in siRNA targeting CLIC1 or siCTL is also shown. Data are presented as the mean ± SD, n=3 biological replicates. Statistical analysis was performed using a student t-test. *$p < 0.05$, **$p < 0.01$, ***$p < 0.001$.

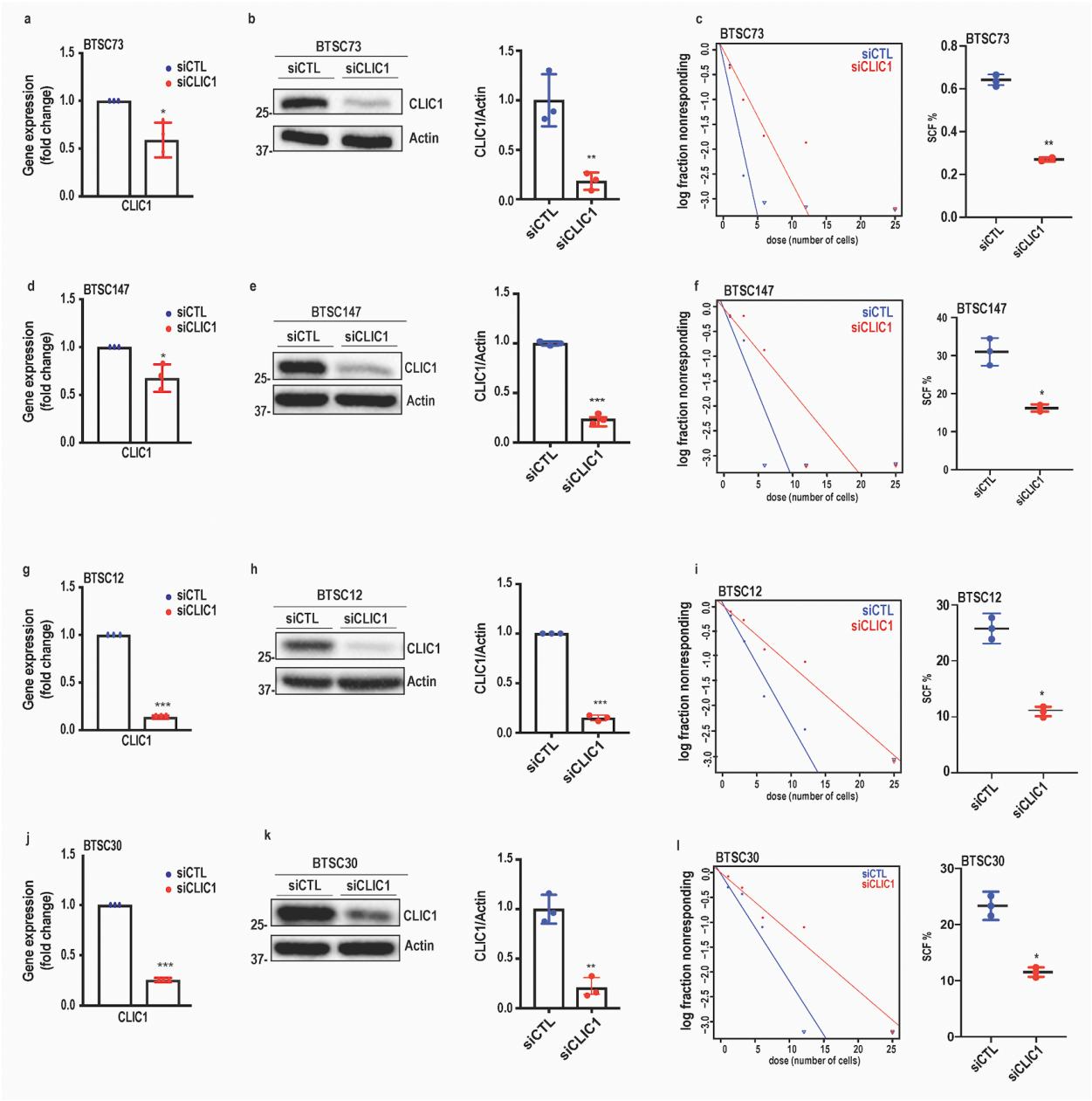
a
BTSC73
siCTL
siCLIC1
Gene expression (fold change)
CLIC1
b
BTSC73
siCTL
siCLIC1
CLIC1
Actin
25-
37-
CLIC1/Actin
c
BTSC73
siCTL
siCLIC1
log fraction nonresponding
dose (number of cells)
SCF %
d
BTSC147
e
BTSC147
f
BTSC147
g
BTSC12
h
BTSC12
i
BTSC12
j
BTSC30
k
BTSC30
l
BTSC30

### 3.3. CLIC1 colocalizes with both OSMR and EGFRvIII in BTSCs

Having established that CLIC1 regulates self-renewal of BTSCs, we set out to validate the MaMTH-HTS data. MaMTH-HTS analyses was performed in HEK293T cells which identified CLIC1 as a high-confidence binding partner of OSMR in the presence and absence of EGFRvIII. First, we performed colocalization analysis using primary antibodies against CLIC1 and OSMR in BTSC12, BTSC30, BTSC73, and BTSC147, demonstrating colocalization in all lines tested **(Figure 13a-d).** Next, we assessed the colocalization of CLIC1 and EGFRvIII in the EGFRvIII excessing cell lines, BTSC73 and BTSC147, which also demonstrated colocalization **(Figure 14a,b).** To ensure specificity of antibodies, each experiment was conducted with a primary antibody omitted control condition.

**Figure 13. Colocalization of CLIC1 and OSMR.**
(a-d) BTSCs were dissociated and plated for immunostaining with antibodies directed against CLIC1 and OSMR. Images in *Merged* shows representative panels of CLIC1 (green), colocalized with OSMR (red). One representative image is shown per BTSC line. Scale bar, 10μm. Each experiment was conducted with a primary antibody omitted control group, n=3 biological replicates.

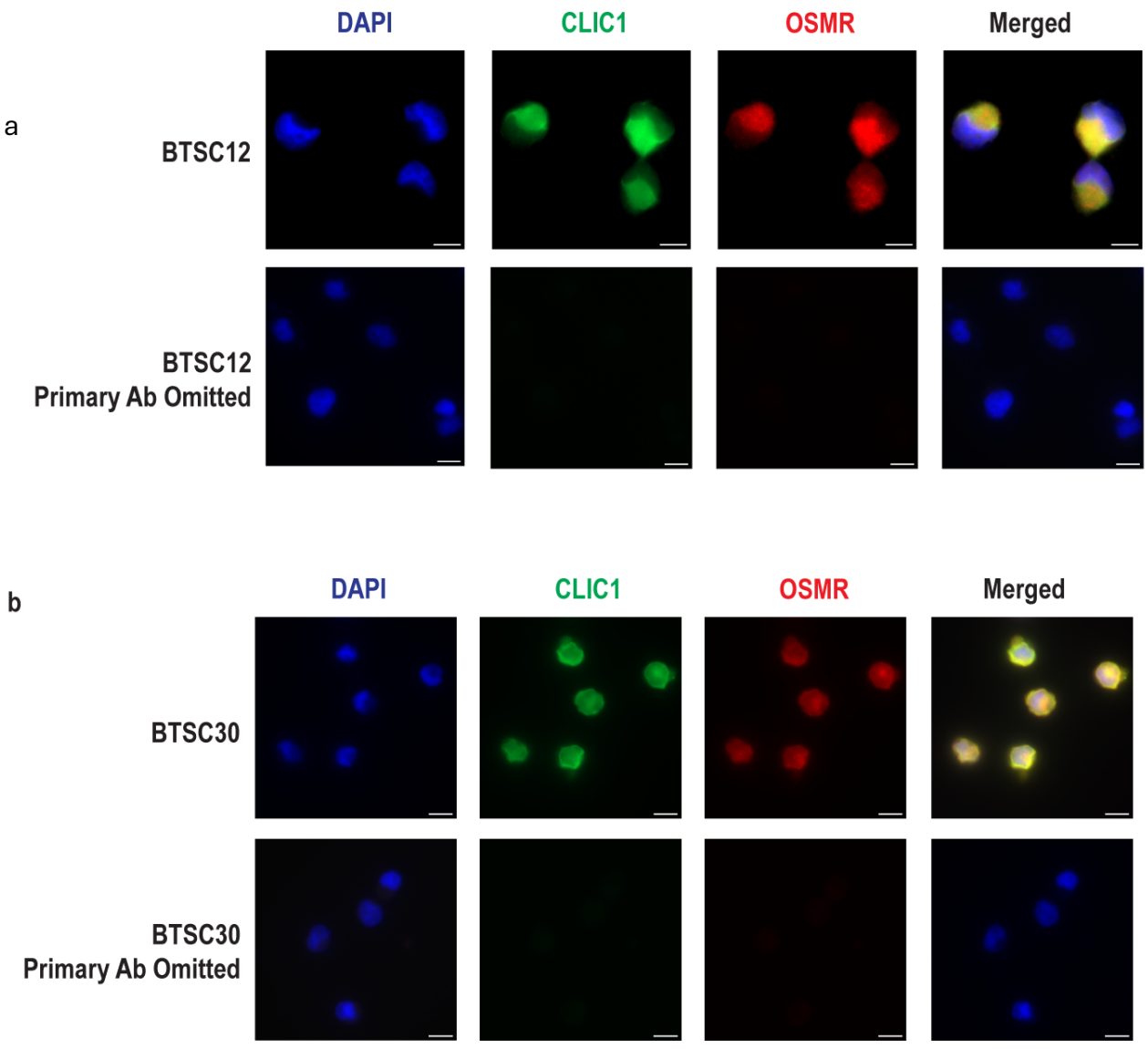
a
DAPI
CLIC1
OSMR
Merged
BTSC12
BTSC12
Primary Ab Omitted
b
DAPI
CLIC1
OSMR
Merged
BTSC30
BTSC30
Primary Ab Omitted

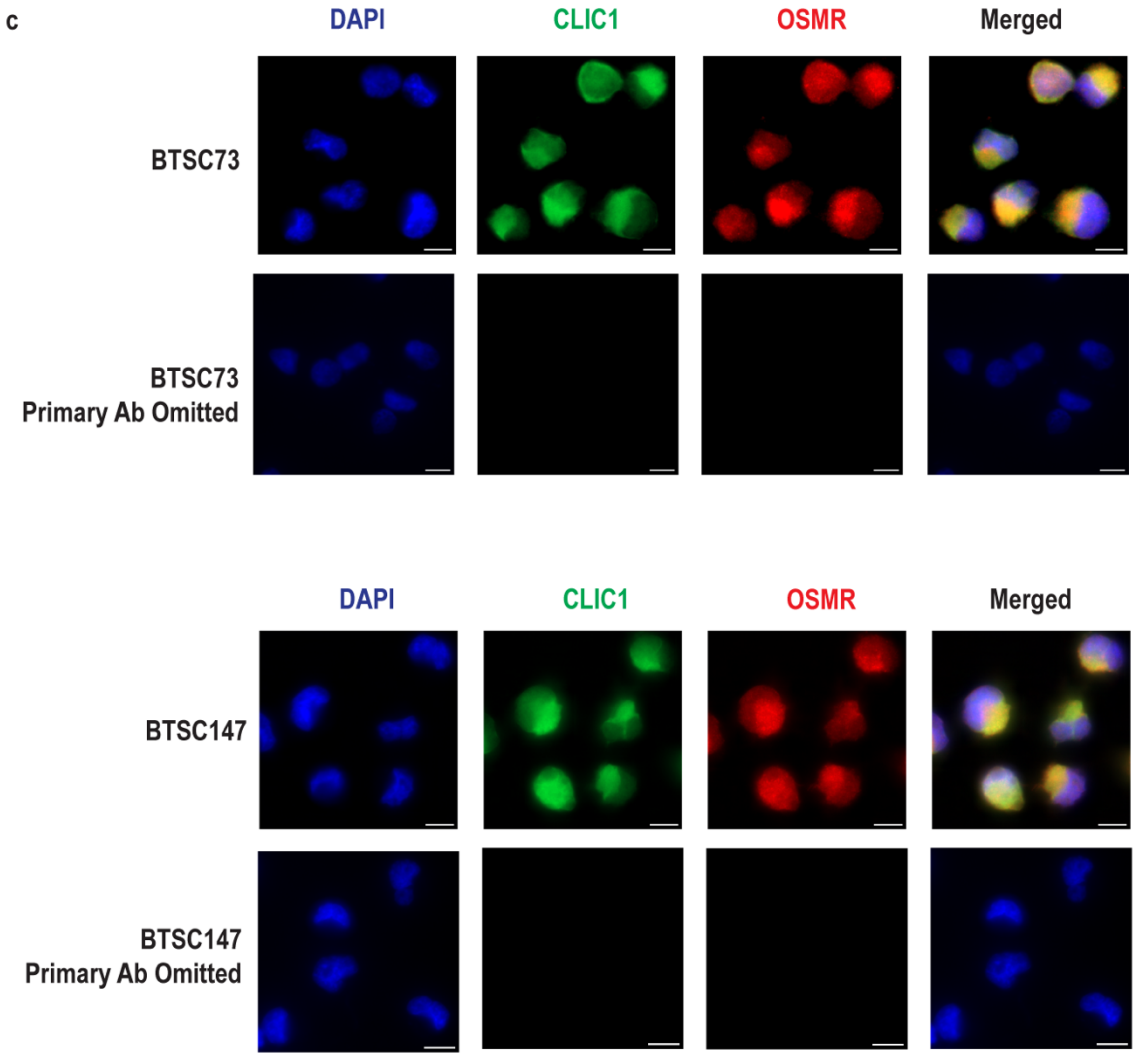
c
DAPI
CLIC1
OSMR
Merged
BTSC73
BTSC73
Primary Ab Omitted
d
DAPI
CLIC1
OSMR
Merged
BTSC147
BTSC147
Primary Ab Omitted

**Figure 14. Colocalization of CLIC1 and EGFRvIII**
(a,b) BTSCs were dissociated and plated for immunostaining with antibodies directed against CLIC1 and OSMR. Images in *Merged* shows representative panels of CLIC1 (green), colocalized with EGFRvIII (red). One representative image is shown per BTSC line. Scale bar, 10μm. Each experiment was conducted with a primary antibody omitted control group, n=3 biological replicates.

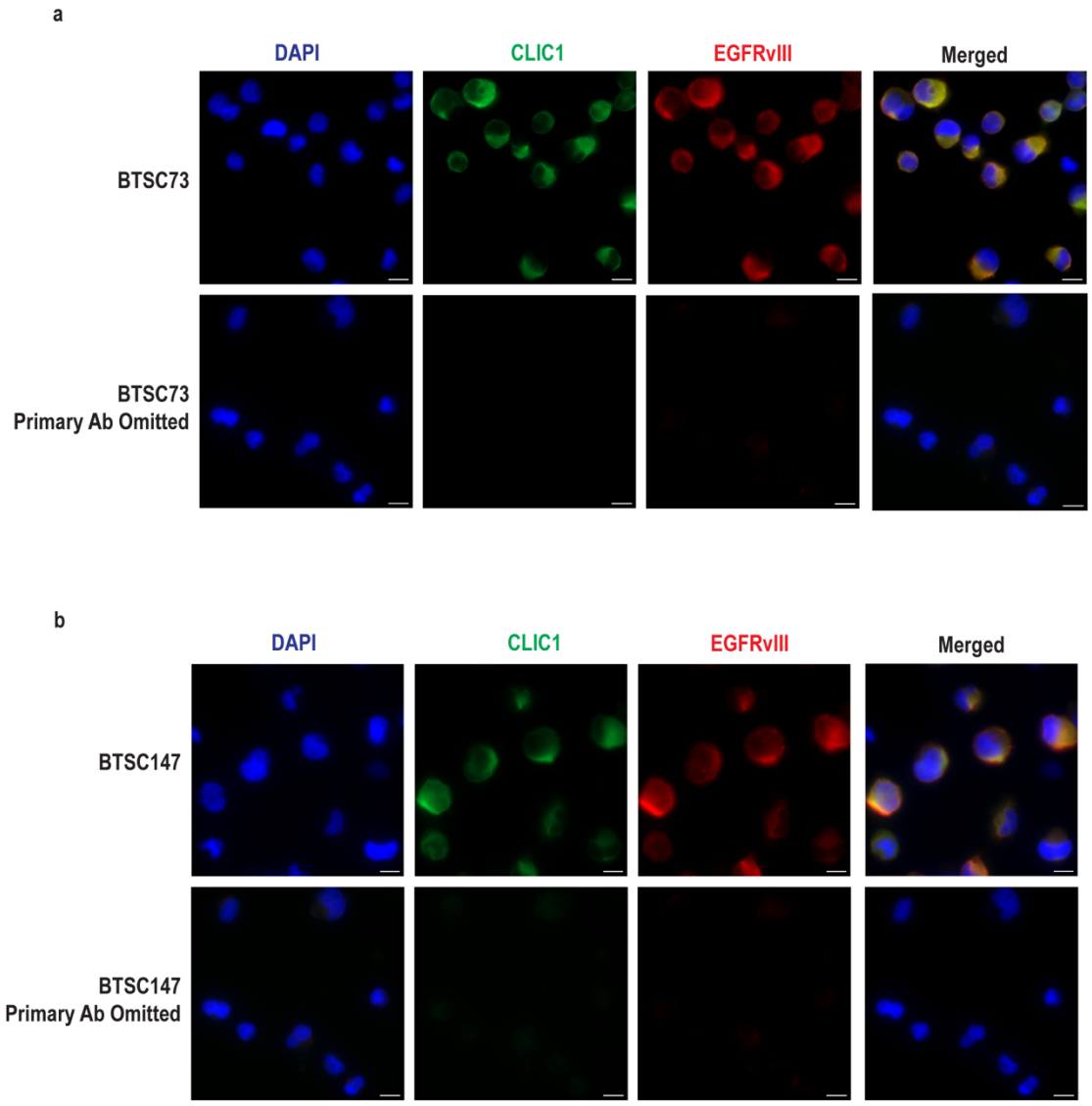
a
DAPI
CLIC1
EGFRvIII
Merged
BTSC73
BTSC73
Primary Ab Omitted
b
DAPI
CLIC1
EGFRvIII
Merged
BTSC147
BTSC147
Primary Ab Omitted

### 3.4. CLIC1 forms a complex with OSMR and OSMR/EGFRvIII

Our data revealing the colocalization of CLIC1 with OSMR and EGFRvIII suggests the hypothesis that these proteins may interacts physically. To address this hypothesis, we conducted a proximity ligation assay (PLA) which allows for in situ detection of endogenous protein-protein interactions if they are less than 40nm apart. We used OSMR and CLIC1 antibodies in two EGFRvIII expressing BTSC lines (BTSC73 and BTSC147). This assay established that CLIC1 endogenously interacts with OSMR across each BTSC line tested. Each interaction is represented by a red puncta that forms after oligonucleotide probes directed against the two proteins of interest (CLIC1 and OSMR) are ligated, amplified, and hybridized with fluorescent probes **(Figure 15a,b).** To ensure specificity of the interaction, the assay was conducted on a no primary antibody control. PLA results demonstrated a robust interaction between CLIC1 and OSMR.

We next generated transgenic BTSCs in which we introduced a genetic deletion in CLIC1 using CRISPR-Cas9 in two EGFRvIII expressing BTSC lines (BTSC73 and BTSC147). Genetic deletion was confirmed with RT-qPCR and western blotting **(Figure 16a-d).** Using trypan blue and ELDA, we confirmed that genetic deletion of CLIC1 impairs proliferation and self-renewal **(Figure 17).** To confirm the specificity of the in situ interaction, in parallel we conducted a PLA on CTL-BTSCs and CLIC1-CRISPR-BTSCs and observed a complete reduction of the PLA signal. Primary antibodies were first directed against CLIC1 and OSMR **(Figure 18a).** Next, were looked at the interaction between CLIC1 and P-EGFR and noted a robust interaction. **(Figure 18c)**. The plugin Stardist on Fiji, a puncta detection method, was used to count the number of PLA interactions **(Figure 18b,d).**

**Figure 15. CLIC1 interacts with OSMR endogenously**
(a-b) PLA of CLIC1 and OSMR performed in BTSC73 and BTSC147. Each red puncta represents an interaction between CLIC1 and OSMR. one representative image is shown. Assays were conducted with a primary antibody omitted control group. Nuclei were stained with DAPI. Scale bar, 10μm.

a

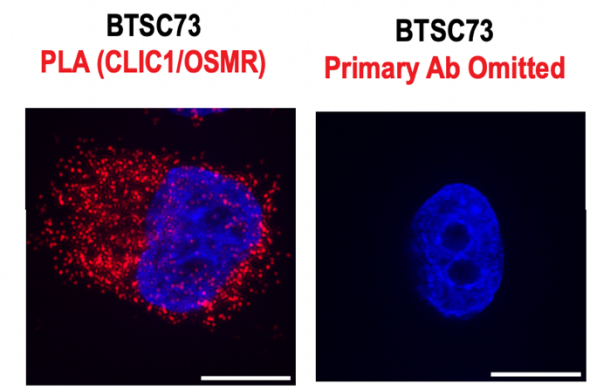
BTSC73
PLA (CLIC1/OSMR)
BTSC73
Primary Ab Omitted

b

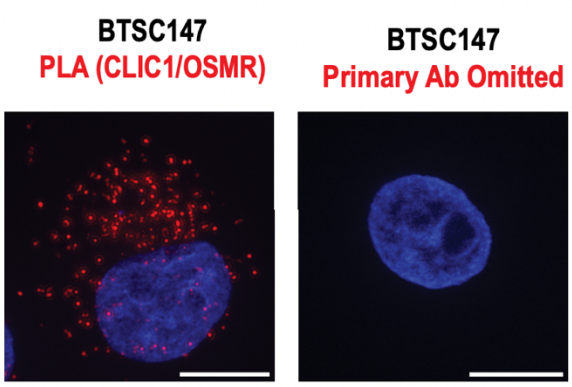
BTSC147
PLA (CLIC1/OSMR)
BTSC147
Primary Ab Omitted

**Figure 16. Validation of transgenic BTSCs using CRISPR-Cas9**
(a,c) CLIC1 mRNA levels assessed via RT-qPCR across CTL BTSCs (BTSC73 and BTSC147*)* and CLIC1-CRISPR-BTSCs (CRISPR-a, and CRISPR-b).
(b,d) Western blot analysis comparing CLIC1 protein levels across CTL BTSCs, CRISPR-a, and CRISPR-b.

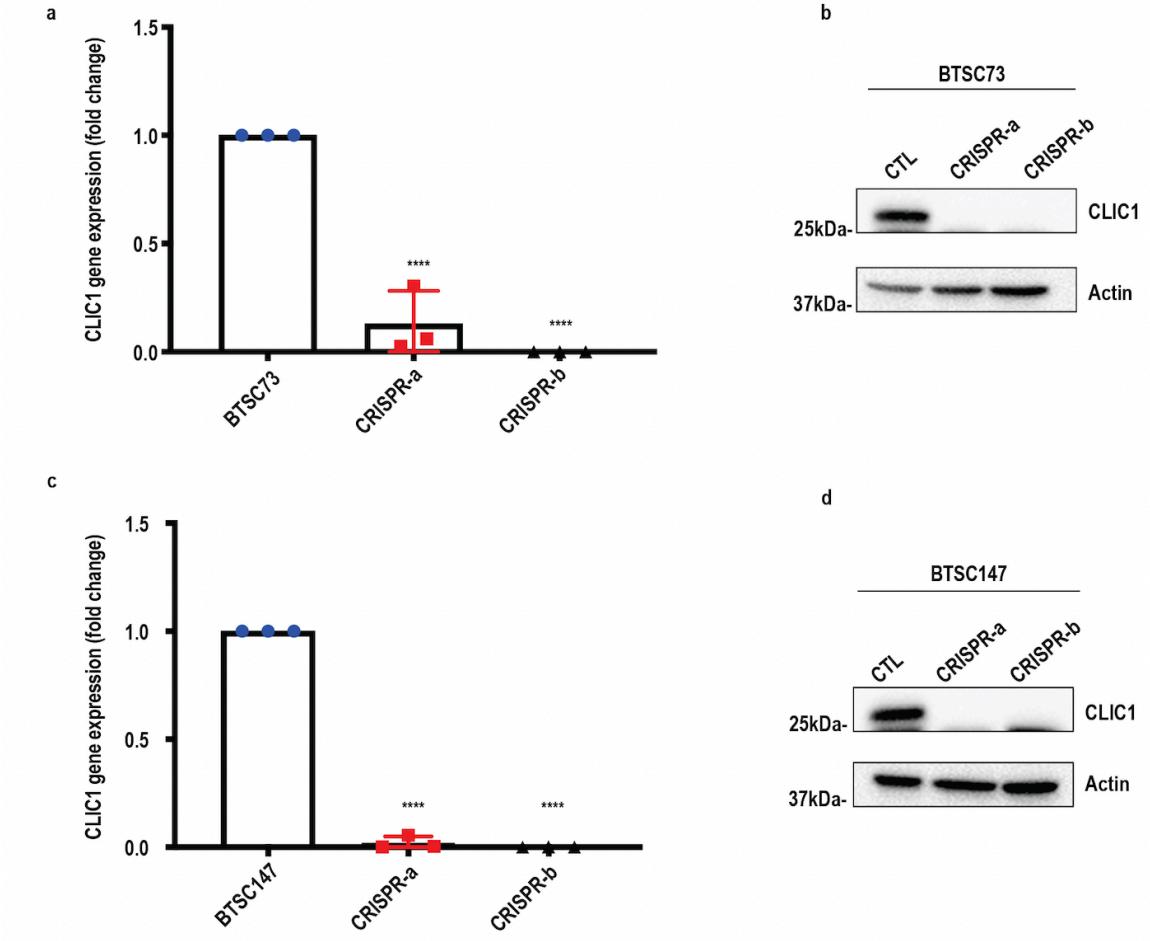
a
CLIC1 gene expression (fold change)
1.5
1.0
0.5
0.0
****
****
BTSC73
CRISPR-a
CRISPR-b
b
BTSC73
CTL
CRISPR-a
CRISPR-b
25kDa-
CLIC1
37kDa-
Actin
c
CLIC1 gene expression (fold change)
1.5
1.0
0.5
0.0
****
****
BTSC147
CRISPR-a
CRISPR-b
d
BTSC147
CTL
CRISPR-a
CRISPR-b
25kDa-
CLIC1
37kDa-
Actin

**Figure 17. Genetic deletion of CLIC1 impairs proliferative and self-renewal capacity**

(a) Proliferation ability plotted based on the number of viable cells counted using trypan blue exclusion dye. Data are presented as mean ± SD, n=3 biological replicates.
(b) Proliferation capability plotted as fold change based on the initial count on day 1 for each condition. Data are presented as mean ± SD, n=3 biological replicates.
(c) Cells were subject to extreme limiting dilution assay.
(d) (SCF %) in control BTSC73 and CRISPR-a and CRISPR-b. Data are presented as mean ± SD. Statistical analysis was performed using a student's t test. *$p < 0.05$, **$p < 0.01$, ***$p < 0.001$, n = 3 biological replicates.

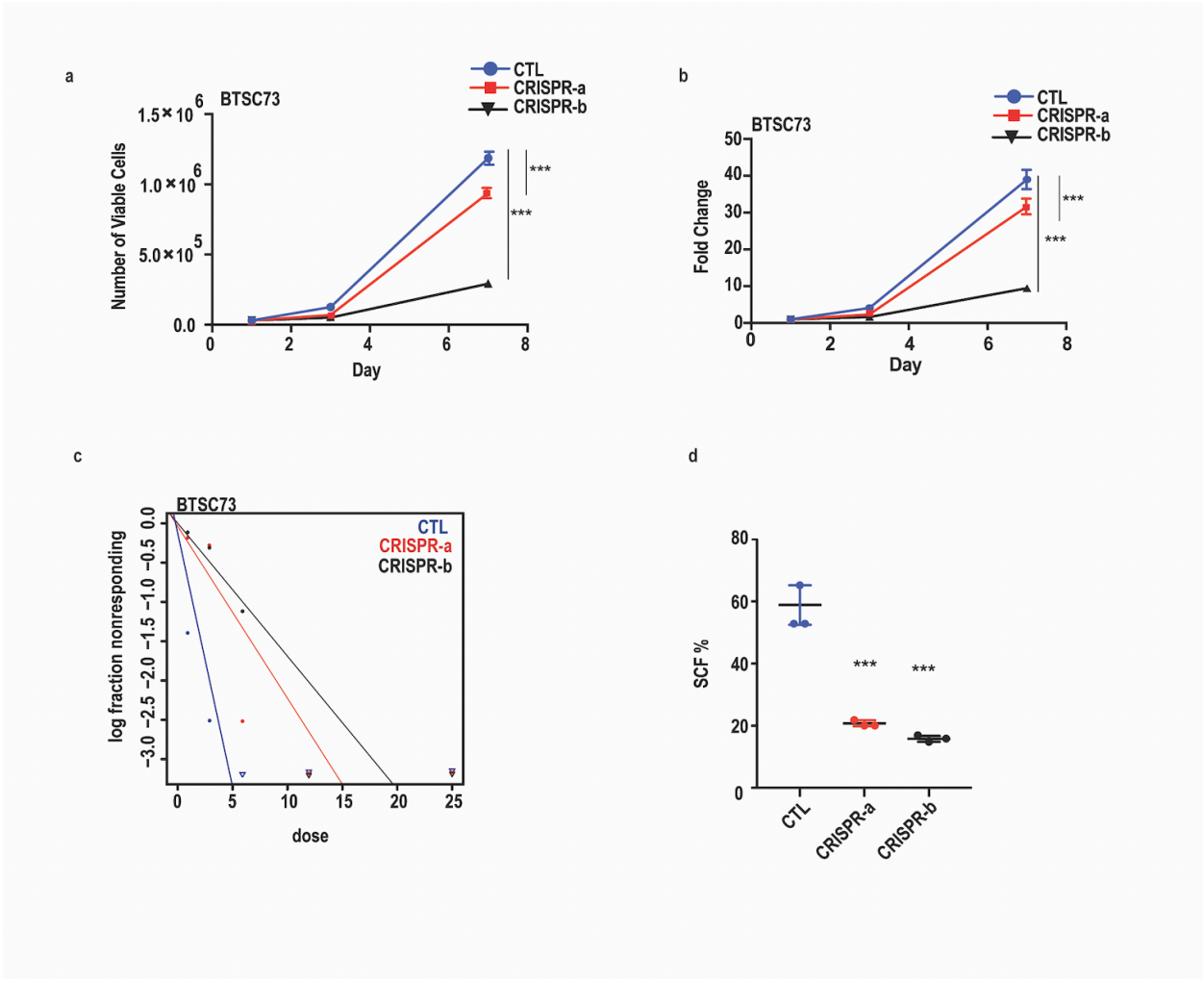
a
BTSC73
CTL
CRISPR-a
CRISPR-b
Number of Viable Cells
1.5×10^6
1.0×10^6
5.0×10^5
0.0
0
2
4
6
8
Day
***
***
b
BTSC73
CTL
CRISPR-a
CRISPR-b
Fold Change
50
40
30
20
10
0
0
2
4
6
8
Day
***
***
c
BTSC73
CTL
CRISPR-a
CRISPR-b
log fraction nonresponding
0.0
−0.5
−1.0
−1.5
−2.0
−2.5
−3.0
0
5
10
15
20
25
dose
d
SCF %
80
60
40
20
0
***
***
CTL
CRISPR-a
CRISPR-b

**Figure 18. CLIC1 interacts with OSMR and P-EGFR**
(a) PLA of CLIC1 and OSMR performed in BTSC147. PLA in CLIC1 CRISPR-b was used as a negative control. Primary antibodies were omitted for additional controls. Nuclei were stained with DAPI. Scale bar, 10μm. The number of PLA puncta per nucleus was determined based on BTSC147WT and CLIC1 CRISPR-b.
(b,d) Stardist plugin in Fiji was used to quantify the number of PLA puncta per nucleus. Statistical analysis was performed using a student's t test. *$p < 0.05$, **$p < 0.01$, ***$p < 0.001$.
(c) PLA of CLIC1 and P-EGFR performed in BTSC147. PLA in CLIC1 CRISPR-b clone was used as a negative control. Primary antibodies were omitted for additional controls. Nuclei were stained with DAPI. Scale bar, 10μm. The number of PLA puncta per nucleus was determined based on BTSC147WT and CLIC1 CRISPR-b lines.

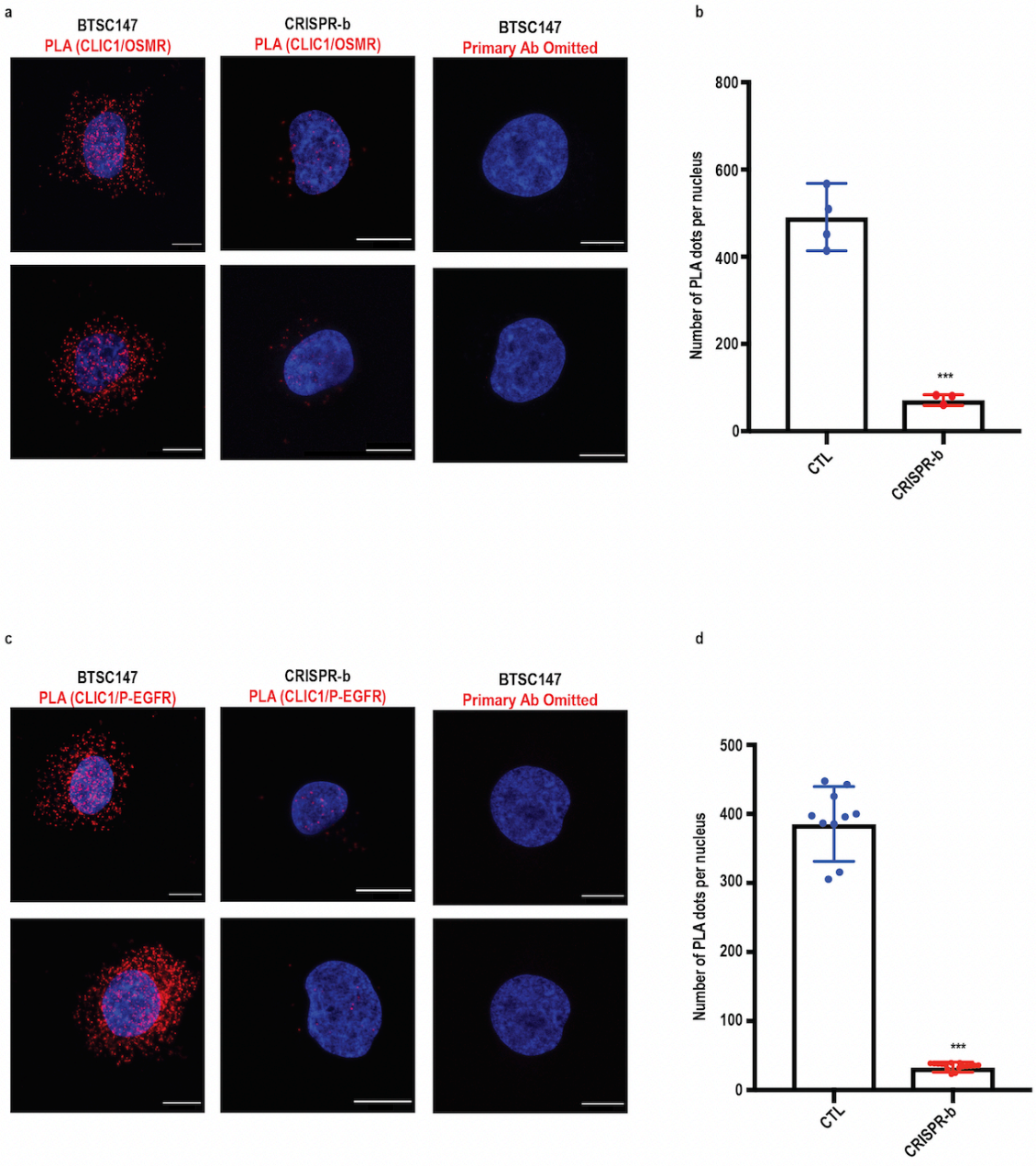
a
BTSC147
PLA (CLIC1/OSMR)
CRISPR-b
PLA (CLIC1/OSMR)
BTSC147
Primary Ab Omitted
b
Number of PLA dots per nucleus
800
600
400
200
0
***
CTL
CRISPR-b
c
BTSC147
PLA (CLIC1/P-EGFR)
CRISPR-b
PLA (CLIC1/P-EGFR)
BTSC147
Primary Ab Omitted
d
Number of PLA dots per nucleus
500
400
300
200
100
0
***
CTL
CRISPR-b

### 3.5. Genetic deletion of CLIC1 impairs EGFRvIII levels and STAT3 phosphorylation in BTSCs and GB tumourigenesis

Our data revealing that CLIC1 interacts with OSMR in EGFRvIII expressing BTSCs raised the question whether CLIC1 is functionally required for maintaining oncogenic signalling mediated by the OSMR/EGFRvIII complex. OSMR orchestrates a feedforward mechanism with EGFRvIII-STAT3 by acting as a co-receptor for EGFRvIII or phosphorylated (active) wild-type EGFR in both human BTSCs and murine astrocytes. This leads to aberrant activation of STAT3. Concurrently, STAT3 binds to the OSMR promoter to upregulate its expression thus orchestrating a feed-forward mechanism in GB[20]. Interestingly, we found that genetically deleting CLIC1 significantly impairs phosphorylation of key oncogenic proteins, EGFRvIII and STAT3 in CLIC1-CRISPR-BTSCs **(Figure 19).** These results prompted us to examine if CLIC1 contributes to GB tumourigenesis. To answer this question, we performed stereotaxic intracranial injections of BTSC73 and BTSC147 along with their corresponding CLIC1-CRISPR-BTSC lines in 6-week old Severe Combined Immunodeficiency (SCID) mice. Mice receiving CLIC1-CRISPR-BTSCs or CTL-BTSCs were subjected to live imaging of luciferase activity in the brains which was performed using the In Vivo Imaging System (IVIS) to trace BTSCs and tumour volume **(Figure 20a,d).** At 7 days following surgery, mice receiving CTL BTSC73 formed malignant brain tumours and were at endpoints as assessed by major weight loss and neurological signs by day 20 **(Figure 20c).** Mice receive CRISPR-a were at endpoints at 26days, while mice receiving CRISPR-b survived until day 49 **(Figure 20c).** Furthermore, mice receiving CTL BTSC147 were at endpoints at 28 days while mice receiving either CRISPR-a or CRISPR-b are still alive **(Figure 20e).** Our data suggest that CLIC1 is required for EGFRvIII/STAT3 phosphorylation and GB tumourigenesis.

**Figure 19. Genetic deletion of CLIC attenuates STAT3 and EGFRvIII phosphorylation**
(a,c) BTSCs were subject to immunoblotting using P-STAT3 and total STAT3 antibodies Actin was used as a loading control.
(b,d)Densitometric quantification is normalized to total STAT3. Statistical analysis was performed using a student t-test. *p<0.05, **p<0.01, ***p<0.001, n=3 biological replicates.
(e,g) BTSCs were subject to immunoblotting using antibodies indicated on the blots Actin was used as a loading control.
Densitometric quantification is normalized to total actin and total EGFR. Statistical analysis was performed using a student t-test. *p<0.05, **p<0.01 ***p<0.001, n=3 biological replicates.

h

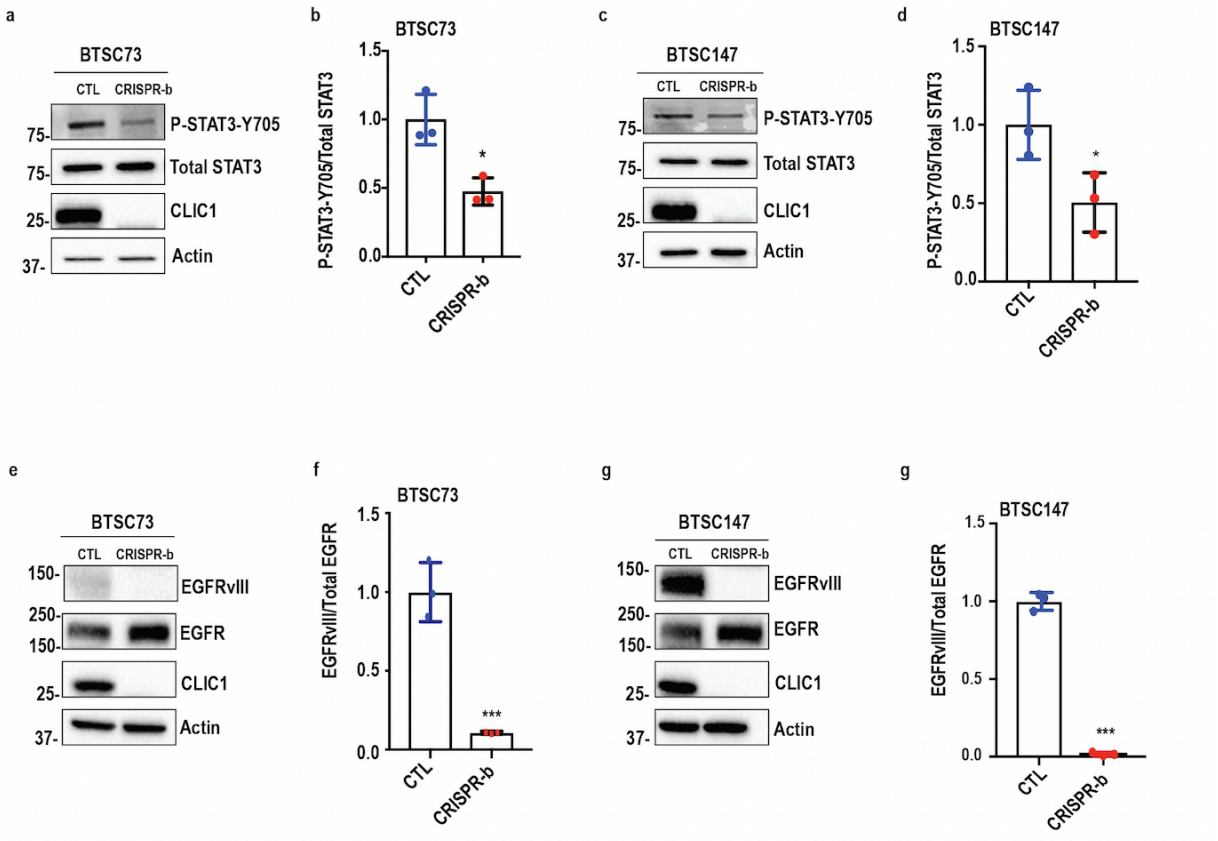
a
BTSC73
CTL
CRISPR-b
75-
P-STAT3-Y705
75-
Total STAT3
25-
CLIC1
37-
Actin
b
BTSC73
P-STAT3-Y705/Total STAT3
1.5
1.0
0.5
0.0
*
CTL
CRISPR-b
c
BTSC147
CTL
CRISPR-b
75-
P-STAT3-Y705
75-
Total STAT3
25-
CLIC1
37-
Actin
d
BTSC147
P-STAT3-Y705/Total STAT3
1.5
1.0
0.5
0.0
*
CTL
CRISPR-b
e
BTSC73
CTL
CRISPR-b
150-
EGFRvIII
250-
150-
EGFR
25-
CLIC1
37-
Actin
f
BTSC73
EGFRvIII/Total EGFR
1.5
1.0
0.5
0.0
***
CTL
CRISPR-b
g
BTSC147
CTL
CRISPR-b
150-
EGFRvIII
250-
150-
EGFR
25-
CLIC1
37-
Actin
g
BTSC147
EGFRvIII/Total EGFR
1.5
1.0
0.5
0.0
***
CTL
CRISPR-b

**Figure 20. CLIC1 regulates the ability of EGFRvIII-expressing human BTSCs to form tumors *in vivo***
(a,d) IVIS imaging of tumour size in SCID mice after intracranial injection of WT or CLIC1 CRISPR BTSCs (CRISPR-a and CRISPR-b).
(b,e) Quantification of IVIS signals.
(c,f) Kaplan-Meier survival plot was graphed to evaluate animal lifespan in each group.

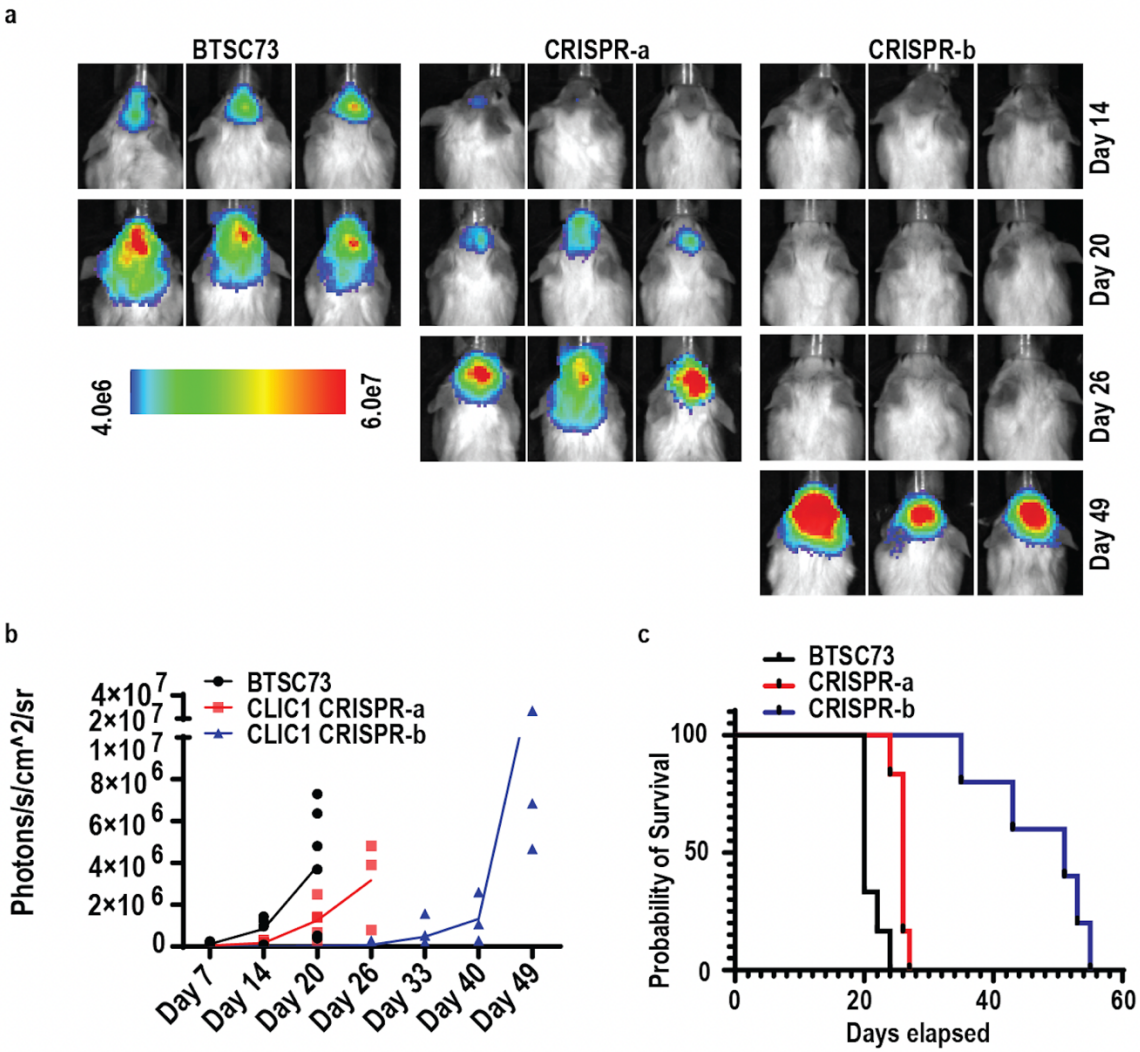
a
BTSC73
CRISPR-a
CRISPR-b
Day 14
Day 20
Day 26
Day 49
4.0e6
6.0e7
b
Photons/s/cm^2/sr
4×10^7
2×10^7
1×10^7
8×10^6
6×10^6
4×10^6
2×10^6
0
BTSC73
CLIC1 CRISPR-a
CLIC1 CRISPR-b
Day 7
Day 14
Day 20
Day 26
Day 33
Day 40
Day 49
c
BTSC73
CRISPR-a
CRISPR-b
Probability of Survival
100
50
0
0
20
40
60
Days elapsed

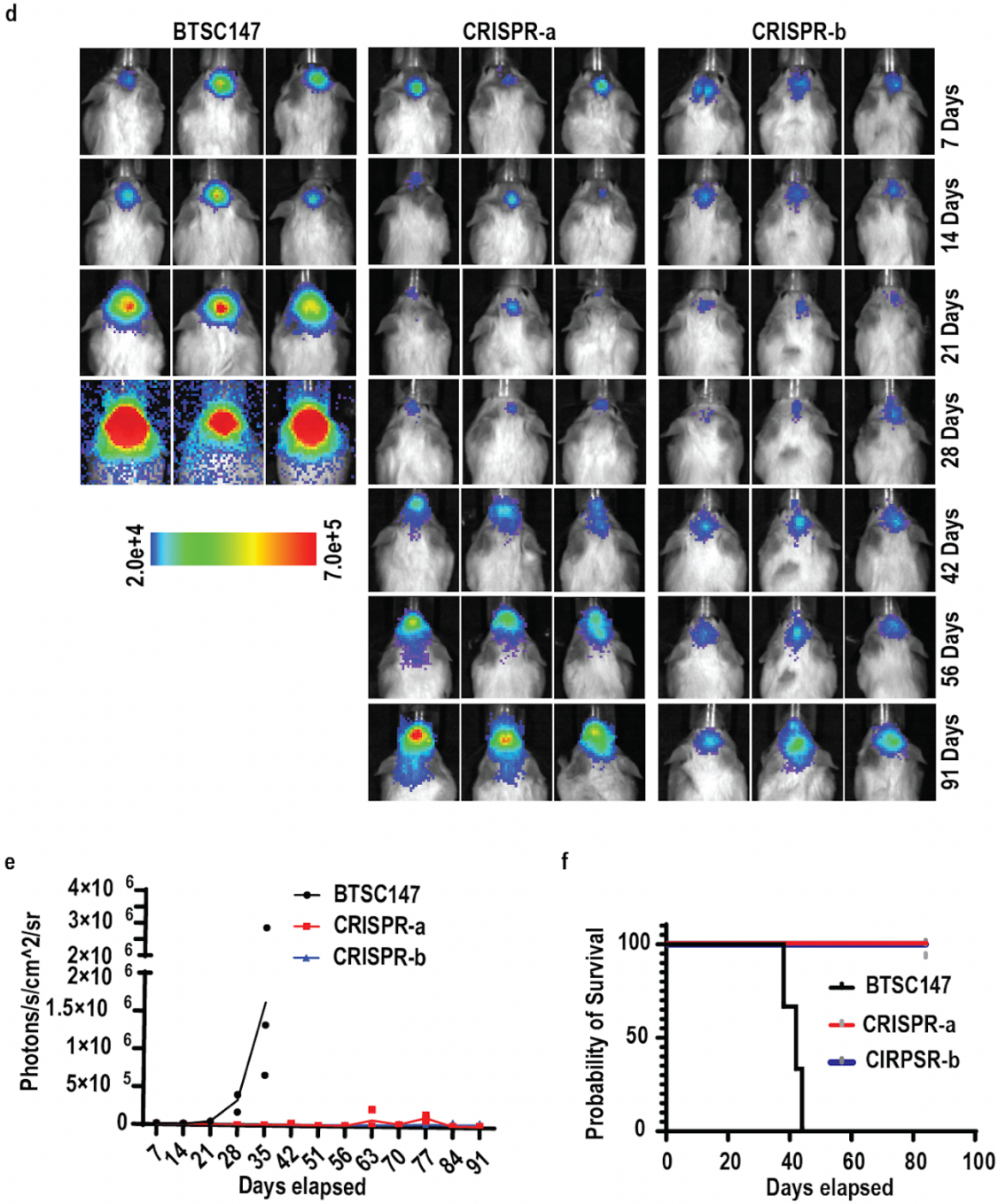
d
BTSC147
CRISPR-a
CRISPR-b
7 Days
14 Days
21 Days
28 Days
42 Days
56 Days
91 Days
2.0e+4
7.0e+5
e
Photons/s/cm^2/sr
4×10 6
3×10 6
2×10 6
2×10 6
1.5×10 6
1×10 6
5×10 5
0
BTSC147
CRISPR-a
CRISPR-b
7 14 21 28 35 42 51 56 63 70 77 84 91
Days elapsed
f
Probability of Survival
100
50
0
BTSC147
CRISPR-a
CIRPSR-b
0 20 40 60 80 100
Days elapsed

### 3.6. CLIC1 is expressed constitutively at the plasma membrane

Having observed decreased proliferation, self-renewal and tumourigenesis upon genetic deletion of CLIC1, we aimed to discern the role PM-CLIC1 in oncogenic behaviour. CLIC1 exists in an equilibrium between cytoplasmic form and PM-form. Previous studies have highlighted the significance of PM-CLIC1 in driving proliferation, and self-renewal[249,250,315]. To assess the question of whether CLIC1 is found in the PM of BTSCs, we first performed cell fractionation across two EGFRvIII expressing BTSCs (BTSC73 and BTSC147) and confirmed the presence of CLIC1 at the plasma membrane **(Figure 21a, b).** We utilized GAPDH (cytosolic marker) and $Na^+/K^+$ ATPase (plasma membrane) antibodies to ensure purity of the fractions. In parallel, we performed immunofluorescence on non-permeabilized BTSCs which validated the presence of CLIC1 at the plasma membrane (**Figure 22a-d).**

**Figure 21. CLIC1 is localized to the plasma membrane in BTSCs**
(a,b) Subcellular fractionation for membrane-associated versus cytosolic proteins. $Na^+/K^+$ ATPase was used as a membranous marker, GAPDH, a cytosolic marker. Both high exposure and low exposure images are shown for CLIC levels, n = 3 biological replicates.

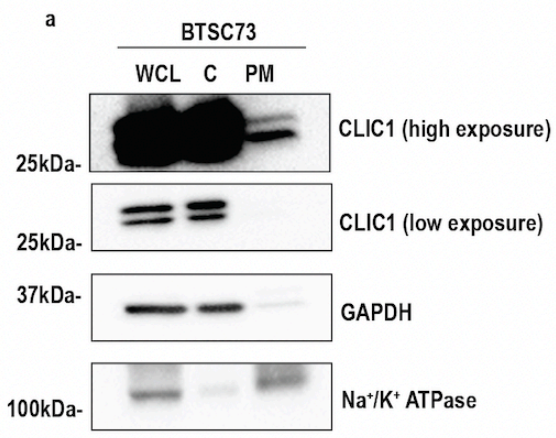
a
BTSC73
WCL
C
PM
25kDa-
CLIC1 (high exposure)
25kDa-
CLIC1 (low exposure)
37kDa-
GAPDH
100kDa-
Na+/K+ ATPase

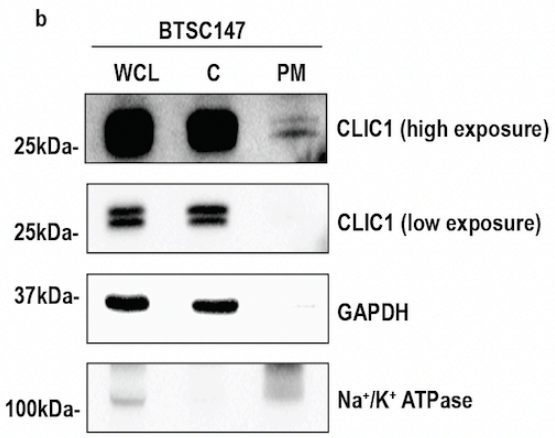
b
BTSC147
WCL
C
PM
25kDa-
CLIC1 (high exposure)
25kDa-
CLIC1 (low exposure)
37kDa-
GAPDH
100kDa-
Na+/K+ ATPase

**Figure 22. CLIC1 is detected at the plasma membrane of non-permeabilized BTSCs**
(a-d) BTSCs were subject to immunoblotting. Images in *Merged* shows the example of CLIC1 (green) overlapping with DAPI (blue). Scale bar, 10μm. One representative image is shown per BTSC line. Each experiment was conducted with a primary antibody omitted control group, n=3 biological replicates.

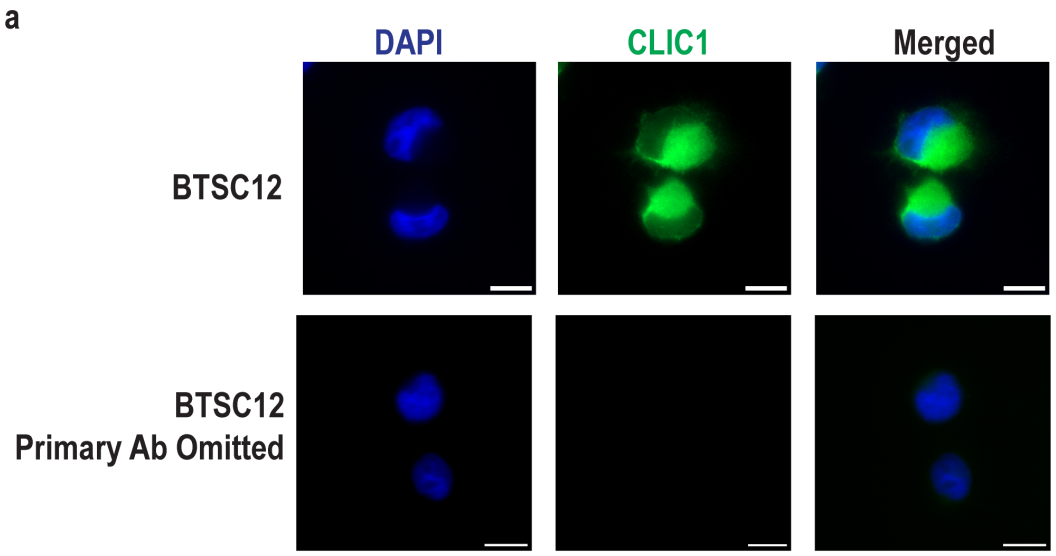
a
DAPI
CLIC1
Merged
BTSC12
BTSC12
Primary Ab Omitted

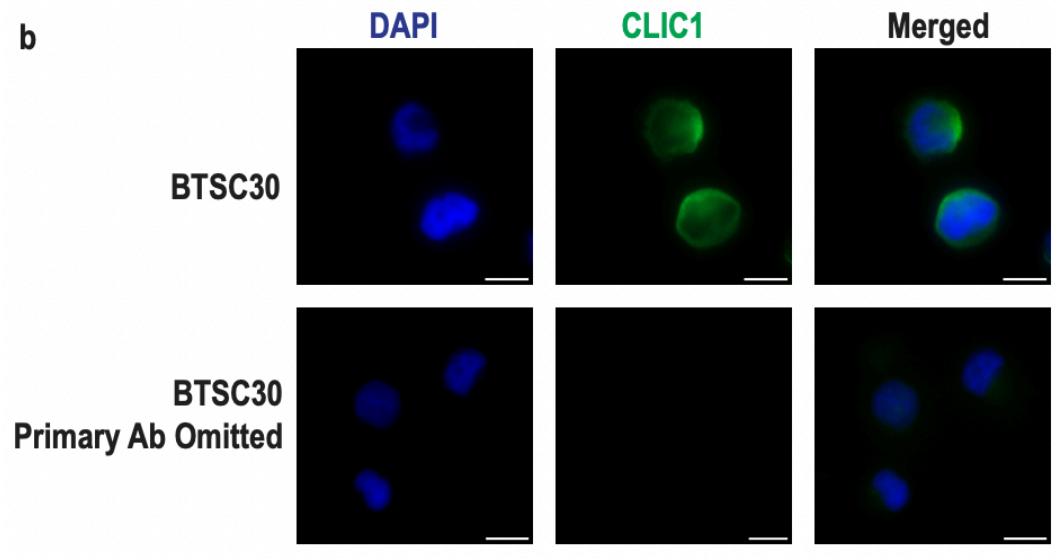
b
DAPI
CLIC1
Merged
BTSC30
BTSC30
Primary Ab Omitted

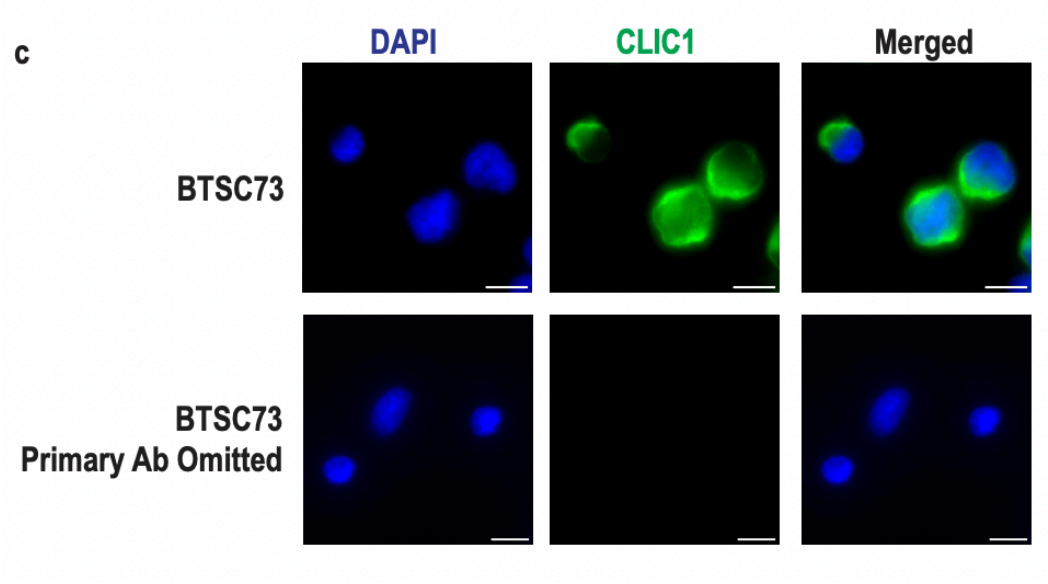
c
DAPI
CLIC1
Merged
BTSC73
BTSC73
Primary Ab Omitted

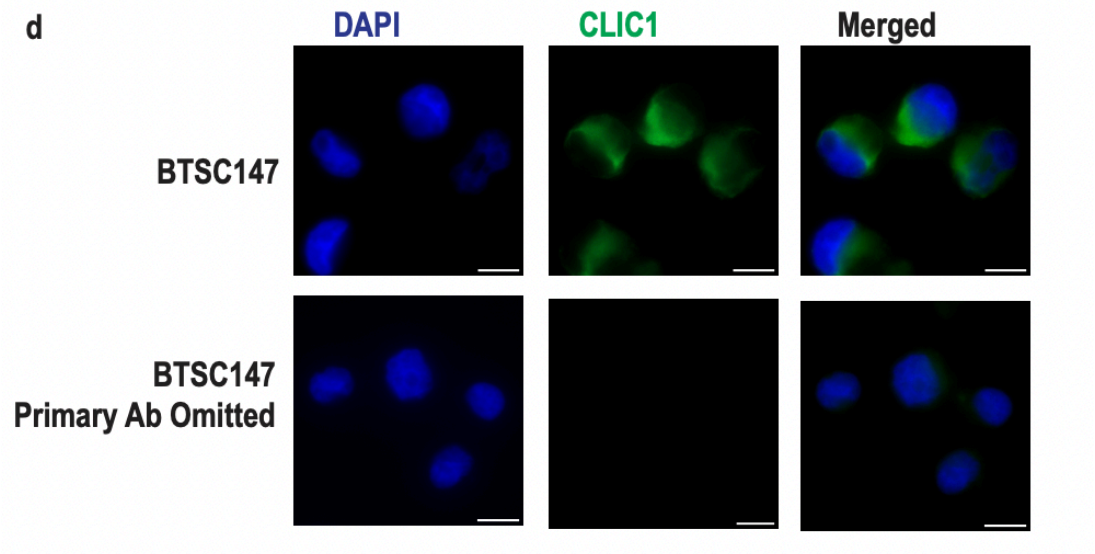
d
DAPI
CLIC1
Merged
BTSC147
BTSC147
Primary Ab Omitted

### 3.7. Impact of OSMR suppression on CLIC1-mediated Cl- Current

We have established that CLIC1 physically and functionally interact with OSMR to maintain EGFRvIII/STAT3 phosphorylation in BTSCs. Next, we set out to determine if OSMR is required for the CLIC1-mediated current. We utilized siRNA knockdown of OSMR in GBM1 cells, a GB CSC cell line, followed by patch clamp experiments in non-targeting (NT) control and OSMR knockdown cells to evaluate the association between reduced OSMR protein levels and alterations in $Cl^-$ current. Cell currents were assessed both prior to (baseline) and following the addition of 100uM of IAA94 to the bath solution **(Figure 23a,b).** Strikingly, the corresponding current-voltage relationship demonstrated that knockdown of OSMR attenuates the CLIC1 mediated current **(Figure 23c-e).** Taken together, we provide data that CLIC1 regulates EGFRvIII/STAT3 phosphorylation and at the same time OSMR is required for CLIC1 function at the plasma membrane. We establish that cooperation of OSMR with CLIC1 is required to drive GB progression.

**Figure 23. Electrophysiological evaluation of the effect of shOSMR on CLIC1 in Glioblastoma human primary culture (GBM1)**

(a,b) Representative whole-cell current recording from GBM1 cells in control (NC, a) and in transfected cells with shOSMR (b). The voltage step protocol used consisted of 800 msec pulses from -60 mV to +60 mV (20 mV voltage steps). The holding potential was set at -40 mV in all the current recordings. The panels show total currents (top), currents after the perfusion of IAA94 (middle), and the IAA94 sensitive current (bottom).

(c,d) Current-voltage relationships from average current recordings at different test potentials c, NC, n = 7; d, transfected shOSMR, n = 5). Average current values before and after IAA94 inhibition (top plots), and average IAA94 sensitive current values (bottom) plotted at the different test potentials.

(e) Histogram displaying current density at +60 mV in the NC cells and transfected with shOSMR. Statistical analysis was performed using a student t-test. *$p < 0.05$, **$p < 0.01$, ***$p < 0.001$.

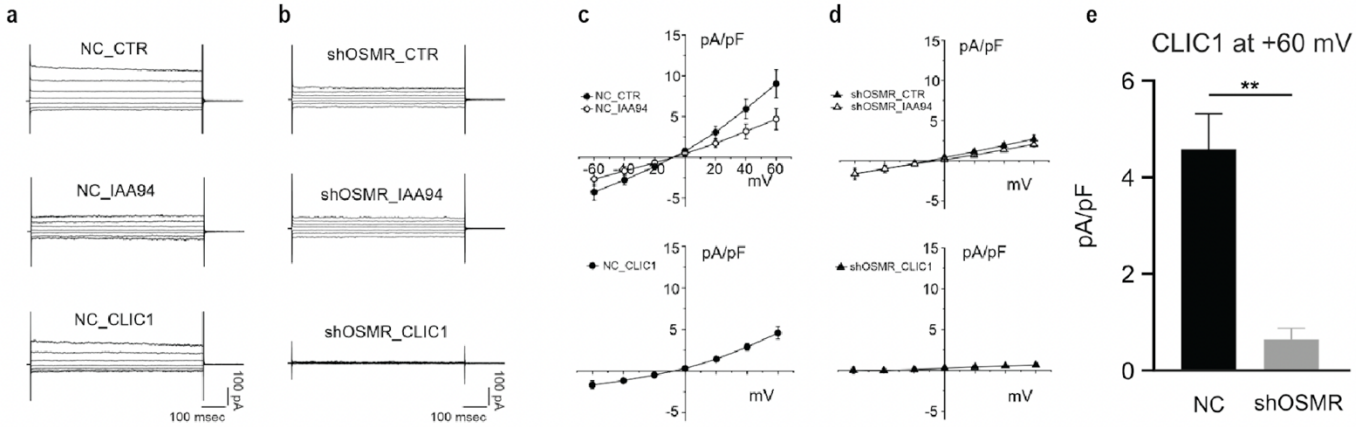
a
NC_CTR
NC_IAA94
NC_CLIC1
100 pA
100 msec
b
shOSMR_CTR
shOSMR_IAA94
shOSMR_CLIC1
100 pA
100 msec
c
pA/pF
NC_CTR
NC_IAA94
mV
NC_CLIC1
pA/pF
mV
d
pA/pF
shOSMR_CTR
shOSMR_IAA94
mV
shOSMR_CLIC1
pA/pF
mV
e
CLIC1 at +60 mV
**
pA/pF
NC
shOSMR

## 4. Discussion and Future Directions

GB is the most lethal central nervous system malignancy with a median survival of 18 months[1,2]. Despite intense treatment with IR and TMZ following surgical resection, recurrence is inevitable[8]. Recurrence of GB is in part driven by resistant BTSCs which evade treatment modalities[45–49]. One approach to combat GB recurrence is to map and target the signalling pathways that sustain BTSCs. Elevated expression of the cytokine receptor, OSMR, and the co-occurrence of commonly active mutant of the EGFR gene, EGFRvIII, within BTSCs are known to establish highly tumourigenic and treatment resistance BTSCs[17,103]. How the OSMR/EGFRvIII complex operates to maintain BTSCs and promote oncogenesis remains to be explored. Here, we report the discovery of CLIC1 as an essential common binding partner of OSMR, in the presence and absence of EGFRvIII that promotes BTSC tumourigenesis. CLIC1 is implicated in many aggressive cancers including HCC, lung cancer, gallbladder carcinoma, gastric carcinoma, colorectal cancer, medulloblastoma, and glioblastoma[224,225,228,278–280,316]. As an ion channel, CLIC1 is expressed at the plasma membrane of BTSCs where it supports cell cycle progression[249,250]. We found that CLIC1 affects the viability, proliferation, and self-renewal of BTSCs *in vitro*, and tumour progression *in vivo*. CLIC1 regulates BTSC growth by inducing STAT3 and EGFRvIII phosphorylation. Importantly, we show the requirement of OSMR for CLIC1 mediated ionic conductance. Our data suggest that CLIC1 is potentially a viable therapeutic target for suppressing OSMR/EGFRvIII/STAT3 oncogenic signalling and depleting the resistant BTSCs in GB.

### 4.1. Impact of CLIC1 on cell cycle progression

In this study, we employed different approaches including transient siRNA-mediated knockdown and genetic deletion of CLIC1 via CRISPR-Cas9 in different patient derived BTSC and established that CLIC1 suppressed self-renewal and proliferation of BTSCs, as evidenced by ELDA and trypan blue assays, respectively. Since both processes of self-renewal and proliferation critically rely on cell division, our data suggest that CLIC1 may tightly regulate cell division. Notably, considerable evidence exists that suggests a role of CLIC1 in cell cycle progression. Peretti et al. demonstrated that CLIC1 regulates the G1/S phase transition in BTSCs. Treatment of BTSCs with the CLIC1 inhibitor, IAA94, delays transition from the G1 phase, consequently increasing the total time required to complete the cell cycle.

IAA94 treatment also delays the expression of cyclin D1, an important regulator of G1/S transition[249]. In another study by Francisco and colleagues, the genetic deletion of CLIC1 resulted in cell swelling, mitotic defects, and reduced proliferation in MB cells[224]. It is possible that CLIC1 acts as a cell cycle regulator by mediating cell volume changes. For instance, during the prophase to metaphase transition, cells undergo a significant volume decrease, reaching a minimum size at metaphase. This reduced volume is preferred by the cell and is referred to as pre-mitotic condensation[289,290]. Pre-mitotic condensation requires the efflux of $Cl^-$ which may be mediated by CLIC1.

Future investigations on cell cycle analysis in BTSCs warrants insights on the role of CLIC1 in regulation of self-renewal and proliferation. This can be accomplished by arresting cells at each phase of the cell cycle and track the subcellular localization of CLIC1 to determine influence of CLIC1 on cell cycle progression. Rapamycin can be used for G1 inhibition, while treatment with hydroxyurea and nocodazole can be employed for S phase and M phase inhibition, respectively. Concurrently, using the whole cell patch clamp method, the CLIC1 current can be measured at each phase of the cell cycle to determine which phase is regulated by CLIC1 and to what degree. Finally, the distribution of cells across different cell cycle phases should be determined using flow cytometry between CTL and CLIC1-CRISPR-BTSCs. To assess the involvement of CLIC1 in altering cell volume during cell cycle progression, pairwise comparison of cell volume between CTL wild type and CLIC1-CRISPR-BTSCs can also be measured by expressing a soluble GFP in BTSCs and performing serial confocal imaging. Image stacks with a Z-step size of 1 µm per optical slice using a 63x 1.4NA oil lens can acquire images throughout the entire thickness of cells. Subsequently, using Imaris software, cells can be reconstructed three dimensionally and cell volume can be measured using the “Surface” function. These experiments will shed light on the role of CLIC1 in cell division and its regulation of cell volume during this process. We expect that in line with previous reports, dysregulation in cell volume homeostasis hinders successful completion of the cell cycle which may explain the reductions in self-renewal and proliferation demonstrated upon CLIC1 supression[224,317].

### 4.2. Impact of CLIC1 on cell identity

CRISPR-Cas9 technology was utilized to generate a constitutive silencing of CLIC1 in two patients derived BTSC lines (BTSC73 and BTSC147). We found that genetic deletion of CLIC1 prolonged the survival of mice, which were intracranially implanted with BTSCs, and slowed brain tumour formation as compared to control BTSCs. As a binding partner of OSMR, CLIC1 is implicated in establishing a highly malignant subset of BTSCs. However, the exact mechanisms underlying CLIC1-mediated tumorigenicity remained elusive. Our follow up investigation revealed the downregulation of oncogenic signaling pathways, such as STAT3 activation and EGFRvIII expression, in CLIC1-deleted BTSCs suggesting a shift towards a more differentiated phenotype. Previous research on cell fate dynamics supports this notion. Stockhausen et al. demonstrated that induced differentiation of BTSCs with serum leads to loss of EGFRvIII expression and decreased tumourigenic potential[318]. In another study by Gritti et al., CLIC1 expression was lost upon induction of differentiation with FBS[250]. These results suggest that both EGFRvIII and CLIC1 are important in maintaining the BTSCs in an undifferentiated state. Previous research has demonstrated that gene deletions can profoundly alter cell identity. For example, the loss of the transcription factor OCT4 disrupts the pluripotency network in embryonic stem cells (ESCs), leading to differentiation[319]. Similarly, in another study by He et al., the chloride channel, Ano1, was found to limit differentiation of epithelial progenitors towards cells of the secretory lineage[320]. Further studies are required to determine if CLIC1 aids in establishing a cellular network that supports stemness of BTSCs. These studies can encompass global gene expression analysis (e.g. RNA sequencing) to evaluate the expression of key BTSC markers, OCT4, OLIG2, SOX2, and NESTIN, and the differentiation markers, GFAP and TUJ1, in response to CLIC1 deletion. In addition, flow cytometry can be employed as another approach since differentiated cells often express distinct sets of cell surface markers (NeuN) compared to undifferentiated stem cells. By labeling cells with fluorescently conjugated antibodies targeting lineage-specific markers such as CD133 for BTSCs, and NeuN for differentiated cells, flow cytometry can quantify the proportion of cells expressing these markers, indicating the degree of differentiation towards a particular lineage. Unraveling the molecular mechanisms that underly CLIC1-mediated tumorigenicity will lay the foundation for the design of novel therapeutic strategies in combating aggressive brain tumours. Moreover, this research

paradigm underscores the need for deeper investigations into the interplay between gene alterations, cell identity, and tumour behavior.

### 4.3. Impact of CLIC1 on therapeutic resistance

BTSCs possess the defining features of tumourigenesis and multidrug resistance (MDR)[321,322]. It is possible that by suppressing CLIC1, the functional characteristics of BTSCs are disrupted. Ionic homeostasis is critical in cancer cells and CSCs and recently, ion channel blockers have been widely used in clinical practice. For instance, inhibition of KCa3.1 channel was found to sensitize BTSCs to TMZ. In another study, bis-chloroethylnitrosourea (BCNU) resistant BTSCs became sensitized to the chemotherapeutic after treatment with the $Cl^-$ channel blocker 4,4′-diisothiocyanostilbene-2,2′-disulfonic acid (DIDS). These BTSCs were noted to have upregulation of CLIC1, suggesting its role in chemotherapy resistance[323,324]. In view of these findings and our own results, future investigation should focus on combination therapy with TMZ and IAA94 to address whether blockade of CLIC1 facilitates response to TMZ in chemo-resistant BTSCs and GB.

Resistance to therapy is a major challenge in cancer treatment. One mechanism used to render cells resistant is through drug efflux. This is accomplished by membrane transporter protein, including Multi-Drug Resistance Protein 1 (MDR1), MDR-Associated Protein 1 (MRP1), and Breast Cancer Resistance Protein (BCRP)[325,326]. Interestingly, like other chloride channels (e.g. ClC-3), CLIC1 seems to confer resistance to cancer therapy[327–329]. Choriocarcinoma cell (JeG3) induced chemotherapy resistant lines were found to have upregulated CLIC1 expression and CLIC1 was found to induce the expression of MRP1[330]. CLIC1 is also shown in exosomes in gastric cancer whereby it mediates resistance to vincristine. Importantly, exosomes collected from the supernatant of resistant cell lines were able to transform vincristine sensitive cell to make them resistant to therapy. This data suggests that CLIC1 may be impacting drug resistance through EV transfer to neighbouring cell populations[331]. Concurrently, CLIC1 vesicle transfer has further been implicated in glioma stem cells proliferation and mediation of the extracellular environment[244]. By blocking the $Cl^-$ current in stem-like cells through the re-purposing of known pharmacological drugs, CLIC1 was shown to be a promising target for therapy[250,315]. These data suggest that the expression of CLIC1 may be an adaptive mechanism used by cancer cells to become resistant to

chemotherapy. Importantly, we show that OSMR, the binding partner of CLC1, confers resistance to therapy[314]. Whether CLIC1 cooperates with OSMR to confer resistance to the present standards of care in GB remains an exciting avenue for future research.

### 4.4. CLIC1 regulation of EGFRvIII

EGFR amplification and the presence of EGFRvIII are the most common genetic alterations in GB. EGFRvIII has been implicated in therapeutic resistance, tumour growth, invasiveness, migration, and tumour initiation in GB[114,332–335]. EGFRvIII also regulates angiogenesis by mediating VEGF secretion[336]. Furthermore, the presence of EGFRvIII confers CSC features by stimulating the expression of NSC markers, such as CD133 and SOX2, in addition to mediating heightened self-renewal capacity[100,337]. In the present study, both BTSC73 and BTSC147 naturally harbour EGFRvIII amplification. Strikingly, genetic deletion of CLIC1, significantly reduced EGFRvIII levels. This is a significant finding as direct targeting of EGFRvIII is very challenging due to chemotherapy induced mutations, toxicity, the blood brain barrier, and tumour heterogeneity[127–130]. Given that PM-CLIC1 is highly expressed in BTSCs and exhibits low expression in normal NSCs[299], targeting of CLIC1 may present an opportunity to indirectly deplete EGFRvIII levels, while sparing normal cells. Further studies are required to elucidate the mechanism of EGFRvIII degradation.

#### 4.4.1. CLIC1 regulation of lysosomes

In cancer, lysosomes are qualitatively and quantitively modified to suit tumour growth[338]. Lysosomal dysfunction has emerged as a critical factor in the pathogenesis of GB, influencing the accumulation of key proteins such as EGFRvIII and impacting cellular homeostasis[99,203]. EGFRvIII is known for its resistance to degradation due to impairments in reuptake and lysosome degradation pathways. One significant contributor to this phenomenon is the dysregulation of acidity. Lysosome and endosomes are acidified by the action of vacuole ATPase (V-ATPase) proton pumps, which enable activation of various hydrolytic enzymes required for intracellular digestion and recycling of macromolecules[339,340]. In GB, however, upregulation of the $Na^+/H^+$ exchanger NHE9 counteracts the acidifying potential of V-ATPase proton pumps by forming a proton leak channel. This leak pathway leads to excessive luminal alkalization (pH 5.71±0.23 to pH 6.90±0.47) and disrupts proper degradation of EGFRvIII[203].

One possibility to explain our findings on loss of CLIC1-mediated EGFRvIII depletion could be via the role of CLIC1 in mediating lysosomal acidification thereby influencing the stability of EGFRvIII. In support of this idea, previous studies by Jiang et al. demonstrated that suppression of CLIC1 in macrophages led to a defect in phagosome acidification, impaired phagosome proteolytic capacity and reduced ROS production[341]. Future studies should utilize live imaging of cells to track the subcellular localization of EGFRvIII in the presence and absence of CLIC1 to determine the influence of CLIC1 on EGFRvIII stability. In addition, endosomal pH can be measured using flow cytometry whereby BTSCs can be exposed to a pH-sensitive fluorescent dye, such as fluorescein isothiocyanate (FITC) and a pH-insensitive reference, such as Alexa Fluor 647.

### 4.5. OSMR oxidatively regulates CLIC1

OSMR has been reported to interact with Complex I of mitochondrial respiratory chain, promoting oxidative phosphorylation (OXPHOS), regulating ROS levels, and conferring resistance to IR[314]. Interestingly, CLIC1 is proposed to be a target of biguanide related drugs, including metformin, and it has been shown to regulate ROS levels[250,316]. The CLIC1 mediated current plays a critical role in BTSCs and notably, CLIC1's membrane insertion mechanism appears to be regulated by reduction-oxidation (REDOX), whereby oxidative conditions favour the formation of ion channels by CLIC1[259,266,342].

In the present study, we observed that knockdown of OSMR attenuates the CLIC1 mediated current. Given that OSMR regulates ROS levels and CLIC1 is redox sensitive, future studies should evaluate how OSMR regulates CLIC1 membrane insertion. It is plausible that OSMR creates an oxidative environment that favours membrane insertion of CLIC1. ROS generation can be measured using the probe 2′,7′-dichlorodihydrofluorescein diacetate (H2DCFDA), which becomes the highly fluorescent 2',7'-dichlorofluorescein (DCF) molecule under oxidizing conditions. To specifically analyze mitochondrial ROS, MitoSOX™ Mitochondrial Superoxide Indicators can be used. In addition, the subcellular localization of CLIC1 should be tracked in the presence and absence of OSMR. It is worth mentioning that previous studies have shown that suppression of OSMR leads to increased ROS levels, which may contradict this hypothesis[314] . As such, the effect of OSMR on pH should also be explored further as pH

also influences CLIC1's membrane insertion. To assess pH levels, the ratiometric $Cl^-$ and $H^+$ Clophensor plasmid, optimized for the nervous system, can be utilized in BTSCs[343].

### 4.5.1. Transcriptional regulation of CLIC1 by OSMR

Previous studies by Jahani-Asl et al. have shown that suppression of OSMR reduces activity of the transcription factor STAT3[20]. Notably, a STAT3 binding site is present in the promoter region of CLIC1[344]. It is possible that in the absence of OSMR and STAT3 activity, the transcription of CLIC1 is downregulated which may explain our results demonstrating reduced CLIC1 mediated currents in the absence of OSMR. To assess the effect of OSMR on CLIC1 mRNA levels, future studies should utilize RT-qPCR and immunoblotting to compare CLIC1 levels in CTL BTSCs and OSMR-CRISPR-BTSCs. In addition, a luciferase assay can establish a functional relationship between the presence of OSMR and the amount of CLIC1 that is produced.

## 4.6. Conclusion

The present study identified a novel OSMR binding partner, Chloride Intracellular Channel 1 (CLIC1), in patient-derived BTSCs. This protein was identified through MaMTH-HTS and endogenous validation in BTSCs. CLIC1 was found to promote BTSC viability, proliferation, and self-renewal *in vitro*, while promoting tumorigenesis *in vivo*. The decreased functional capacity of BTSCs is believed to be mediated by the EGFRvIII-STAT3 pathway, as genetic deletion of CLIC1 was found to impair both STAT3 activation and EGFRvIII levels. This work lays the foundation for future studies aimed at establishing the mechanistic link between CLIC1 and EGFRvIII stability. Further research should focus on elucidating the precise molecular interactions between CLIC1 and EGFRvIII, and how these interactions influence the stability and function of EGFRvIII. Investigating the role of CLIC1 in endosomal acidification and receptor recycling processes could provide valuable insights into the regulation of EGFRvIII by chloride channels. Additionally, exploring the therapeutic potential of targeting CLIC1 in GB could open new avenues for treatment strategies, particularly in overcoming the challenges associated with direct EGFRvIII targeting. Overall, our findings underscore the critical role of CLIC1 in GB pathogenesis and highlight its potential as a promising therapeutic target.

## 5. References


1. Gilard, V. *et al.* Diagnosis and Management of Glioblastoma: A Comprehensive Perspective. *J Pers Med* **11**, (2021).
2. Shergalis, A., Bankhead, A., Luesakul, U., Muangsin, N. & Neamati, N. Current Challenges and Opportunities in Treating Glioblastoma. *Pharmacol Rev* **70**, 412–445 (2018).
3. Grech, N. *et al.* Rising Incidence of Glioblastoma Multiforme in a Well-Defined Population. *Cureus* **12**, e8195 (2020).
4. Puchalski, R. B. *et al.* An anatomic transcriptional atlas of human glioblastoma. *Science (1979)* **360**, 660–663 (2018).
5. Bao, S. *et al.* Glioma stem cells promote radioresistance by preferential activation of the DNA damage response. *Nature* **444**, 756–760 (2006).
6. Lan, X. *et al.* Fate mapping of human glioblastoma reveals an invariant stem cell hierarchy. *Nature* **549**, 227–232 (2017).
7. Oliveira, M. N. *et al.* Glioblastoma cell invasiveness and epithelial-to-mesenchymal transitioning are modulated by kinin receptors. *Advances in Cancer Biology - Metastasis* **4**, 100045 (2022).
8. Kanderi, T. & Gupta, V. *Glioblastoma Multiforme*. (2024).
9. Becker, A., Sells, B., Haque, S. & Chakravarti, A. Tumor Heterogeneity in Glioblastomas: From Light Microscopy to Molecular Pathology. *Cancers (Basel)* **13**, 761 (2021).
10. Kawauchi, D. *et al.* Early Diagnosis and Surgical Intervention Within 3 Weeks From Symptom Onset Are Associated With Prolonged Survival of Patients With Glioblastoma. *Neurosurgery* **91**, 741–748 (2022).
11. Brennan, C. W. *et al.* The Somatic Genomic Landscape of Glioblastoma. *Cell* **155**, 462–477 (2013).
12. Reifenberger, G., Liu, L., Ichimura, K., Schmidt, E. E. & Collins, V. P. Amplification and overexpression of the MDM2 gene in a subset of human malignant gliomas without p53 mutations. *Cancer Res* **53**, 2736–9 (1993).
13. Larsson, I. *et al.* Modeling glioblastoma heterogeneity as a dynamic network of cell states. *Mol Syst Biol* **17**, (2021).
14. Zhang, Y. *et al.* The p53 Pathway in Glioblastoma. *Cancers (Basel)* **10**, (2018).
15. Wang, S. I. *et al.* Somatic mutations of PTEN in glioblastoma multiforme. *Cancer Res* **57**, 4183–6 (1997).
16. Scheer, M. *et al.* Neurofibromatosis Type 1 Gene Alterations Define Specific Features of a Subset of Glioblastomas. *Int J Mol Sci* **23**, (2021).
17. An, Z., Aksoy, O., Zheng, T., Fan, Q.-W. & Weiss, W. A. Epidermal growth factor receptor and EGFRvIII in glioblastoma: signaling pathways and targeted therapies. *Oncogene* **37**, 1561–1575 (2018).
18. Higa, N. *et al.* Prognostic impact of PDGFRA gain/amplification and MGMT promoter methylation status in patients with IDH wild-type glioblastoma. *Neurooncol Adv* **4**, vdac097 (2022).

19. Reifenberger, G., Liu, L., Ichimura, K., Schmidt, E. E. & Collins, V. P. Amplification and overexpression of the MDM2 gene in a subset of human malignant gliomas without p53 mutations. *Cancer Res* **53**, 2736–9 (1993).
20. Jahani-Asl, A. *et al.* Control of glioblastoma tumorigenesis by feed-forward cytokine signaling. *Nat Neurosci* **19**, 798–806 (2016).
21. Choi, S. W. *et al.* Mutation-specific non-canonical pathway of PTEN as a distinct therapeutic target for glioblastoma. *Cell Death Dis* **12**, 374 (2021).
22. You, Y. *et al.* Evaluation of combination gene therapy with PTEN and antisense hTERT for malignant glioma in vitro and xenografts. *Cellular and Molecular Life Sciences* **64**, 621–631 (2007).
23. Abdulkareem, I. H. & Blair, M. Phosphatase and tensin homologue deleted on chromosome 10. *Niger Med J* **54**, 79–86 (2013).
24. Eisenbarth, D. & Wang, Y. A. Glioblastoma heterogeneity at single cell resolution. *Oncogene* **42**, 2155–2165 (2023).
25. Abdelfattah, N. *et al.* Single-cell analysis of human glioma and immune cells identifies S100A4 as an immunotherapy target. *Nat Commun* **13**, 767 (2022).
26. Sidaway, P. Glioblastoma subtypes revisited. *Nat Rev Clin Oncol* **14**, 587–587 (2017).
27. Verhaak, R. G. W. *et al.* Integrated Genomic Analysis Identifies Clinically Relevant Subtypes of Glioblastoma Characterized by Abnormalities in PDGFRA, IDH1, EGFR, and NF1. *Cancer Cell* **17**, 98–110 (2010).
28. Zhang, P., Xia, Q., Liu, L., Li, S. & Dong, L. Current Opinion on Molecular Characterization for GBM Classification in Guiding Clinical Diagnosis, Prognosis, and Therapy. *Front Mol Biosci* **7**, (2020).
29. Steponaitis, G. & Tamasauskas, A. Mesenchymal and Proneural Subtypes of Glioblastoma Disclose Branching Based on GSC Associated Signature. *Int J Mol Sci* **22**, (2021).
30. Wu, L. *et al.* Evolution-driven crosstalk between glioblastoma and the tumor microenvironment. *Cancer Biol Med* **20**, 319–24 (2023).
31. Wang, Q. *et al.* Tumor Evolution of Glioma-Intrinsic Gene Expression Subtypes Associates with Immunological Changes in the Microenvironment. *Cancer Cell* **32**, 42-56.e6 (2017).
32. Wang, Q. *et al.* Tumor Evolution of Glioma-Intrinsic Gene Expression Subtypes Associates with Immunological Changes in the Microenvironment. *Cancer Cell* **32**, 42-56.e6 (2017).
33. Wang, Q. *et al.* Tumor Evolution of Glioma-Intrinsic Gene Expression Subtypes Associates with Immunological Changes in the Microenvironment. *Cancer Cell* **32**, 42-56.e6 (2017).
34. Hutóczki, G., Virga, J., Birkó, Z. & Klekner, A. Novel Concepts of Glioblastoma Therapy Concerning Its Heterogeneity. *Int J Mol Sci* **22**, (2021).
35. Erratum to: Cancer cell heterogeneity and plasticity: A paradigm shift in glioblastoma. *Neuro Oncol* **24**, 2011–2011 (2022).
36. Reya, T., Morrison, S. J., Clarke, M. F. & Weissman, I. L. Stem cells, cancer, and cancer stem cells. *Nature* **414**, 105–111 (2001).

37. Chandler, J. M. & Lagasse, E. Cancerous stem cells: deviant stem cells with cancer-causing misbehavior. *Stem Cell Res Ther* **1**, 13 (2010).
38. Prasetyanti, P. R. & Medema, J. P. Intra-tumor heterogeneity from a cancer stem cell perspective. *Mol Cancer* **16**, 41 (2017).
39. Nowell, P. C. The Clonal Evolution of Tumor Cell Populations. *Science (1979)* **194**, 23–28 (1976).
40. Shackleton, M., Quintana, E., Fearon, E. R. & Morrison, S. J. Heterogeneity in Cancer: Cancer Stem Cells versus Clonal Evolution. *Cell* **138**, 822–829 (2009).
41. Dick, J. E. Stem cell concepts renew cancer research. *Blood* **112**, 4793–4807 (2008).
42. Patel, A. P. *et al.* Single-cell RNA-seq highlights intratumoral heterogeneity in primary glioblastoma. *Science (1979)* **344**, 1396–1401 (2014).
43. Dirkse, A. *et al.* Stem cell-associated heterogeneity in Glioblastoma results from intrinsic tumor plasticity shaped by the microenvironment. *Nat Commun* **10**, 1787 (2019).
44. Nallasamy, P. *et al.* Tumor microenvironment enriches the stemness features: the architectural event of therapy resistance and metastasis. *Mol Cancer* **21**, 225 (2022).
45. Furst, L. *et al.* Identification and isolation of slow-cycling glioma stem cells. in 21–30 (2022). doi:10.1016/bs.mcb.2022.02.004.
46. Piccirillo, S. G. M. *et al.* Genetic and Functional Diversity of Propagating Cells in Glioblastoma. *Stem Cell Reports* **4**, 7–15 (2015).
47. Singh, S. K. *et al.* Identification of human brain tumour initiating cells. *Nature* **432**, 396–401 (2004).
48. Vescovi, A. L., Galli, R. & Reynolds, B. A. Brain tumour stem cells. *Nat Rev Cancer* **6**, 425–436 (2006).
49. Galli, R. *et al.* Isolation and characterization of tumorigenic, stem-like neural precursors from human glioblastoma. *Cancer Res* **64**, 7011–21 (2004).
50. Chen, J. *et al.* A restricted cell population propagates glioblastoma growth after chemotherapy. *Nature* **488**, 522–526 (2012).
51. Johnson, M. S. & Cook, J. G. Cell cycle exits and U-turns: Quiescence as multiple reversible forms of arrest. *Fac Rev* **12**, 5 (2023).
52. Miyashita, S. & Hoshino, M. Transit Amplifying Progenitors in the Cerebellum: Similarities to and Differences from Transit Amplifying Cells in Other Brain Regions and between Species. *Cells* **11**, 726 (2022).
53. Cusulin, C. *et al.* Precursor States of Brain Tumor Initiating Cell Lines Are Predictive of Survival in Xenografts and Associated with Glioblastoma Subtypes. *Stem Cell Reports* **5**, 1–9 (2015).
54. Codega, P. *et al.* Prospective Identification and Purification of Quiescent Adult Neural Stem Cells from Their In Vivo Niche. *Neuron* **82**, 545–559 (2014).
55. Binda, E., Reynolds, B. A. & Vescovi, A. L. Glioma stem cells: turpis omen in nomen? (the evil in the name?). *J Intern Med* **276**, 25–40 (2014).
56. Wan, F. *et al.* The utility and limitations of neurosphere assay, CD133 immunophenotyping and side population assay in glioma stem cell research. *Brain Pathol* **20**, 877–89 (2010).

57. Davis, B. *et al.* Comparative genomic and genetic analysis of glioblastoma-derived brain tumor-initiating cells and their parent tumors. *Neuro Oncol* **18**, 350–360 (2016).
58. Agarwal, S. *et al.* Tumor Derived Mutations of Protein Tyrosine Phosphatase Receptor Type K Affect Its Function and Alter Sensitivity to Chemotherapeutics in Glioma. *PLoS One* **8**, e62852 (2013).
59. Comprehensive genomic characterization defines human glioblastoma genes and core pathways. *Nature* **455**, 1061–1068 (2008).
60. Assem, M. *et al.* Enhancing Diagnosis, Prognosis, and Therapeutic Outcome Prediction of Gliomas Using Genomics. *OMICS* **16**, 113–122 (2012).
61. Silva, C. M. Role of STATs as downstream signal transducers in Src family kinase-mediated tumorigenesis. *Oncogene* **23**, 8017–8023 (2004).
62. Price, J. T., Tiganis, T., Agarwal, A., Djakiew, D. & Thompson, E. W. Epidermal growth factor promotes MDA-MB-231 breast cancer cell migration through a phosphatidylinositol 3'-kinase and phospholipase C-dependent mechanism. *Cancer Res* **59**, 5475–8 (1999).
63. Wise, R. & Zolkiewska, A. Metalloprotease-dependent activation of EGFR modulates CD44+/CD24− populations in triple negative breast cancer cells through the MEK/ERK pathway. *Breast Cancer Res Treat* **166**, 421–433 (2017).
64. García-Aranda, M. & Redondo, M. Targeting Receptor Kinases in Colorectal Cancer. *Cancers (Basel)* **11**, (2019).
65. Comoglio, P. M., Trusolino, L. & Boccaccio, C. Known and novel roles of the MET oncogene in cancer: a coherent approach to targeted therapy. *Nat Rev Cancer* **18**, 341–358 (2018).
66. Li, X., Wang, C., Xiao, J., McKeehan, W. L. & Wang, F. Fibroblast growth factors, old kids on the new block. *Semin Cell Dev Biol* **53**, 155–167 (2016).
67. Shibuya, M. Vascular Endothelial Growth Factor (VEGF) and Its Receptor (VEGFR) Signaling in Angiogenesis: A Crucial Target for Anti- and Pro-Angiogenic Therapies. *Genes Cancer* **2**, 1097–105 (2011).
68. Silva Paiva, R., Gomes, I., Casimiro, S., Fernandes, I. & Costa, L. c-Met expression in renal cell carcinoma with bone metastases. *J Bone Oncol* **25**, 100315 (2020).
69. Chen, J., Song, W. & Amato, K. Eph receptor tyrosine kinases in cancer stem cells. *Cytokine Growth Factor Rev* **26**, 1–6 (2015).
70. Rajasekhar, V. K. *et al.* Oncogenic Ras and Akt Signaling Contribute to Glioblastoma Formation by Differential Recruitment of Existing mRNAs to Polysomes. *Mol Cell* **12**, 889–901 (2003).
71. Stacey, D. W. Cyclin D1 serves as a cell cycle regulatory switch in actively proliferating cells. *Curr Opin Cell Biol* **15**, 158–163 (2003).
72. Boonstra, J. *et al.* The epidermal growth factor. *Cell Biol Int* **19**, 413–430 (1995).
73. Cary, L. A., Han, D. C. & Guan, J. L. Integrin-mediated signal transduction pathways. *Histol Histopathol* **14**, 1001–9 (1999).
74. Schlesinger, T. K. The TAO of MEKK. *Frontiers in Bioscience* **3**, A354 (1998).
75. Kranenburg, O., Gebbink, M. F. B. G. & Voest, E. E. Stimulation of angiogenesis by Ras proteins. *Biochimica et Biophysica Acta (BBA) - Reviews on Cancer* **1654**, 23–37 (2004).

76. Zhao, L. & Vogt, P. K. Class I PI3K in oncogenic cellular transformation. *Oncogene* **27**, 5486–5496 (2008).
77. Li, X. *et al.* PI3K/Akt/mTOR signaling pathway and targeted therapy for glioblastoma. *Oncotarget* **7**, 33440–50 (2016).
78. Cetintas, V. B. & Batada, N. N. Is there a causal link between PTEN deficient tumors and immunosuppressive tumor microenvironment? *J Transl Med* **18**, 45 (2020).
79. Levy, D. E. & Inghirami, G. STAT3: A multifaceted oncogene. *Proceedings of the National Academy of Sciences* **103**, 10151–10152 (2006).
80. Fu, W., Hou, X., Dong, L. & Hou, W. Roles of STAT3 in the pathogenesis and treatment of glioblastoma. *Front Cell Dev Biol* **11**, (2023).
81. Xu, C., Fan, C. D. & Wang, X. Regulation of Mdm2 protein stability and the p53 response by NEDD4-1 E3 ligase. *Oncogene* **34**, 281–289 (2015).
82. Ozaki, T. & Nakagawara, A. Role of p53 in Cell Death and Human Cancers. *Cancers (Basel)* **3**, 994–1013 (2011).
83. Park, C.-M. *et al.* Induction of p53-mediated apoptosis and recovery of chemosensitivity through p53 transduction in human glioblastoma cells by cisplatin. *Int J Oncol* **28**, 119–25 (2006).
84. Zheng, H. *et al.* p53 and Pten control neural and glioma stem/progenitor cell renewal and differentiation. *Nature* **455**, 1129–1133 (2008).
85. England, B., Huang, T. & Karsy, M. Current understanding of the role and targeting of tumor suppressor p53 in glioblastoma multiforme. *Tumor Biology* **34**, 2063–2074 (2013).
86. Park, C.-M. *et al.* Induction of p53-mediated apoptosis and recovery of chemosensitivity through p53 transduction in human glioblastoma cells by cisplatin. *Int J Oncol* **28**, 119–25 (2006).
87. Djuzenova, C. S. *et al.* Actin cytoskeleton organization, cell surface modification and invasion rate of 5 glioblastoma cell lines differing in PTEN and p53 status. *Exp Cell Res* **330**, 346–357 (2015).
88. Murphrey, M. B., Quaim, L. & Varacallo, M. *Biochemistry, Epidermal Growth Factor Receptor*. (2022).
89. Hoogstrate, Y. *et al.* The EGFRvIII transcriptome in glioblastoma: A meta-omics analysis. *Neuro Oncol* **24**, 429–441 (2022).
90. Kleinschmidt-DeMasters, B. K., Lillehei, K. O. & Varella-Garcia, M. Glioblastomas in the Older Old. *Arch Pathol Lab Med* **129**, 624–631 (2005).
91. Rayego-Mateos, S. *et al.* Connective tissue growth factor is a new ligand of epidermal growth factor receptor. *J Mol Cell Biol* **5**, 323–335 (2013).
92. Isobe, T. *et al.* Epiregulin. *Journal of Biological Chemistry* **270**, 7495–7500 (1995).
93. Shing, Y. *et al.* Betacellulin: a mitogen from pancreatic beta cell tumors. *Science (1979)* **259**, 1604–1607 (1993).
94. Higashiyama, S., Abraham, J. A., Miller, J., Fiddes, J. C. & Klagsbrun, M. A Heparin-Binding Growth Factor Secreted by Macrophage-Like Cells That Is Related to EGF. *Science (1979)* **251**, 936–939 (1991).
95. Slamon, D. J. *et al.* Human Breast Cancer: Correlation of Relapse and Survival with Amplification of the HER-2/ *neu* Oncogene. *Science (1979)* **235**, 177–182 (1987).

96. Marquardt, H., Hunkapiller, M. W., Hood, L. E. & Todaro, G. J. Rat Transforming Growth Factor Type 1: Structure and Relation to Epidermal Growth Factor. *Science (1979)* **223**, 1079–1082 (1984).
97. An, Z., Aksoy, O., Zheng, T., Fan, Q.-W. & Weiss, W. A. Epidermal growth factor receptor and EGFRvIII in glioblastoma: signaling pathways and targeted therapies. *Oncogene* **37**, 1561–1575 (2018).
98. Schmidt, M. H. H., Furnari, F. B., Cavenee, W. K. & Bögler, O. Epidermal growth factor receptor signaling intensity determines intracellular protein interactions, ubiquitination, and internalization. *Proceedings of the National Academy of Sciences* **100**, 6505–6510 (2003).
99. Grandal, M. V. *et al.* EGFRvIII escapes down-regulation due to impaired internalization and sorting to lysosomes. *Carcinogenesis* **28**, 1408–1417 (2007).
100. Emlet, D. R. *et al.* Targeting a glioblastoma cancer stem-cell population defined by EGF receptor variant III. *Cancer Res* **74**, 1238–49 (2014).
101. Wheeler, D. L., Dunn, E. F. & Harari, P. M. Understanding resistance to EGFR inhibitors—impact on future treatment strategies. *Nat Rev Clin Oncol* **7**, 493–507 (2010).
102. Wikstrand, C. J. *et al.* Investigation of a synthetic peptide as immunogen for a variant epidermal growth factor receptor associated with gliomas. *J Neuroimmunol* **46**, 165–173 (1993).
103. Padfield, E., Ellis, H. P. & Kurian, K. M. Current Therapeutic Advances Targeting EGFR and EGFRvIII in Glioblastoma. *Front Oncol* **5**, (2015).
104. Shibata, T. *et al.* Enhancing Effects of Epidermal Growth Factor on Human Squamous Cell Carcinoma Motility and Matrix Degradation But Not Growth. *Tumor Biology* **17**, 168–175 (1996).
105. Bonavia, R. *et al.* EGFRvIII promotes glioma angiogenesis and growth through the NF-κB, interleukin-8 pathway. *Oncogene* **31**, 4054–4066 (2012).
106. Borrett, M. J. *et al.* A Shared Transcriptional Identity for Forebrain and Dentate Gyrus Neural Stem Cells from Embryogenesis to Adulthood. *eNeuro* **9**, ENEURO.0271-21.2021 (2022).
107. Lee, J. H. *et al.* Human glioblastoma arises from subventricular zone cells with low-level driver mutations. *Nature* **560**, 243–247 (2018).
108. Matarredona, E. R. & Pastor, A. M. Neural Stem Cells of the Subventricular Zone as the Origin of Human Glioblastoma Stem Cells. Therapeutic Implications. *Front Oncol* **9**, (2019).
109. Holland, E. C., Hively, W. P., DePinho, R. A. & Varmus, H. E. A constitutively active epidermal growth factor receptor cooperates with disruption of $G_1$ cell-cycle arrest pathways to induce glioma-like lesions in mice. *Genes Dev* **12**, 3675–3685 (1998).
110. Serrano, M., Hannon, G. J. & Beach, D. A new regulatory motif in cell-cycle control causing specific inhibition of cyclin D/CDK4. *Nature* **366**, 704–707 (1993).
111. Ouelle, D. E., Zindy, F., Ashmun, R. A. & Sherr, C. J. Alternative reading frames of the INK4a tumor suppressor gene encode two unrelated proteins capable of inducing cell cycle arrest. *Cell* **83**, 993–1000 (1995).

112. Bachoo, R. M. *et al.* Epidermal growth factor receptor and Ink4a/Arf. *Cancer Cell* **1**, 269–277 (2002).
113. de la Iglesia, N. *et al.* Identification of a PTEN-regulated STAT3 brain tumor suppressor pathway. *Genes Dev* **22**, 449–62 (2008).
114. Puram, S. V. *et al.* STAT3-iNOS Signaling Mediates EGFRvIII-Induced Glial Proliferation and Transformation. *Journal of Neuroscience* **32**, 7806–7818 (2012).
115. Singh, N., Miner, A., Hennis, L. & Mittal, S. Mechanisms of temozolomide resistance in glioblastoma - a comprehensive review. *Cancer Drug Resist* **4**, 17–43 (2021).
116. Ahmed, A. U., Auffinger, B. & Lesniak, M. S. Understanding glioma stem cells: rationale, clinical relevance and therapeutic strategies. *Expert Rev Neurother* **13**, 545–55 (2013).
117. Yekula, A. *et al.* The role of extracellular vesicles in acquisition of resistance to therapy in glioblastomas. *Cancer Drug Resistance* (2020) doi:10.20517/cdr.2020.61.
118. Oliver, L. *et al.* Drug resistance in glioblastoma: are persisters the key to therapy? *Cancer Drug Resistance* (2020) doi:10.20517/cdr.2020.29.
119. Egaña, L. *et al.* Methylation of MGMT promoter does not predict response to temozolomide in patients with glioblastoma in Donostia Hospital. *Sci Rep* **10**, 18445 (2020).
120. Polyak, K. & Weinberg, R. A. Transitions between epithelial and mesenchymal states: acquisition of malignant and stem cell traits. *Nat Rev Cancer* **9**, 265–273 (2009).
121. Mani, S. A. *et al.* The epithelial-mesenchymal transition generates cells with properties of stem cells. *Cell* **133**, 704–15 (2008).
122. Kim, Y. *et al.* Perspective of mesenchymal transformation in glioblastoma. *Acta Neuropathol Commun* **9**, 50 (2021).
123. Chen, Z. *et al.* FOSL1 promotes proneural-to-mesenchymal transition of glioblastoma stem cells via UBC9/CYLD/NF-κB axis. *Molecular Therapy* **30**, 2568–2583 (2022).
124. Fedele, M., Cerchia, L., Pegoraro, S., Sgarra, R. & Manfioletti, G. Proneural-Mesenchymal Transition: Phenotypic Plasticity to Acquire Multitherapy Resistance in Glioblastoma. *Int J Mol Sci* **20**, 2746 (2019).
125. Reardon, D. A. *et al.* A Phase I/II Trial of Pazopanib in Combination with Lapatinib in Adult Patients with Relapsed Malignant Glioma. *Clinical Cancer Research* **19**, 900–908 (2013).
126. Halatsch, M.-E. *et al.* Inverse correlation of epidermal growth factor receptor messenger RNA induction and suppression of anchorage-independent growth by OSI-774, an epidermal growth factor receptor tyrosine kinase inhibitor, in glioblastoma multiforme cell lines. *J Neurosurg* **100**, 523–533 (2004).
127. Sampson, J. H. *et al.* An epidermal growth factor receptor variant III-targeted vaccine is safe and immunogenic in patients with glioblastoma multiforme. *Mol Cancer Ther* **8**, 2773–9 (2009).
128. Zussman, B. M. & Engh, J. A. Outcomes of the ACT III Study. *Neurosurgery* **76**, N17 (2015).
129. Schuster, J. *et al.* A phase II, multicenter trial of rindopepimut (CDX-110) in newly diagnosed glioblastoma: the ACT III study. *Neuro Oncol* **17**, 854–861 (2015).

130. Malkki, H. Glioblastoma vaccine therapy disappointment in Phase III trial. *Nat Rev Neurol* **12**, 190–190 (2016).
131. Liu, F. & Mischel, P. S. Targeting epidermal growth factor receptor co-dependent signaling pathways in glioblastoma. *WIREs Systems Biology and Medicine* **10**, (2018).
132. Mellinghoff, I. K. *et al.* Molecular Determinants of the Response of Glioblastomas to EGFR Kinase Inhibitors. *New England Journal of Medicine* **353**, 2012–2024 (2005).
133. Singh, S. R., Rameshwar, P. & Siegel, P. Targeting tumor microenvironment in cancer therapy. *Cancer Lett* **380**, 203–204 (2016).
134. Quail, D. F. & Joyce, J. A. Microenvironmental regulation of tumor progression and metastasis. *Nat Med* **19**, 1423–1437 (2013).
135. Astekar, M., Metgud, R., Sharma, A. & Soni, A. Hidden keys in stroma: Unlocking the tumor progression. *J Oral Maxillofac Pathol* **17**, 82–8 (2013).
136. Propper, D. J. & Balkwill, F. R. Harnessing cytokines and chemokines for cancer therapy. *Nat Rev Clin Oncol* **19**, 237–253 (2022).
137. Anderson, N. M. & Simon, M. C. The tumor microenvironment. *Curr Biol* **30**, R921–R925 (2020).
138. Fridman, W. H. *et al.* B cells and tertiary lymphoid structures as determinants of tumour immune contexture and clinical outcome. *Nat Rev Clin Oncol* **19**, 441–457 (2022).
139. Kartikasari, A. E. R., Huertas, C. S., Mitchell, A. & Plebanski, M. Tumor-Induced Inflammatory Cytokines and the Emerging Diagnostic Devices for Cancer Detection and Prognosis. *Front Oncol* **11**, 692142 (2021).
140. Baghban, R. *et al.* Tumor microenvironment complexity and therapeutic implications at a glance. *Cell Communication and Signaling* **18**, 59 (2020).
141. Xuan, W., Lesniak, M. S., James, C. D., Heimberger, A. B. & Chen, P. Context-Dependent Glioblastoma–Macrophage/Microglia Symbiosis and Associated Mechanisms. *Trends Immunol* **42**, 280–292 (2021).
142. Cova, T. F. G. G., Bento, D. J. & Nunes, S. C. C. Computational Approaches in Theranostics: Mining and Predicting Cancer Data. *Pharmaceutics* **11**, 119 (2019).
143. Tsao, A. S. *et al.* Scientific Advances in Lung Cancer 2015. *Journal of Thoracic Oncology* **11**, 613–638 (2016).
144. Li, W., Ng, J. M.-K., Wong, C. C., Ng, E. K. W. & Yu, J. Molecular alterations of cancer cell and tumour microenvironment in metastatic gastric cancer. *Oncogene* **37**, 4903–4920 (2018).
145. Ungefroren, H., Sebens, S., Seidl, D., Lehnert, H. & Hass, R. Interaction of tumor cells with the microenvironment. *Cell Communication and Signaling* **9**, 18 (2011).
146. Soler, M. F., Abaurrea, A., Azcoaga, P., Araujo, A. M. & Caffarel, M. M. New perspectives in cancer immunotherapy: targeting IL-6 cytokine family. *J Immunother Cancer* **11**, e007530 (2023).
147. Hambardzumyan, D., Gutmann, D. H. & Kettenmann, H. The role of microglia and macrophages in glioma maintenance and progression. *Nat Neurosci* **19**, 20–27 (2016).
148. Johnson, D. E., O'Keefe, R. A. & Grandis, J. R. Targeting the IL-6/JAK/STAT3 signalling axis in cancer. *Nat Rev Clin Oncol* **15**, 234–248 (2018).

149. Lee, B. Y. *et al.* Heterocellular OSM-OSMR signalling reprograms fibroblasts to promote pancreatic cancer growth and metastasis. *Nat Commun* **12**, 7336 (2021).
150. Araujo, A. M. *et al.* Stromal oncostatin M cytokine promotes breast cancer progression by reprogramming the tumor microenvironment. *Journal of Clinical Investigation* **132**, (2022).
151. Nishina, T. *et al.* Interleukin-11-expressing fibroblasts have a unique gene signature correlated with poor prognosis of colorectal cancer. *Nat Commun* **12**, 2281 (2021).
152. Peñuelas, S. *et al.* TGF-β Increases Glioma-Initiating Cell Self-Renewal through the Induction of LIF in Human Glioblastoma. *Cancer Cell* **15**, 315–327 (2009).
153. Zhang, C., Liu, J., Wang, J., Hu, W. & Feng, Z. The emerging role of leukemia inhibitory factor in cancer and therapy. *Pharmacol Ther* **221**, 107754 (2021).
154. Soler, M. F., Abaurrea, A., Azcoaga, P., Araujo, A. M. & Caffarel, M. M. New perspectives in cancer immunotherapy: targeting IL-6 cytokine family. *J Immunother Cancer* **11**, e007530 (2023).
155. Zegeye, M. M. *et al.* Activation of the JAK/STAT3 and PI3K/AKT pathways are crucial for IL-6 trans-signaling-mediated pro-inflammatory response in human vascular endothelial cells. *Cell Commun Signal* **16**, 55 (2018).
156. Hara, T. *et al.* Interactions between cancer cells and immune cells drive transitions to mesenchymal-like states in glioblastoma. *Cancer Cell* **39**, 779-792.e11 (2021).
157. Chen, M. *et al.* Exploring the oncostatin M (OSM) feed-forward signaling of glioblastoma via STAT3 in pan-cancer analysis. *Cancer Cell Int* **21**, 565 (2021).
158. Houben, E., Hellings, N. & Broux, B. Oncostatin M, an Underestimated Player in the Central Nervous System. *Front Immunol* **10**, (2019).
159. Richards, C. D. The enigmatic cytokine oncostatin m and roles in disease. *ISRN Inflamm* **2013**, 512103 (2013).
160. West, N. R., Owens, B. M. J. & Hegazy, A. N. The oncostatin M-stromal cell axis in health and disease. *Scand J Immunol* **88**, e12694 (2018).
161. Zarling, J. M. *et al.* Oncostatin M: a growth regulator produced by differentiated histiocytic lymphoma cells. *Proc Natl Acad Sci U S A* **83**, 9739–43 (1986).
162. Douglas, A. M. *et al.* Expression and function of members of the cytokine receptor superfamily on breast cancer cells. *Oncogene* **14**, 661–669 (1997).
163. Junk, D. J. *et al.* Oncostatin M promotes cancer cell plasticity through cooperative STAT3-SMAD3 signaling. *Oncogene* **36**, 4001–4013 (2017).
164. Torres, C. *et al.* Serum Cytokine Profile in Patients With Pancreatic Cancer. *Pancreas* **43**, 1042–1049 (2014).
165. Gurluler, E. *et al.* Oncostatin-M as a novel biomarker in colon cancer patients and its association with clinicopathologic variables. *Eur Rev Med Pharmacol Sci* **18**, 2042–7 (2014).
166. Lilja, A., Nordborg, C., Brun, A., Salford, L. & Aman, P. Expression of the IL-6 family cytokines in human brain tumors. *Int J Oncol* (2001) doi:10.3892/ijo.19.3.495.
167. Tanay, A. & Regev, A. Scaling single-cell genomics from phenomenology to mechanism. *Nature* **541**, 331–338 (2017).
168. Tirosh, I. & Suvà, M. L. Deciphering Human Tumor Biology by Single-Cell Expression Profiling. *Annu Rev Cancer Biol* **3**, 151–166 (2019).

169. Natesh, K. *et al.* Oncostatin-M Differentially Regulates Mesenchymal and Proneural Signature Genes in Gliomas via STAT3 Signaling. *Neoplasia* **17**, 225–237 (2015).
170. Coniglio, S. J. *et al.* Microglial Stimulation of Glioblastoma Invasion Involves Epidermal Growth Factor Receptor (EGFR) and Colony Stimulating Factor 1 Receptor (CSF-1R) Signaling. *Molecular Medicine* **18**, 519–527 (2012).
171. Wang, S.-C., Yu, C.-F., Hong, J.-H., Tsai, C.-S. & Chiang, C.-S. Radiation Therapy-Induced Tumor Invasiveness Is Associated with SDF-1-Regulated Macrophage Mobilization and Vasculogenesis. *PLoS One* **8**, e69182 (2013).
172. Wang, D. *et al.* Macrophage-derived CCL22 promotes an immunosuppressive tumor microenvironment via IL-8 in malignant pleural effusion. *Cancer Lett* **452**, 244–253 (2019).
173. Korbecki, J. *et al.* CC Chemokines in a Tumor: A Review of Pro-Cancer and Anti-Cancer Properties of the Ligands of Receptors CCR1, CCR2, CCR3, and CCR4. *Int J Mol Sci* **21**, 8412 (2020).
174. Ebner, F. *et al.* Microglial Activation Milieu Controls Regulatory T Cell Responses. *The Journal of Immunology* **191**, 5594–5602 (2013).
175. Zhang, J. *et al.* A dialog between glioma and microglia that promotes tumor invasiveness through the CCL2/CCR2/interleukin-6 axis. *Carcinogenesis* **33**, 312–319 (2012).
176. Yang, D., Liu, J., Qian, H. & Zhuang, Q. Cancer-associated fibroblasts: from basic science to anticancer therapy. *Exp Mol Med* **55**, 1322–1332 (2023).
177. Araujo, A. M. *et al.* Stromal oncostatin M cytokine promotes breast cancer progression by reprogramming the tumor microenvironment. *Journal of Clinical Investigation* **132**, (2022).
178. Yoshida, G. J. Regulation of heterogeneous cancer-associated fibroblasts: the molecular pathology of activated signaling pathways. *Journal of Experimental & Clinical Cancer Research* **39**, 112 (2020).
179. Desmoulière, A., Chaponnier, C. & Gabbiani, G. Perspective Article: Tissue repair, contraction, and the myofibroblast. *Wound Repair and Regeneration* **13**, 7–12 (2005).
180. Forsthuber, A. *et al.* CXCL5 as Regulator of Neutrophil Function in Cutaneous Melanoma. *Journal of Investigative Dermatology* **139**, 186–194 (2019).
181. Eruslanov, E. B. *et al.* Tumor-associated neutrophils stimulate T cell responses in early-stage human lung cancer. *Journal of Clinical Investigation* **124**, 5466–5480 (2014).
182. Lee, B. Y. *et al.* Heterocellular OSM-OSMR signalling reprograms fibroblasts to promote pancreatic cancer growth and metastasis. *Nat Commun* **12**, 7336 (2021).
183. Clark, C. E. *et al.* Dynamics of the Immune Reaction to Pancreatic Cancer from Inception to Invasion. *Cancer Res* **67**, 9518–9527 (2007).
184. Pylayeva-Gupta, Y., Lee, K. E., Hajdu, C. H., Miller, G. & Bar-Sagi, D. Oncogenic Kras-induced GM-CSF production promotes the development of pancreatic neoplasia. *Cancer Cell* **21**, 836–47 (2012).
185. Nywening, T. M. *et al.* Targeting tumour-associated macrophages with CCR2 inhibition in combination with FOLFIRINOX in patients with borderline resectable and

locally advanced pancreatic cancer: a single-centre, open-label, dose-finding, non-randomised, phase 1b trial. *Lancet Oncol* **17**, 651–662 (2016).
186. Zhang, Y. *et al.* Interleukin-6 Is Required for Pancreatic Cancer Progression by Promoting MAPK Signaling Activation and Oxidative Stress Resistance. *Cancer Res* **73**, 6359–6374 (2013).
187. Waghray, M. *et al.* GM-CSF Mediates Mesenchymal–Epithelial Cross-talk in Pancreatic Cancer. *Cancer Discov* **6**, 886–899 (2016).
188. Shi, Y. *et al.* Targeting LIF-mediated paracrine interaction for pancreatic cancer therapy and monitoring. *Nature* **569**, 131–135 (2019).
189. Bayne, L. J. *et al.* Tumor-derived granulocyte-macrophage colony-stimulating factor regulates myeloid inflammation and T cell immunity in pancreatic cancer. *Cancer Cell* **21**, 822–35 (2012).
190. Doherty, M., Smigiel, J., Junk, D. & Jackson, M. Cancer Stem Cell Plasticity Drives Therapeutic Resistance. *Cancers (Basel)* **8**, 8 (2016).
191. Meacham, C. E. & Morrison, S. J. Tumour heterogeneity and cancer cell plasticity. *Nature* **501**, 328–337 (2013).
192. Scheel, C. & Weinberg, R. A. Cancer stem cells and epithelial–mesenchymal transition: Concepts and molecular links. *Semin Cancer Biol* **22**, 396–403 (2012).
193. Polak, K. L. *et al.* Oncostatin-M and OSM-Receptor Feed-Forward Activation of MAPK Induces Separable Stem-like and Mesenchymal Programs. *Molecular Cancer Research* **21**, 975–990 (2023).
194. Onder, T. T. *et al.* Loss of E-Cadherin Promotes Metastasis via Multiple Downstream Transcriptional Pathways. *Cancer Res* **68**, 3645–3654 (2008).
195. Gadsby, D. C. Ion channels versus ion pumps: the principal difference, in principle. *Nat Rev Mol Cell Biol* **10**, 344–52 (2009).
196. Terlau, H. & Stühmer, W. Structure and Function of Voltage-Gated Ion Channels. *Naturwissenschaften* **85**, 437–444 (1998).
197. Alexander, S., Mathie, A. & Peters, J. Ligand-gated ion channels. *Br J Pharmacol* **164**, (2011).
198. Martinac, B. Mechanosensitive ion channels: an evolutionary and scientific tour de force in mechanobiology. *Channels (Austin)* **6**, 211–3 (2012).
199. Cheng, Q. *et al.* Novel insights into ion channels in cancer stem cells (Review). *Int J Oncol* (2018) doi:10.3892/ijo.2018.4500.
200. Molenaar, R. J. Ion channels in glioblastoma. *ISRN Neurol* **2011**, 590249 (2011).
201. Lang, F. & Stournaras, C. Ion channels in cancer: future perspectives and clinical potential. *Philos Trans R Soc Lond B Biol Sci* **369**, 20130108 (2014).
202. Bahcheli, A. T. *et al.* Pan-cancer ion transport signature reveals functional regulators of glioblastoma aggression. *EMBO J* **43**, 196–224 (2024).
203. Kondapalli, K. C. *et al.* A leak pathway for luminal protons in endosomes drives oncogenic signalling in glioblastoma. *Nat Commun* **6**, 6289 (2015).
204. Chen, X. *et al.* A Feedforward Mechanism Mediated by Mechanosensitive Ion Channel PIEZO1 and Tissue Mechanics Promotes Glioma Aggression. *Neuron* **100**, 799-815.e7 (2018).

205. Folcher, A. *et al.* NALCN-mediated sodium influx confers metastatic prostate cancer cell invasiveness. *EMBO J* **42**, (2023).
206. Leanza, L. *et al.* Direct Pharmacological Targeting of a Mitochondrial Ion Channel Selectively Kills Tumor Cells In Vivo. *Cancer Cell* **31**, 516-531.e10 (2017).
207. Arcangeli, A. *et al.* Targeting Ion Channels in Cancer: A Novel Frontier in Antineoplastic Therapy. *Curr Med Chem* **16**, 66–93 (2009).
208. Comes, N. *et al.* The voltage-dependent K+ channels Kv1.3 and Kv1.5 in human cancer. *Front Physiol* **4**, (2013).
209. Than, B. L. N. *et al.* CFTR is a tumor suppressor gene in murine and human intestinal cancer. *Oncogene* **35**, 4191–4199 (2016).
210. Elinder, F. *et al.* Opening of plasma membrane voltage-dependent anion channels (VDAC) precedes caspase activation in neuronal apoptosis induced by toxic stimuli. *Cell Death Differ* **12**, 1134–1140 (2005).
211. Sabirov, R. Z. *et al.* The ATP-Releasing Maxi-Cl Channel: Its Identity, Molecular Partners and Physiological/Pathophysiological Implications. *Life (Basel)* **11**, (2021).
212. Crottès, D. & Jan, L. Y. The multifaceted role of TMEM16A in cancer. *Cell Calcium* **82**, 102050 (2019).
213. Guan, Y.-T. *et al.* Overexpression of chloride channel-3 (ClC-3) is associated with human cervical carcinoma development and prognosis. *Cancer Cell Int* **19**, 8 (2019).
214. Hoffmann, E. K., Sørensen, B. H., Sauter, D. P. R. & Lambert, I. H. Role of volume-regulated and calcium-activated anion channels in cell volume homeostasis, cancer and drug resistance. *Channels (Austin)* **9**, 380–96 (2015).
215. Kim, H. J., Lee, P. C.-W. & Hong, J. H. Chloride Channels and Transporters: Roles beyond Classical Cellular Homeostatic pH or Ion Balance in Cancers. *Cancers (Basel)* **14**, (2022).
216. Murray, E. *et al.* Quantitative Proteomic Profiling of Pleomorphic Human Sarcoma Identifies CLIC1 as a Dominant Pro-Oncogenic Receptor Expressed in Diverse Sarcoma Types. *J Proteome Res* **13**, 2543–2559 (2014).
217. Fernández-Salas, E. *et al.* mtCLIC/CLIC4, an Organellular Chloride Channel Protein, Is Increased by DNA Damage and Participates in the Apoptotic Response to p53. *Mol Cell Biol* **22**, 3610–3620 (2002).
218. Padmakumar, V. C. *et al.* Spontaneous Skin Erosions and Reduced Skin and Corneal Wound Healing Characterize CLIC4NULL Mice. *Am J Pathol* **181**, 74–84 (2012).
219. Zheng, D. *et al.* PA28β regulates cell invasion of gastric cancer via modulating the expression of chloride intracellular channel 1. *J Cell Biochem* **113**, 1537–1546 (2012).
220. Tang, H.-Y. *et al.* Protein isoform-specific validation defines multiple chloride intracellular channel and tropomyosin isoforms as serological biomarkers of ovarian cancer. *J Proteomics* **89**, 165–178 (2013).
221. Shukla, A. *et al.* CLIC4 regulates TGF-β-dependent myofibroblast differentiation to produce a cancer stroma. *Oncogene* **33**, 842–850 (2014).
222. Okudela, K. *et al.* Proteome Analysis for Downstream Targets of Oncogenic KRAS - the Potential Participation of CLIC4 in Carcinogenesis in the Lung. *PLoS One* **9**, e87193 (2014).

223. Deng, Y.-J. *et al.* CLIC4, ERp29, and Smac/DIABLO Derived from Metastatic Cancer Stem–like Cells Stratify Prognostic Risks of Colorectal Cancer. *Clinical Cancer Research* **20**, 3809–3817 (2014).
224. Francisco, M. A. *et al.* Chloride intracellular channel 1 cooperates with potassium channel EAG2 to promote medulloblastoma growth. *Journal of Experimental Medicine* **217**, (2020).
225. Wang, P. Chloride intracellular channel 1 regulates colon cancer cell migration and invasion through ROS/ERK pathway. *World J Gastroenterol* **20**, 2071 (2014).
226. Ding, Q. *et al.* CLIC1 overexpression is associated with poor prognosis in gallbladder cancer. *Tumor Biology* **36**, 193–198 (2015).
227. Yu, W. *et al.* Expression and prognostic value of CLIC1 in epithelial ovarian cancer. *Exp Ther Med* (2018) doi:10.3892/etm.2018.6000.
228. Chen, C.-D. *et al.* Overexpression of CLIC1 in human gastric carcinoma and its clinicopathological significance. *Proteomics* **7**, 155–167 (2007).
229. Peng, J.-M., Lin, S.-H., Yu, M.-C. & Hsieh, S.-Y. CLIC1 recruits PIP5K1A/C to induce cell-matrix adhesions for tumor metastasis. *Journal of Clinical Investigation* **131**, (2021).
230. Setti, M. *et al.* Functional Role of CLIC1 Ion Channel in Glioblastoma-Derived Stem/Progenitor Cells. *JNCI: Journal of the National Cancer Institute* **105**, 1644–1655 (2013).
231. Thuringer, D., Chanteloup, G., Winckler, P. & Garrido, C. The vesicular transfer of CLIC1 from glioblastoma to microvascular endothelial cells requires TRPM7. *Oncotarget* **9**, 33302–33311 (2018).
232. Valenzuela, S. M. *et al.* Molecular Cloning and Expression of a Chloride Ion Channel of Cell Nuclei. *Journal of Biological Chemistry* **272**, 12575–12582 (1997).
233. Heiss, N. S. & Poustka, A. Genomic Structure of a Novel Chloride Channel Gene, CLIC2, in Xq28. *Genomics* **45**, 224–228 (1997).
234. Qian, Z., Okuhara, D., Abe, M. K. & Rosner, M. R. Molecular Cloning and Characterization of a Mitogen-activated Protein Kinase-associated Intracellular Chloride Channel. *Journal of Biological Chemistry* **274**, 1621–1627 (1999).
235. Duncan, R. R., Westwood, P. K., Boyd, A. & Ashley, R. H. Rat Brain p64H1, Expression of a New Member of the p64 Chloride Channel Protein Family in Endoplasmic Reticulum. *Journal of Biological Chemistry* **272**, 23880–23886 (1997).
236. Berryman, M. & Bretscher, A. Identification of a Novel Member of the Chloride Intracellular Channel Gene Family (CLIC5) That Associates with the Actin Cytoskeleton of Placental Microvilli. *Mol Biol Cell* **11**, 1509–1521 (2000).
237. Nishizawa, T., Nagao, T., Iwatsubo, T., Forte, J. G. & Urushidani, T. Molecular Cloning and Characterization of a Novel Chloride Intracellular Channel-related Protein, Parchorin, Expressed in Water-secreting Cells. *Journal of Biological Chemistry* **275**, 11164–11173 (2000).
238. Al Khamici, H. *et al.* Members of the Chloride Intracellular Ion Channel Protein Family Demonstrate Glutaredoxin-Like Enzymatic Activity. *PLoS One* **10**, e115699 (2015).

239. Dulhunty, A., Gage, P., Curtis, S., Chelvanayagam, G. & Board, P. The Glutathione Transferase Structural Family Includes a Nuclear Chloride Channel and a Ryanodine Receptor Calcium Release Channel Modulator. *Journal of Biological Chemistry* **276**, 3319–3323 (2001).
240. Singh, H. Two decades with dimorphic Chloride Intracellular Channels (CLICs). *FEBS Lett* **584**, 2112–2121 (2010).
241. Ulmasov, B. *et al.* CLIC1 null mice demonstrate a role for CLIC1 in macrophage superoxide production and tissue injury. *Physiol Rep* **5**, e13169 (2017).
242. Fernández-Salas, E., Sagar, M., Cheng, C., Yuspa, S. H. & Weinberg, W. C. p53 and Tumor Necrosis Factor α Regulate the Expression of a Mitochondrial Chloride Channel Protein. *Journal of Biological Chemistry* **274**, 36488–36497 (1999).
243. Ponnalagu, D. *et al.* Data supporting characterization of CLIC1, CLIC4, CLIC5 and DmCLIC antibodies and localization of CLICs in endoplasmic reticulum of cardiomyocytes. *Data Brief* **7**, 1038–1044 (2016).
244. Setti, M. *et al.* Extracellular vesicle-mediated transfer of CLIC1 protein is a novel mechanism for the regulation of glioblastoma growth. *Oncotarget* **6**, 31413–31427 (2015).
245. Gururaja Rao, S., Ponnalagu, D., Patel, N. J. & Singh, H. Three Decades of Chloride Intracellular Channel Proteins: From Organelle to Organ Physiology. *Curr Protoc Pharmacol* **80**, (2018).
246. Tang, T. *et al.* CLICs-dependent chloride efflux is an essential and proximal upstream event for NLRP3 inflammasome activation. *Nat Commun* **8**, 202 (2017).
247. Jiang, L. *et al.* Intracellular chloride channel protein CLIC1 regulates macrophage functions via modulation of phagosomal acidification. *J Cell Sci* (2012) doi:10.1242/jcs.110072.
248. Ponnalagu, D. *et al.* Molecular identity of cardiac mitochondrial chloride intracellular channel proteins. *Mitochondrion* **27**, 6–14 (2016).
249. Peretti, M. *et al.* Mutual Influence of ROS, pH, and CLIC1 Membrane Protein in the Regulation of G1–S Phase Progression in Human Glioblastoma Stem Cells. *Mol Cancer Ther* **17**, 2451–2461 (2018).
250. Gritti, M. *et al.* Metformin repositioning as antitumoral agent: selective antiproliferative effects in human glioblastoma stem cells, via inhibition of CLIC1-mediated ion current. *Oncotarget* **5**, 11252–11268 (2014).
251. Suh, K. & Yuspa, S. Intracellular Chloride Channels: Critical Mediators of Cell Viability and Potential Targets for Cancer Therapy. *Curr Pharm Des* **11**, 2753–2764 (2005).
252. Takano, K. *et al.* An X-linked channelopathy with cardiomegaly due to a CLIC2 mutation enhancing ryanodine receptor channel activity. *Hum Mol Genet* **21**, 4497–4507 (2012).
253. Wojciak-Stothard, B. *et al.* Aberrant Chloride Intracellular Channel 4 Expression Contributes to Endothelial Dysfunction in Pulmonary Arterial Hypertension. *Circulation* **129**, 1770–1780 (2014).
254. Hernandez-Fernaud, J. R. *et al.* Secreted CLIC3 drives cancer progression through its glutathione-dependent oxidoreductase activity. *Nat Commun* **8**, 14206 (2017).

255. Flores-Téllez, T. N. J., Lopez, T. V., Vásquez Garzón, V. R. & Villa-Treviño, S. Co-Expression of Ezrin-CLIC5-Podocalyxin Is Associated with Migration and Invasiveness in Hepatocellular Carcinoma. *PLoS One* **10**, e0131605 (2015).
256. Novarino, G. Involvement of the Intracellular Ion Channel CLIC1 in Microglia-Mediated -Amyloid-Induced Neurotoxicity. *Journal of Neuroscience* **24**, 5322–5330 (2004).
257. Milton, R. H. *et al.* CLIC1 Function Is Required for β-Amyloid-Induced Generation of Reactive Oxygen Species by Microglia. *The Journal of Neuroscience* **28**, 11488–11499 (2008).
258. Gagnon, L. H. *et al.* The Chloride Intracellular Channel Protein CLIC5 Is Expressed at High Levels in Hair Cell Stereocilia and Is Essential for Normal Inner Ear Function. *The Journal of Neuroscience* **26**, 10188–10198 (2006).
259. Averaimo, S., Milton, R. H., Duchen, M. R. & Mazzanti, M. Chloride intracellular channel 1 (CLIC1): Sensor and effector during oxidative stress. *FEBS Lett* **584**, 2076–2084 (2010).
260. Harrop, S. J. *et al.* Crystal Structure of a Soluble Form of the Intracellular Chloride Ion Channel CLIC1 (NCC27) at 1.4-Å Resolution. *Journal of Biological Chemistry* **276**, 44993–45000 (2001).
261. Tulk, B. M., Schlesinger, P. H., Kapadia, S. A. & Edwards, J. C. CLIC-1 Functions as a Chloride Channel When Expressed and Purified from Bacteria. *Journal of Biological Chemistry* **275**, 26986–26993 (2000).
262. Littler, D. R. *et al.* The Intracellular Chloride Ion Channel Protein CLIC1 Undergoes a Redox-controlled Structural Transition. *Journal of Biological Chemistry* **279**, 9298–9305 (2004).
263. Varela, L. *et al.* A Zn2+-triggered two-step mechanism of CLIC1 membrane insertion and activation into chloride channels. *J Cell Sci* **135**, (2022).
264. Warton, K. *et al.* Recombinant CLIC1 (NCC27) Assembles in Lipid Bilayers via a pH-dependent Two-state Process to Form Chloride Ion Channels with Identical Characteristics to Those Observed in Chinese Hamster Ovary Cells Expressing CLIC1. *Journal of Biological Chemistry* **277**, 26003–26011 (2002).
265. Randhawa, K. & Jahani-Asl, A. CLIC1 regulation of cancer stem cells in glioblastoma. in 99–123 (2023). doi:10.1016/bs.ctm.2023.09.004.
266. Littler, D. R. *et al.* The enigma of the CLIC proteins: Ion channels, redox proteins, enzymes, scaffolding proteins? *FEBS Lett* **584**, 2093–2101 (2010).
267. Singh, H. & Ashley, R. H. Redox Regulation of CLIC1 by Cysteine Residues Associated with the Putative Channel Pore. *Biophys J* **90**, 1628–1638 (2006).
268. Averaimo, S. *et al.* Point Mutations in the Transmembrane Region of the Clic1 Ion Channel Selectively Modify Its Biophysical Properties. *PLoS One* **8**, e74523 (2013).
269. Tulk, B. M., Kapadia, S. & Edwards, J. C. CLIC1 inserts from the aqueous phase into phospholipid membranes, where it functions as an anion channel. *American Journal of Physiology-Cell Physiology* **282**, C1103–C1112 (2002).
270. Warton, K. *et al.* Recombinant CLIC1 (NCC27) Assembles in Lipid Bilayers via a pH-dependent Two-state Process to Form Chloride Ion Channels with Identical

Characteristics to Those Observed in Chinese Hamster Ovary Cells Expressing CLIC1. *Journal of Biological Chemistry* **277**, 26003–26011 (2002).
271. Spear, J. S. & White, K. A. Single-cell intracellular pH dynamics regulate the cell cycle by timing the G1 exit and G2 transition. *J Cell Sci* **136**, (2023).
272. Dubé, M., Etienne, L., Fels, M. & Kielian, M. Calcium-Dependent Rubella Virus Fusion Occurs in Early Endosomes. *J Virol* **90**, 6303–6313 (2016).
273. Rosengarth, A. & Luecke, H. A Calcium-driven Conformational Switch of the N-terminal and Core Domains of Annexin A1. *J Mol Biol* **326**, 1317–1325 (2003).
274. Sciacca, M. F. M. *et al.* Cations as Switches of Amyloid-Mediated Membrane Disruption Mechanisms: Calcium and IAPP. *Biophys J* **104**, 173–184 (2013).
275. Littler, D. R. *et al.* Comparison of vertebrate and invertebrate CLIC proteins: The crystal structures ofCaenorhabditis elegans EXC-4 andDrosophila melanogaster DmCLIC. *Proteins: Structure, Function, and Bioinformatics* **71**, 364–378 (2008).
276. Tulk, B. M., Kapadia, S. & Edwards, J. C. CLIC1 inserts from the aqueous phase into phospholipid membranes, where it functions as an anion channel. *American Journal of Physiology-Cell Physiology* **282**, C1103–C1112 (2002).
277. Chalothorn, D., Zhang, H., Smith, J. E., Edwards, J. C. & Faber, J. E. Chloride intracellular channel-4 is a determinant of native collateral formation in skeletal muscle and brain. *Circ Res* **105**, 89–98 (2009).
278. Jiang, X. *et al.* Up-regulation of CLIC1 activates MYC signaling and forms a positive feedback regulatory loop with MYC in Hepatocellular carcinoma. *Am J Cancer Res* **10**, 2355–2370 (2020).
279. Wang, J.-W. *et al.* Identification of metastasis-associated proteins involved in gallbladder carcinoma metastasis by proteomic analysis and functional exploration of chloride intracellular channel 1. *Cancer Lett* **281**, 71–81 (2009).
280. Wang, P. *et al.* Regulation of colon cancer cell migration and invasion by CLIC1-mediated RVD. *Mol Cell Biochem* **365**, 313–321 (2012).
281. Valenzuela, S. M. *et al.* The nuclear chloride ion channel NCC27 is involved in regulation of the cell cycle. *J Physiol* **529**, 541–552 (2000).
282. Inaba, M. & Yamashita, Y. M. Asymmetric Stem Cell Division: Precision for Robustness. *Cell Stem Cell* **11**, 461–469 (2012).
283. Hjelmeland, A. B. *et al.* Acidic stress promotes a glioma stem cell phenotype. *Cell Death Differ* **18**, 829–840 (2011).
284. Lee, J.-R. *et al.* The inhibition of chloride intracellular channel 1 enhances Ca2+ and reactive oxygen species signaling in A549 human lung cancer cells. *Exp Mol Med* **51**, 1–11 (2019).
285. Macknight, A. D. C. Principles of Cell Volume Regulation. *Kidney Blood Press Res* **11**, 114–141 (1988).
286. Neurohr, G. E. & Amon, A. Relevance and Regulation of Cell Density. *Trends Cell Biol* **30**, 213–225 (2020).
287. Jentsch, T. J. VRACs and other ion channels and transporters in the regulation of cell volume and beyond. *Nat Rev Mol Cell Biol* **17**, 293–307 (2016).
288. Lang, F. *et al.* Functional Significance of Cell Volume Regulatory Mechanisms. *Physiol Rev* **78**, 247–306 (1998).

289. Boucrot, E. & Kirchhausen, T. Mammalian Cells Change Volume during Mitosis. *PLoS One* **3**, e1477 (2008).
290. Habela, C. W. & Sontheimer, H. Cytoplasmic Volume Condensation Is an Integral Part of Mitosis. *Cell Cycle* **6**, 1613–1620 (2007).
291. Habela, C. W., Ernest, N. J., Swindall, A. F. & Sontheimer, H. Chloride Accumulation Drives Volume Dynamics Underlying Cell Proliferation and Migration. *J Neurophysiol* **101**, 750–757 (2009).
292. Huang, X. *et al.* EAG2 potassium channel with evolutionarily conserved function as a brain tumor target. *Nat Neurosci* **18**, 1236–1246 (2015).
293. Bakhshinyan, D., Savage, N., Salim, S. K., Venugopal, C. & Singh, S. K. The Strange Case of Jekyll and Hyde: Parallels Between Neural Stem Cells and Glioblastoma-Initiating Cells. *Front Oncol* **10**, (2021).
294. Menon, S. G. *et al.* Redox regulation of the G1 to S phase transition in the mouse embryo fibroblast cell cycle. *Cancer Res* **63**, 2109–17 (2003).
295. Orlicka-Płocka, M. *et al.* Implications of Oxidative Stress in Glioblastoma Multiforme Following Treatment with Purine Derivatives. *Antioxidants* **10**, 950 (2021).
296. Menon, S. G. & Goswami, P. C. A redox cycle within the cell cycle: ring in the old with the new. *Oncogene* **26**, 1101–1109 (2007).
297. Alao, J. P. The regulation of cyclin D1 degradation: roles in cancer development and the potential for therapeutic invention. *Mol Cancer* **6**, 24 (2007).
298. Vélez-Cruz, R. & Johnson, D. The Retinoblastoma (RB) Tumor Suppressor: Pushing Back against Genome Instability on Multiple Fronts. *Int J Mol Sci* **18**, 1776 (2017).
299. Setti, M. *et al.* Functional role of CLIC1 ion channel in glioblastoma-derived stem/progenitor cells. *J Natl Cancer Inst* **105**, 1644–55 (2013).
300. Kim, D. *et al.* Epithelial Mesenchymal Transition in Embryonic Development, Tissue Repair and Cancer: A Comprehensive Overview. *J Clin Med* **7**, 1 (2017).
301. Kim, Y.-S., Yi, B.-R., Kim, N.-H. & Choi, K.-C. Role of the epithelial–mesenchymal transition and its effects on embryonic stem cells. *Exp Mol Med* **46**, e108–e108 (2014).
302. Thiery, J. P., Acloque, H., Huang, R. Y. J. & Nieto, M. A. Epithelial-Mesenchymal Transitions in Development and Disease. *Cell* **139**, 871–890 (2009).
303. Molenaar, R. J. Ion channels in glioblastoma. *ISRN Neurol* **2011**, 590249 (2011).
304. Sontheimer, H. Malignant gliomas: perverting glutamate and ion homeostasis for selective advantage. *Trends Neurosci* **26**, 543–549 (2003).
305. Carro, M. S. *et al.* The transcriptional network for mesenchymal transformation of brain tumours. *Nature* **463**, 318–325 (2010).
306. Phillips, H. S. *et al.* Molecular subclasses of high-grade glioma predict prognosis, delineate a pattern of disease progression, and resemble stages in neurogenesis. *Cancer Cell* **9**, 157–173 (2006).
307. Ahir, B. K., Engelhard, H. H. & Lakka, S. S. Tumor Development and Angiogenesis in Adult Brain Tumor: Glioblastoma. *Mol Neurobiol* **57**, 2461–2478 (2020).
308. Sendoel, A. & Hengartner, M. O. Apoptotic Cell Death Under Hypoxia. *Physiology* **29**, 168–176 (2014).

309. Yang, X. *et al*. A public genome-scale lentiviral expression library of human ORFs. *Nat Methods* **8**, 659–661 (2011).
310. Kelly, J. J. P. *et al*. Proliferation of Human Glioblastoma Stem Cells Occurs Independently of Exogenous Mitogens. *Stem Cells* **27**, 1722–1733 (2009).
311. Lavictoire, S. J., Parolin, D. A. E., Klimowicz, A. C., Kelly, J. F. & Lorimer, I. A. J. Interaction of Hsp90 with the Nascent Form of the Mutant Epidermal Growth Factor Receptor EGFRvIII. *Journal of Biological Chemistry* **278**, 5292–5299 (2003).
312. Luchman, H. A. *et al*. An in vivo patient-derived model of endogenous IDH1-mutant glioma. *Neuro Oncol* **14**, 184–191 (2012).
313. Sarsour, E. H., Kumar, M. G., Chaudhuri, L., Kalen, A. L. & Goswami, P. C. Redox Control of the Cell Cycle in Health and Disease. *Antioxid Redox Signal* **11**, 2985–3011 (2009).
314. Sharanek, A. *et al*. OSMR controls glioma stem cell respiration and confers resistance of glioblastoma to ionizing radiation. *Nat Commun* **11**, 4116 (2020).
315. Barbieri, F. *et al*. Inhibition of Chloride Intracellular Channel 1 (CLIC1) as Biguanide Class-Effect to Impair Human Glioblastoma Stem Cell Viability. *Front Pharmacol* **9**, (2018).
316. Lee, J.-R. *et al*. The inhibition of chloride intracellular channel 1 enhances Ca2+ and reactive oxygen species signaling in A549 human lung cancer cells. *Exp Mol Med* **51**, 1–11 (2019).
317. Huang, X. *et al*. Voltage-gated potassium channel EAG2 controls mitotic entry and tumor growth in medulloblastoma via regulating cell volume dynamics. *Genes Dev* **26**, 1780–1796 (2012).
318. Stockhausen, M.-T., Kristoffersen, K., Stobbe, L. & Poulsen, H. S. Differentiation of glioblastoma multiforme stem-like cells leads to downregulation of EGFR and EGFRvIII and decreased tumorigenic and stem-like cell potential. *Cancer Biol Ther* **15**, 216–24 (2014).
319. Niwa, H., Miyazaki, J. & Smith, A. G. Quantitative expression of Oct-3/4 defines differentiation, dedifferentiation or self-renewal of ES cells. *Nat Genet* **24**, 372–376 (2000).
320. He, M. *et al*. Chloride channels regulate differentiation and barrier functions of the mammalian airway. *Elife* **9**, (2020).
321. Clevers, H. The cancer stem cell: premises, promises and challenges. *Nat Med* **17**, 313–319 (2011).
322. Chearwae, W. & Bright, J. J. PPARγ agonists inhibit growth and expansion of CD133+ brain tumour stem cells. *Br J Cancer* **99**, 2044–2053 (2008).
323. Kang, M.-K. & Kang, S.-K. Pharmacologic blockade of chloride channel synergistically enhances apoptosis of chemotherapeutic drug-resistant cancer stem cells. *Biochem Biophys Res Commun* **373**, 539–544 (2008).
324. Higgins, C. F. Volume-activated chloride currents associated with the multidrug resistance P-glycoprotein. *J Physiol* **482**, 31–36 (1995).
325. Holohan, C., Van Schaeybroeck, S., Longley, D. B. & Johnston, P. G. Cancer drug resistance: an evolving paradigm. *Nat Rev Cancer* **13**, 714–726 (2013).

326. Gottesman, M. M., Fojo, T. & Bates, S. E. Multidrug resistance in cancer: role of ATP–dependent transporters. *Nat Rev Cancer* **2**, 48–58 (2002).
327. Liu, Y. *et al.* Chloride intracellular channel 1 regulates the antineoplastic effects of metformin in gallbladder cancer cells. *Cancer Sci* **108**, 1240–1252 (2017).
328. Nong, Z.-L. *et al.* CLIC1-mediated autophagy confers resistance to DDP in gastric cancer. *Anticancer Drugs* **35**, 1–11 (2024).
329. Feng, J. *et al.* ClC-3 promotes paclitaxel resistance via modulating tubulins polymerization in ovarian cancer cells. *Biomedicine & Pharmacotherapy* **138**, 111407 (2021).
330. Wu, J. & Wang, D. CLIC1 Induces Drug Resistance in Human Choriocarcinoma Through Positive Regulation of MRP1. *Oncology Research Featuring Preclinical and Clinical Cancer Therapeutics* **25**, 863–871 (2017).
331. Zhao, K. *et al.* Exosome-mediated transfer of CLIC1 contributes to the vincristine-resistance in gastric cancer. *Mol Cell Biochem* **462**, 97–105 (2019).
332. Mukherjee, B. *et al.* EGFRvIII and DNA Double-Strand Break Repair: A Molecular Mechanism for Radioresistance in Glioblastoma. *Cancer Res* **69**, 4252–4259 (2009).
333. Hatanpaa, K. J., Burma, S., Zhao, D. & Habib, A. A. Epidermal Growth Factor Receptor in Glioma: Signal Transduction, Neuropathology, Imaging, and Radioresistance. *Neoplasia* **12**, 675–684 (2010).
334. Huang, P. H. *et al.* Quantitative analysis of EGFRvIII cellular signaling networks reveals a combinatorial therapeutic strategy for glioblastoma. *Proceedings of the National Academy of Sciences* **104**, 12867–12872 (2007).
335. An, Z., Aksoy, O., Zheng, T., Fan, Q.-W. & Weiss, W. A. Epidermal growth factor receptor and EGFRvIII in glioblastoma: signaling pathways and targeted therapies. *Oncogene* **37**, 1561–1575 (2018).
336. Eskilsson, E. *et al.* EGFRvIII mutations can emerge as late and heterogenous events in glioblastoma development and promote angiogenesis through Src activation. *Neuro Oncol* **18**, 1644–1655 (2016).
337. Yin, J. *et al.* Pigment Epithelium-Derived Factor (PEDF) Expression Induced by EGFRvIII Promotes Self-renewal and Tumor Progression of Glioma Stem Cells. *PLoS Biol* **13**, e1002152 (2015).
338. Jacobs, K. A., Maghe, C. & Gavard, J. Lysosomes in glioblastoma: pump up the volume. *Cell Cycle* **19**, 2094–2104 (2020).
339. DiCiccio, J. E. & Steinberg, B. E. Lysosomal pH and analysis of the counter ion pathways that support acidification. *J Gen Physiol* **137**, 385–90 (2011).
340. Van Dyke, R. W. Acidification of Lysosomes and Endosomes. in 331–360 (1996). doi:10.1007/978-1-4615-5833-0_10.
341. Jiang, L. *et al.* Intracellular chloride channel protein CLIC1 regulates macrophage functions via modulation of phagosomal acidification. *J Cell Sci* (2012) doi:10.1242/jcs.110072.
342. Goodchild, S. C. *et al.* Oxidation promotes insertion of the CLIC1 chloride intracellular channel into the membrane. *European Biophysics Journal* **39**, 129–138 (2009).

343. Raimondo, J. A genetically-encoded chloride and pH sensor for dissociating ion dynamics in the nervous system. *Front Cell Neurosci* **7**, (2013).
344. Rouillard, A. D. *et al*. The harmonizome: a collection of processed datasets gathered to serve and mine knowledge about genes and proteins. *Database* **2016**, baw100 (2016).